

Investigating biologically inert platinum(IV)-  
glutamine complexes to maximise their  
selectivity and utility in personalised cancer  
therapy.



THE UNIVERSITY OF  
**SYDNEY**

**Vinitha M**

Supervisors: Professor Trevor Hambley  
Professor Renae Ryan

*A thesis submitted to fulfil requirements for the degree of  
Master of Philosophy*

School of Chemistry  
The University of Sydney

2023

## **Statement of Originality**

This is to certify to the best of my knowledge, that the content of this thesis is my own work. This thesis has not been submitted for the award of any degree or other purposes. I certify that the intellectual content of this thesis is the product of my own work and that all assistance received in the preparation of this thesis and sources have been acknowledged.

**Vinitha M**

## ABSTRACT

This project is aimed at studying the targeted delivery of biologically inert platinum(IV)-glutamine complexes into cancer cells by exploiting their overexpression of the glutamine transporter, ASCT2. It addresses the limitations of current platinum(II) drugs in clinics. Biologically inert bis(amino acid)platinum(II) complexes were synthesised as precursors. The transport of modified glutamine compounds via ASCT2 was concurrently investigated to elucidate if the modification of glutamine impacted its transport. *trans*-[Pt(L-alanine)<sub>2</sub>] and *trans*-[Pt(L-glycine)<sub>2</sub>] were synthesised but were determined as unsuitable precursors due to their poor solubility in many solvents which hindered their oxidation. A synthetic procedure using *cis*-[PtCl<sub>2</sub>(DMSO)<sub>2</sub>] as a starting material was developed to synthesise *cis*-bis(amino acid)platinum(II) complexes with greater solubility. A series of experiments were conducted in different reaction conditions with L-isoleucine, L-tryptophan, and L-alanine to design an optimal procedure. *cis*-[Pt(L-alanine)<sub>2</sub>] was synthesised in high purity when *cis*-[PtCl<sub>2</sub>(DMSO)<sub>2</sub>] was reacted with 2 equivalents of L-alanine and base in methanol. A modified glutamine compound was synthesised by attaching a 2-(2-aminoethoxy)ethanol linker to the  $\alpha$ -carboxylic acid of L-glutamine (compound 1). Compound 1 and L-theanine were applied to *Xenopus laevis* oocytes expressing ASCT2. Two-electrode voltage clamp electrophysiology was used to measure substrate-elicited currents over a range of membrane potentials. Compound 1 is neither a substrate nor an inhibitor of ASCT2 while L-theanine was identified as an inhibitor. This revealed that the modification of glutamine prevents it from acting as a substrate of ASCT2. This suggests that ASCT2 may not be a suitable target for the delivery of platinum(IV)-glutamine complexes. The synthesis of *cis*-[Pt(L-alanine)<sub>2</sub>] revealed that *cis*-[PtCl<sub>2</sub>(DMSO)<sub>2</sub>] can be utilised as a starting material to synthesise *cis*-bis(amino acid)platinum(II) complexes.

## ACKNOWLEDGEMENTS

I would like to begin by showing my appreciation to my supervisor, Professor Trevor Hambley, for giving me the opportunity to do this research project. I appreciate you waiting 2 years for me to commence my degree due to border closures and for accepting me as your student despite your retirement. Thank you for being so patient and for teaching me the chemistry and laboratory skills needed to be a good researcher. Thank you for also providing me with support with matters outside of the degree and for always believing in me. I would also like to acknowledge Dr Adnan Bani-Saad. I would like to express my gratitude for the time you have spent helping me with my experiments and training me on instruments. Thank you for making our lab such a pleasant environment to work in.

I would like to thank my co-supervisor, Professor Renae Ryan, for this opportunity as well. Thank you for your guidance and support throughout this degree. To the members of TBG, Chelsea, Amy, Irina, Julian, and Alice, it has been an enjoyable experience working with all of you even through the late nights. I would like to especially thank Chelsea Briot for your guidance, and for teaching me everything I needed. I truly could not have completed this degree without your help.

I would also like to thank Professor Elizabeth New for adopting me as your student and for including me in all of your group activities and meetings. I appreciate the additional support you have provided me with and thank you for allowing me to join your group where I have made amazing friends. Nian Kee, Hazel, Haobo, Dr. Joy, Dr. Monika, Jay, Ivy, Prem, and Louis, thank you for welcoming me into your group, for your friendship and for encouraging me throughout my highs and lows. I am excited to see you all become great researchers and I am grateful to have met you all. Thank you to the postdocs, Dr. Marcus, Dr. Liam, Dr. Tom, and Dr. Leila for the help you have provided me with as well.

I would like to thank Dr. Aviva Levina for training me in cell culture and Dr. Nick Proschogo for training me in mass spectrometry and the staff of the mass spectrometry facility for processing my samples.

I would like to acknowledge St. Paul's College Graduate House for providing me with a safe and supportive environment to live in while I complete my degree. To Han Lun, Ryan, Anya, Jethro, Tommy, Eva, Lauren, Vered, Raven, Charlie, Srijai, Supeli, and Fostina, thank you for encouraging me throughout this journey, listening to me practice my presentations and for accompanying me while I wrote my thesis. Thank you for being my support system away from home. To baby Idun, thank you for adding so much love and happiness to my life. You never fail to make my day better and it has been my pleasure to look after you and watch you grow up.

Most importantly, I would like to end by thanking my family in Singapore for encouraging me to further my education. Thank you for believing in me and for providing me with the emotional and financial support that has allowed me to live in Sydney and pursue my goal of becoming a scientist. I would like to thank my best friend, Shalini, for always being present and supporting me throughout my journey, even from a distance. I would like to also thank my close friends in Singapore and overseas, Clarissa, Sheetal, Nellie, Ru Hui, and Amos for all the support you have provided me with throughout the years.

## TABLE OF CONTENTS

ABSTRACT.....	i
ACKNOWLEDGEMENTS .....	ii
LIST OF APPENDICES.....	viii
LIST OF ABBREVIATIONS.....	x
CHAPTER 1: INTRODUCTION.....	
1.1 Overview of cancer .....	1
1.2 Platinum(II) anticancer drugs .....	1
1.2.1 Cisplatin .....	1
1.2.2 Mechanism of action of cisplatin .....	2
1.2.3 Limitations of cisplatin .....	3
1.2.4 Carboplatin.....	4
1.2.5 Oxaliplatin.....	5
1.3 Platinum(IV) drugs .....	5
1.4 Targeted delivery .....	6
1.4.1 Targeted drug delivery .....	6
1.4.2 Warburg effect .....	7
1.5 Glutamine targeting in cancers .....	7
1.5.1 Glutamine.....	7
1.5.2 Glutamine metabolism in cancers .....	8
1.5.3 Glutamine transporters.....	9
1.5.4 Mechanism of ASCT2 .....	9
1.5.5 Targeting ASCT2 for anticancer therapy .....	11
1.6 Objectives of project.....	11
CHAPTER 2: THE SYNTHESIS OF PLATINUM(II) PRECURSORS .....	
2.1. Introduction.....	13
2.1.1. Synthesis of <i>trans</i> -bis(amino acid)platinum(II) complexes.....	13
2.1.2. Synthesis of <i>cis</i> -platinum(II) complexes .....	13
2.2 Materials and Instrumentation .....	13
2.2.1 Infrared spectroscopy (IR) .....	13
2.2.2 <sup>1</sup> H NMR spectroscopy .....	14
2.2.3 Mass spectrometry .....	14
2.3 Synthesis of <i>trans</i> -platinum complexes from K <sub>2</sub> PtCl <sub>4</sub> .....	14
2.3.1 Synthesis of <i>trans</i> -[Pt(β-alanine) <sub>2</sub> ] .....	14
2.3.2 Synthesis of <i>trans</i> -[Pt(L-alanine) <sub>2</sub> ] .....	15
2.3.3 Synthesis of <i>trans</i> -[Pt(glycine) <sub>2</sub> (OH)(CH <sub>3</sub> COO <sup>-</sup> )] .....	15
2.3.4 Synthesis of <i>trans</i> -[Pt(glycine) <sub>2</sub> (OH) <sub>2</sub> ].....	16
2.3.5 Synthesis of <i>trans</i> -[Pt(glycine) <sub>2</sub> (succinate) <sub>2</sub> ].....	16
2.4 Synthesis of platinum(II) complexes from <i>cis</i> -[PtCl <sub>2</sub> (DMSO) <sub>2</sub> ].....	17
2.4.1 Synthesis of <i>cis</i> -[PtCl <sub>2</sub> (DMSO) <sub>2</sub> ] .....	17

2.4.2	Synthesis of <i>cis</i> -[Pt(L- tryptophan) <sub>2</sub> ] .....	17
2.4.3	Synthesis of <i>cis</i> -[Pt(L-isoleucine) <sub>2</sub> ] .....	17
2.4.4	Synthesis of <i>cis</i> -[Pt(L-alanine) <sub>2</sub> ] in 1-butanol .....	18
2.4.5	Synthesis of <i>cis</i> -[Pt(L-alanine) <sub>2</sub> ] in methanol .....	20
2.4.6	Synthesis of <i>cis</i> -[Pt(L-alanine) <sub>2</sub> ] in acetone .....	21
2.5	Cytotoxicity studies .....	22
2.5.1	Materials .....	22
2.5.2	Cell passaging .....	22
2.5.3	Isolation of cells .....	22
2.5.4	Dosing A549 cells with platinum .....	23
2.5.5	MTT Assay .....	23
2.5.6	Data analysis .....	23
2.6	Results and Discussion .....	24
2.6.1	Platinum(IV)-glutamine complex synthesis .....	24
2.6.2	Platinum(II) complex design.....	24
2.6.3	Synthesis of <i>trans</i> -platinum(II) complexes.....	25
2.6.4	Cytotoxicity studies of <i>trans</i> -[Pt(L-alanine) <sub>2</sub> ] .....	26
2.6.5	Synthesis of <i>trans</i> -platinum(IV) complexes .....	27
2.6.6	Challenges encountered during the synthesis of <i>trans</i> -platinum(IV) complexes ...	27
2.7	Synthesis of <i>cis</i> -platinum(II) complexes .....	28
2.7.1	Synthesis of <i>cis</i> -[Pt(L-tryptophan) <sub>2</sub> ] .....	29
2.7.2	Synthesis of <i>cis</i> -[Pt(L-isoleucine) <sub>2</sub> ] .....	30
2.7.3	Synthesis of <i>cis</i> -[Pt(L-alanine) <sub>2</sub> ] in 1-butanol .....	31
2.7.4	Synthesis of <i>cis</i> -[Pt(L-alanine) <sub>2</sub> ] in methanol.....	33
2.7.5	Synthesis of <i>cis</i> -[Pt(L-alanine) <sub>2</sub> ] in acetone .....	35
2.8	Reaction conditions for optimal synthesis of <i>cis</i> -[Pt(L-alanine) <sub>2</sub> ].....	36
2.9	Conclusion .....	36
<b>CHAPTER 3: TRANSPORT OF MODIFIED GLUTAMINE COMPLEXES VIA ASCT2 .....</b>		
3.1	Introduction .....	38
3.1.1	Mechanism of amino acid transport of ASCT2 .....	38
	Figure 3.1: Mechanism of amino acid transport of ASCT2.....	38
3.1.2	Compound 1 .....	39
3.1.3	Compound 2 (L-theanine).....	39
3.2	Methods and Materials.....	39
3.2.1	Harvesting of <i>Xenopus laevis</i> oocytes .....	39
3.2.2	Production of human ASCT2 RNA .....	40
3.2.3	Oocytes microinjection .....	40
3.2.4	Electrophysiology studies .....	40
3.2.5	Substrate dose-response relationship .....	41
3.3	Results.....	41
3.3.1	Substrate dose-response curve .....	41
3.3.2	Compound 1 transport studies .....	43
3.3.3	L-theanine transport studies .....	45
3.4	Discussion.....	46
3.5	Conclusion .....	49

<i>CHAPTER 4: SUMMARY OF PROJECT</i> .....	
4.1 Summary of project.....	50
4.2 Future work.....	52
<i>REFERENCES</i> .....	53
<i>APPENDICES</i> .....	62



## LIST OF FIGURES AND TABLE

Figure 1.1:	Structure of cisplatin	1
Figure 1.2:	Mechanism of action of cisplatin.	2
Figure 1.3:	Structure of carboplatin.	5
Figure 1.4:	Structure of oxaliplatin.	5
Figure 1.5:	Structural model of ASCT2.	10
Figure 1.6:	Proposed design of platinum(IV)-glutamine complexes.	12
Figure 2.1:	Proposed synthetic pathway of platinum(IV)-glutamine complexes.	24
Figure 2.2:	Amino acids at neutral pH.	25
Figure 2.3:	Synthetic scheme of <i>trans</i> -[Pt(L-alanine) <sub>2</sub> ].	26
Figure 2.4:	Cytotoxicity studies of <i>trans</i> -[Pt(L-alanine) <sub>2</sub> ] in A549 cells using MTT assay (72 hours).	26
Figure 2.5.	Formation of geometric isomers during oxidation and subsequent linker attachment of <i>trans</i> -platinum(IV) complexes.	28
Figure 2.6.	Hypothesised synthetic pathway of <i>cis</i> -bis(amino acid)platinum(II) complexes using <i>cis</i> -[PtCl <sub>2</sub> (DMSO) <sub>2</sub> ] as a starting material.	28
Figure 2.7:	Amino acids that were investigated to synthesise <i>cis</i> - bis(amino acid)platinum(II) complexes.	29
Figure 2.8:	Intermediates of <i>cis</i> -[Pt(L-isoleucine) <sub>2</sub> ] synthesis.	31
Figure 2.9:	Intermediates of <i>cis</i> -[Pt(L-alanine) <sub>2</sub> ] synthesis.	32
Figure 2.10:	Structure of L-alaninate.	33
Figure 2.11:	Structure of [Pt(L-alanine) <sub>3</sub> ] <sup>-</sup>	34
Figure 3.1:	Mechanism of amino acid transport of ASCT2.	38
Figure 3.2:	Structure of Compound 1	39
Figure 3.3	Structure of L-theanine, and analogue of L-glutamine	39
Figure 3.4	Dose-response relationship of known substrates.	42
Figure 3.5:	Current-voltage relationship elicited by L-glutamine.	43
Figure 3.6:	Transport of compound 1 in oocytes expressing hASCT2 clamped at -30 mV in NO <sub>3</sub> <sup>-</sup> buffer.	44
Figure 3.7:	Transport of theanine in oocytes expressing hASCT2 clamped at -30 mV in NO <sub>3</sub> <sup>-</sup> buffer.	46
Table 3.1:	Predicted substrate Km and I <sub>max</sub> values and ± SEM at +60 mV	43

## LIST OF APPENDICES

Appendix 1:	IR spectrum of <i>trans</i> -[Pt(L-alanine) <sub>2</sub> ].	62
Appendix 2:	<sup>1</sup> H NMR spectrum of <i>trans</i> -[Pt(L-alanine) <sub>2</sub> ].	62
Appendix 3:	IR spectrum of <i>trans</i> -[Pt(glycine) <sub>2</sub> ].	63
Appendix 4:	IR spectrum of <i>trans</i> -[Pt(glycine) <sub>2</sub> (OH) <sub>2</sub> ].	63
Appendix 5:	IR spectrum of <i>cis</i> -[PtCl <sub>2</sub> (DMSO) <sub>2</sub> ].	64
Appendix 6:	Mass spectrometry ESI (+) and (-) analysis of oil (2.4.3 Synthesis of <i>cis</i> -[Pt(L-isoleucine) <sub>2</sub> ])	65
Appendix 7:	Mass spectrometry ESI (-) analysis of solid. (2.4.3 Synthesis of <i>cis</i> -[Pt(L-isoleucine) <sub>2</sub> ])	66
Appendix 8:	Mass spectrometry ESI (-) analysis of solution fraction. (2.4.3 Synthesis of <i>cis</i> -[Pt(L-isoleucine) <sub>2</sub> ])	67
Appendix 9:	Mass spectrometry ESI (-) analysis of precipitate. (2.4.3 Synthesis of <i>cis</i> -[Pt(L-isoleucine) <sub>2</sub> ])	68
Appendix 10:	Mass spectrometry ESI (-) analysis of oil. (2.4.4 Synthesis of <i>cis</i> -[Pt(L-alanine) <sub>2</sub> ] in 1-butanol)	69
Appendix 11:	Mass spectrometry ESI (+) and (-) analysis of precipitate. (2.4.4 Synthesis of <i>cis</i> -[Pt(L-alanine) <sub>2</sub> ] in 1-butanol)	70
Appendix 12:	IR spectrum of L-alanine.	71
Appendix 13:	Mass spectrometry ESI (-) analysis of crystals. (2.4.4 Synthesis of <i>cis</i> -[Pt(L-alanine) <sub>2</sub> ] in 1-butanol)	72
Appendix 14:	<sup>1</sup> H NMR spectrum of crystals. (2.4.4 Synthesis of <i>cis</i> -[Pt(L-alanine) <sub>2</sub> ] in 1-butanol)	73
Appendix 15:	<sup>1</sup> H NMR spectrum of L-alanine.	73
Appendix 16:	Mass spectrometry ESI (+) and (-) analysis of solid. (2.4.4 Synthesis of <i>cis</i> -[Pt(L-alanine) <sub>2</sub> ] in 1-butanol)	74
Appendix 17:	Mass spectrometry ESI (-) analysis of solid. (2.4.5 Synthesis of <i>cis</i> -[Pt(L-alanine) <sub>2</sub> ] in methanol)	75
Appendix 18:	Mass spectrometry ESI (+) and (-) analysis of crystals. (2.4.5 Synthesis of <i>cis</i> -[Pt(L-alanine) <sub>2</sub> ] in methanol)	76,77
Appendix 19:	<sup>1</sup> H NMR spectrum of crystals. (2.4.5 Synthesis of <i>cis</i> -[Pt(L-alanine) <sub>2</sub> ] in methanol)	78
Appendix 20:	Mass spectrometry ESI (+) and (-) analysis of solid.	79

	(2.4.5 Synthesis of <i>cis</i> -[Pt(L-alanine) <sub>2</sub> in methanol)	
Appendix 21:	<sup>1</sup> H NMR spectrum of solid.	80
	(2.4.5 Synthesis of <i>cis</i> -[Pt(L-alanine) <sub>2</sub> in methanol)	
Appendix 22	<sup>1</sup> H NMR spectrum of [Pt(L-alanine) <sub>3</sub> ] <sup>-</sup>	80
	(2.4.5 Synthesis of <i>cis</i> -[Pt(L-alanine) <sub>2</sub> in methanol)	
Appendix 23:	<sup>1</sup> H NMR spectrum of solid.	80
	(2.4.6 Synthesis of <i>cis</i> -[Pt(L-alanine) <sub>2</sub> ] in acetone)	
Appendix 24:	Mass spectrometry ESI (+) and (-) analysis of solid.	81
	(2.4.6 Synthesis of <i>cis</i> -[Pt(L-alanine) <sub>2</sub> ] in acetone)	

## LIST OF ABBREVIATIONS

$\mu\text{L}$	Microliter
%	Percent
$^{\circ}\text{C}$	Degree Celsius
$^1\text{H}$ NMR spectroscopy	Proton Nuclear Magnetic Resonance Spectroscopy
A549	Human Lung Adenocarcinoma cell line
ASCT	Alanine Serine Cysteine transporter
ATP	Adenosine Triphosphate
$\text{Br}^-$	Bromide
$\text{Ca}(\text{NO}_3)_2$	Calcium nitrate
$\text{CaCl}_2$	Calcium chloride
Carboplatin	diammine(1,1-cyclobutanedicarboxylato)platinum(II)
cDNA	Circular DNA
<i>cis</i> -[PtCl <sub>2</sub> (DMSO) <sub>2</sub> ]	<i>cis</i> -Dichlorobis(dimethylsulfoxido)platinum(II)
Cisplatin	<i>cis</i> -diamminedichloroplatinum(II)
$\text{Cl}^-$	Chloride
Cm	Centimetre
CTR1	Copper transporter 1
D <sub>2</sub> O	Deuterium oxide
DMA	<i>N,N</i> -Dimethylacetamide
DMEM	Advanced Dulbecco's modified Eagle's medium
DMF	Dimethylformamide
DMSO	Dimethyl sulfoxide
DNA	Deoxyribonucleic acid
ESI	Electrospray Ionisation
FDA	Food and Drug Administration
GLUT1	Glucose transporter 1
GOT	Glutamic-oxaloacetic transaminase
GPNA	L- $\gamma$ -Glutamyl-p-nitroanilide
GPT	Glutamic-pyruvate transaminase
H <sub>2</sub> O	Water
H <sub>2</sub> O <sub>2</sub>	Hydrogen peroxide

HeLa	Henrietta Lacks
HEPES	N-2-hydroxyethylpiperazine-N-2-ethane sulfonic acid
HepG2	Hepatoblastoma cell line
HP	Helical hairpins
HPLC	High-performance liquid chromatography
HAS	Human serum albumin
Hz	Hertz
I <sup>-</sup>	Iodide
IR	Infrared spectroscopy
IV	Current-voltage
K <sub>2</sub> PtCl <sub>4</sub>	Potassium tetrachloroplatinate(II)
KCl	Potassium chloride
KI	Potassium iodide
KNO <sub>3</sub> ,	Potassium nitrate
<i>m/z</i>	Mass-to-charge ratio
Mg	Milligram
Mg(NO <sub>3</sub> ) <sub>2</sub>	Magnesium nitrate
MgCl <sub>2</sub>	Magnesium chloride
mL	Millilitre
mM	Millimolar
mmol/L	Millimoles per litre
mol	Mole
mRNA	Messenger RNA
MTT	Triazolyl blue tetrazolium bromide
Na <sup>+</sup>	Sodium ion
NaCl	Sodium chloride
NaNO <sub>3</sub>	Sodium nitrate
NaOH	Sodium hydroxide
NEAA	Non-essential amino acids
Nm	Nanometre
NO <sub>3</sub> <sup>-</sup>	Nitrate
Oxaliplatin	<i>cis</i> -oxalato-( <i>trans</i> -l)-1,2-diaminocyclohexaneplatinum(II)
PBS	Phosphate Buffered Saline

pH	Potential of Hydrogen
Ppm	Parts per million
PSAT1	Phosphoserine aminotransferase 1
ROS	Reactive oxygen species
SEM	Standard error of the mean
SLC	Solute carrier
TCA	Tricarboxylic acid

# *CHAPTER 1: INTRODUCTION*

## 1.1 Overview of cancer

Cancer is a global health issue that affects people regardless of nationality, culture, and socioeconomic strata<sup>1</sup>. It is an umbrella term used to describe a wide range of malignant tumours that can affect any organ and tissue in the body<sup>2</sup>. It encompasses over 100 distinct types of cancers<sup>3</sup> which all stem from the uncontrolled proliferation of cells<sup>4</sup>. Although each cancer type has its unique features, they share common characteristics. This includes their origin from normal cells<sup>5</sup>, loss of differentiation<sup>6</sup>, and their ability to metastasise to other sites of the body<sup>7</sup>. The burden of cancer is rapidly growing worldwide<sup>8</sup>. It is predicted that global cancer rates will increase by 47% from 2020 to 2040 to reach 28.4 million cases per annum<sup>1</sup>.

## 1.2 Platinum(II) anticancer drugs

### 1.2.1 Cisplatin

Cisplatin (Figure 1.1) is a neutral, square-planar platinum(II) drug<sup>9</sup> with a  $d^8$  electronic configuration, which has had a major impact on cancer treatments<sup>10</sup>. It was first approved by the Food and Drug Administration (FDA) in 1978 for the treatment of testicular cancer<sup>11</sup>. Since then, cure rates for testicular cancer which was a previously lethal disease have exceeded 95%<sup>12</sup>. Cisplatin is also used to treat solid cancers<sup>13</sup> including ovarian, bladder, lung<sup>14</sup>, and head and neck cancers<sup>15</sup>. Cisplatin is administered intravenously into patients<sup>12</sup> as a sterile saline solution<sup>16</sup>. In the bloodstream, cisplatin is believed to primarily exist in its neutral, intact form<sup>17</sup>. This is as chloride concentration is relatively high in the bloodstream (100 mM)<sup>15,18</sup> which reduces the extent to which the chloride ligands on cisplatin are displaced<sup>15,19</sup>. However, cisplatin is vulnerable to cysteine<sup>20, 21</sup> and proteins present in blood plasma, particularly ones containing thiol groups such as human serum albumin (HSA)<sup>22</sup>. These molecules irreversibly bind<sup>23</sup> to 69% to 98% of the cisplatin administered, leading to an inactivation of a large amount of the administered drug<sup>17</sup>. This occurrence has been blamed for some of the severe side effects of cisplatin treatment<sup>22,23</sup> and cisplatin resistance<sup>17</sup>.

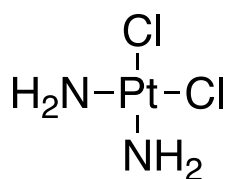


**Figure 1.1: Structure of cisplatin.**



### 1.2.2 Mechanism of action of cisplatin

Free cisplatin mainly enters cells through passive diffusion<sup>19</sup>. Alternatively, it has been suggested that cisplatin can enter cells via active transport through copper transporters (CTR1)<sup>19,24,25</sup>. The intracellular concentration of chloride is relatively low, between 4 to 20 mM, which facilitates the aquation of cisplatin<sup>22</sup> in which the chloro-ligands are replaced by water<sup>26,27</sup>. This leads to the formation of reactive cationic mono-aqua species – *cis*-[PtCl(NH<sub>3</sub>)<sub>2</sub>(H<sub>2</sub>O)]<sup>+</sup><sup>28</sup> or diaqua species [Pt(NH<sub>3</sub>)<sub>2</sub>(H<sub>2</sub>O)<sub>2</sub>]<sup>2+</sup><sup>29</sup> that cannot readily leave the cell<sup>22</sup>. These cationic species can then exert their cytotoxicity by forming DNA adducts, with the most common adduct being at the N7 position of the imidazole ring of two adjacent guanines<sup>30</sup>. Several types of DNA adduct can be formed including interstrand crosslinks, intrastrand crosslinks, and monofunctional adducts<sup>11</sup>. These adducts distort the helical structure of DNA and inhibit DNA transcription which leads to cellular apoptosis<sup>31</sup> (Figure 1.2). However, it has been reported that only 1 to 10% of intracellular cisplatin might eventually enter the nucleus to react with DNA resulting in cell cycle arrest and apoptosis<sup>26</sup>.

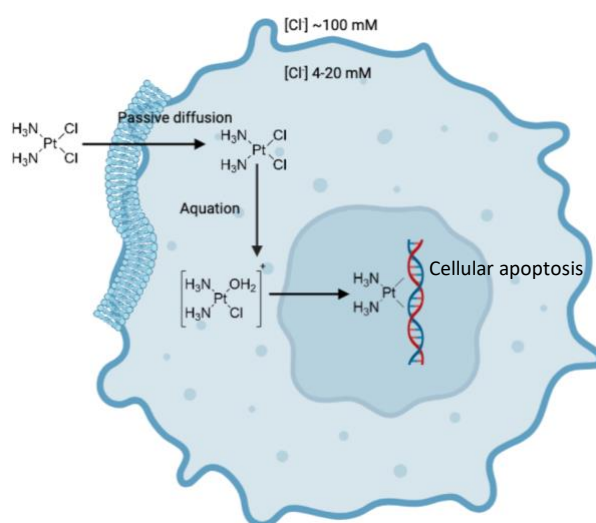


**Figure 1.2: Mechanism of action of cisplatin.** Cisplatin mainly enters cells through passive diffusion<sup>19</sup> where its chloro-ligands are displaced by water<sup>27,28</sup>. The reactive cationic mono-aqua species form adducts in the DNA which leads to cellular apoptosis<sup>26</sup>. The figure was created using BioRender.com.

### **1.2.3 Limitations of cisplatin**

Administration of cisplatin is strictly controlled<sup>6</sup> as it is a highly toxic drug<sup>32</sup>. Limited doses are given to patients with typically 100 mg/day of cisplatin being given on five consecutive days<sup>33,34</sup>. Cisplatin induces the most severe nausea and vomiting of any chemotherapeutic agent<sup>35</sup> which is also the most common side effect of cisplatin<sup>6</sup>. Some patients experience acute emesis within hours of cisplatin administration<sup>36</sup> or delayed emesis which usually peaks around 48 to 72 hours later and may last up to 7 days<sup>37,38</sup>. Female patients over the age of 50 were found to have an increased risk of emesis<sup>39</sup>. This side effect can be reduced by administering prophylactic antiemetics together with corticosteroids<sup>6</sup>. Antiemetic medications such as lorazepam<sup>40</sup> have been shown to reduce the incidence of vomiting substantially. However, it is predicted that approximately 30% to 60% of patients still experience either acute or delayed nausea after the administration of cisplatin<sup>37</sup>.

Nephrotoxicity is a major side effect of cisplatin<sup>6</sup> which develops in patients within 10 days of administration<sup>41</sup>. Kidneys are vulnerable to damage as they accumulate cisplatin in higher levels, as they serve as the major route of drug excretion<sup>42</sup>. Cisplatin-induced nephrotoxicity manifests as acute tubular necrosis<sup>43,44</sup> which is evidenced by a reduction in glomerular function, increased serum creatinine<sup>41</sup>, and lower levels of magnesium and potassium<sup>42</sup>. Hydration protocols involving the coadministration of cisplatin with sodium chloride (NaCl)<sup>45</sup> or mannitol diuresis<sup>40</sup> were developed to reduce nephrotoxicity by reducing the contact time of cisplatin and renal tubes<sup>46</sup>. However, even with careful hydration, approximately one-third of patients still show evidence of kidney damage after cisplatin treatment<sup>45</sup>.

Neurotoxicity is the most serious side effect of cisplatin which mostly affects the peripheral sensory nerves<sup>47</sup>. Peripheral neuropathy develops in approximately 50% of patients<sup>48</sup> and is the most important dose-limiting problem associated with cisplatin<sup>49</sup>. Once developed, there is no effective therapy and treatment is directed towards managing pain over cure<sup>50</sup>. Signs of neurotoxicity involve the upper and lower extremities and include loss of vibration sense, tingling, paraesthesia<sup>50</sup>, weakness, tremor, and loss of taste<sup>51,52</sup>.

Cancer cells can develop drug resistance which has a significant impact on chemotherapy success<sup>12,53</sup>. Several tumours are intrinsically resistant to cisplatin such as colon, non-small cell lung cancer, and renal cancer<sup>54</sup>. Other tumours such as ovarian and small-cell lung cancer<sup>22</sup> can acquire resistance after repeated exposure. Development of cisplatin resistance occurs

frequently and is linked to multiple mechanisms<sup>55</sup>. One primary mechanism is the reduced uptake and accumulation of cisplatin in cancer cells. Some studies have found that cisplatin-resistant cell lines have rigid cell membranes with high sphingomyelin and cholesterol content and have a higher degree of fatty acid saturation<sup>56</sup>. These arrangements make the cell membrane more viscous which reduces drug penetration into cells by passive diffusion<sup>57</sup>. Copper transporter 1 (CTR1)-deficient cells are also cisplatin-resistant<sup>55, 56, 58</sup>. Studies have revealed that copper transporters undergo rapid cytoplasmic internalisation after cisplatin exposure. This reduces the expression of surface transporters, further limiting cisplatin uptake<sup>55</sup>.

Efforts have been directed towards developing new platinum-based anticancer drugs with improved clinical effectiveness and reduced toxicity. Around 3000 derivatives of platinum anticancer drugs have been synthesised and tested in cancer cells<sup>12</sup>. Only 22 of these drugs have advanced to clinical trials<sup>15,59</sup> as most of them have been discontinued due to severe and/or unpredictable side effects<sup>12</sup>, lack of activity in phase II/III trials, or economic reasons<sup>15,60</sup>. Currently, only the derivatives of cisplatin – carboplatin and oxaliplatin have received approval for worldwide use. An additional three derivatives – nedaplatin, lobaplatin, and heptaplatin<sup>13</sup> have been approved for use in Japan, China, and South Korea respectively<sup>60</sup>.

#### **1.2.4 Carboplatin**

Carboplatin (Figure 1.3) was introduced to clinics in the 1980s and is used to treat cancers including, ovarian cancers, small-cell carcinoma, and epidermoid carcinoma of the head and neck<sup>60</sup>. It was designed as a less toxic analogue of cisplatin which still retains its anticancer activity<sup>20</sup>. Upon administration, carboplatin enters cells and undergoes aquation to form the reactive cationic diaqua species  $[\text{Pt}(\text{NH}_3)_2(\text{H}_2\text{O})_2]^{2+}$ , identical to cisplatin metabolites<sup>61</sup>. DNA adducts formed by carboplatin are essentially the same as those formed by cisplatin<sup>20</sup> but are less toxic<sup>12</sup> as its bidentate dicarboxylate ligand undergoes slower displacement compared to the labile chloride ligands of cisplatin<sup>12,26</sup>. This allows a much higher dose of up to 2000 mg/dose to be administered<sup>34,35</sup>. However, patients can still experience side effects such as myelosuppression, clinically manifested as severe thrombocytopenia, neutropenia, and leukopenia which requires monitoring of blood parameters<sup>12</sup>.

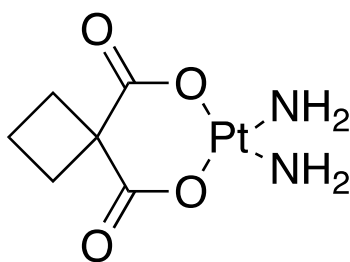


**Figure 1.3: Structure of carboplatin.**

### 1.2.5 Oxaliplatin

Oxaliplatin (Figure 1.4) was designed to overcome the limitations of drug resistance observed in cisplatin<sup>20</sup>. It was first introduced to clinics in 1996<sup>62</sup> and has been proven to be effective in the treatment of some cisplatin-resistant cancers<sup>63</sup>. It is the first platinum anticancer drug to show strong cytotoxic activity and an improved therapeutic index in colon cancer. It is also used in the treatment of other cancers including breast, glioblastoma, and non-small cell lung cancers<sup>12</sup>. Oxaliplatin has a similar mechanism to cisplatin where it causes cellular apoptosis through the formation of DNA-platinum adducts. *In vitro* studies have found that oxaliplatin produces qualitatively similar DNA-Pt adducts as cisplatin with predominantly intrastrand crosslinks (GG>AG)<sup>64</sup>. At equal concentrations, oxaliplatin forms fewer<sup>63,65</sup> but bulkier and more hydrophobic adducts which are more effective in inhibiting DNA synthesis compared to cisplatin adducts<sup>66</sup>. However, oxaliplatin still has dose-limiting side effects such as significant neurotoxicity and tubular necrosis<sup>12</sup>.

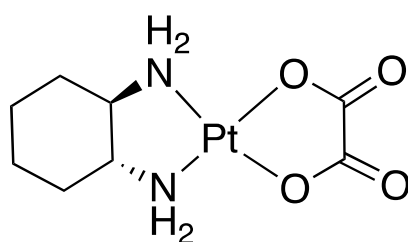


**Figure 1.4: Structure of oxaliplatin.**

### 1.3 Platinum(IV) drugs

During the discovery of cisplatin, the potential anticancer effects of platinum(IV) complexes, *cis*-[PtCl<sub>4</sub>(NH<sub>3</sub>)<sub>2</sub>] and [PtCl<sub>4</sub>(ethane-1,2-diamine)], were studied but paused due to the success of cisplatin<sup>67</sup>. The clinical value of platinum(IV) complexes has been recognised again by researchers in recent decades<sup>66,68</sup>. These complexes are usually prepared by the chemical

oxidation of active square-planar platinum(II) complexes, which have oxidation state of +2. This causes the platinum centre to lose 2 electrons, resulting in two additional axial ligands to be added to the platinum core<sup>68</sup>. Platinum(IV) complexes consist of a central platinum atom<sup>69</sup> in a kinetically inert  $d^6$  electronic configuration and a six-coordinate octahedral geometry<sup>70</sup>. Their inert structure makes them more resistant to substitution in blood<sup>71,72</sup> and less likely to interact with plasma proteins<sup>73</sup>. This reduces the loss of the active drug, preventing side reactions that cause toxic side effects<sup>72</sup>. The improved stability of platinum(IV) complexes may allow them to be administered to patients orally<sup>74,75</sup>. Axial ligands can be modified to enhance the biological profile of platinum(IV) complexes as desired<sup>60</sup>. In cells, platinum(IV) complexes are activated by biological reducing agents such as ascorbic acid, cysteine, glutathione, and other macromolecules<sup>69</sup>. They then lose their axial groups to form their pharmacologically active platinum(II) derivative<sup>72,75</sup>. The resulting platinum(II) complex undergoes hydrolysis and is activated into reactive cationic species. These species then form DNA adducts which lead to cellular apoptosis<sup>76</sup>. Platinum(IV) complexes are referred to as prodrugs as they must undergo biotransformation in vivo before they can exert their pharmacological effects<sup>77</sup>.

## **1.4 Targeted delivery**

### **1.4.1 Targeted drug delivery**

Targeted drug delivery is a concept first postulated by Paul Ehrlich<sup>78,79</sup> which aims to design drugs that directly reach their target site like “magic bullets”<sup>80</sup>. In cancer therapy, the goal is to design a drug that specifically targets tumours to release its toxic payload while leaving normal tissues unaffected<sup>81</sup>. This should reduce the problems caused by conventional chemotherapy such as damage to normal tissues and the development of drug resistance. Targeted drug delivery can work either by active or passive targeting of cancer cells. Some tumours display distinctive characteristics such as increased permeability and retention<sup>82</sup>. Passive targeting takes advantage of these characteristics inherent to tumours for targeted delivery<sup>83</sup>. Cancer cells are also known to specifically express or overexpress certain receptors. This can be exploited for drug delivery through active targeting of cancer cells<sup>84</sup>. In recent years, there has been interest in developing platinum(IV) complexes that specifically deliver their cytotoxic effects to cancer cells<sup>85,86</sup>. Axial ligands of the complexes can be modified for targeted delivery<sup>87</sup>. The platinum pharmacophore can be conjugated to a targeting group which may increase its selectivity to cancer cells<sup>88</sup>. Bioactive substances such as peptides, hormones, and carbohydrates are often used to fulfil the targeting function.

### **1.4.2 Warburg effect**

In the 1920s, Otto Warburg and his colleagues observed a significant increased uptake of glucose in tumours compared to the healthy tissue surrounding them. They also observed that glucose was fermented to produce lactate even in oxygen-rich conditions. Through these observations, they concluded that cancer cells must be deprived of glucose and oxygen to undergo cell death<sup>89, 90</sup>. Warburg hypothesised that mitochondrial dysfunction had disrupted the oxidative phosphorylation pathway, causing cells to switch to aerobic glycolysis, an event he regarded as “the origin of cancer” that has since been disproven<sup>91</sup>. Aerobic glycolysis only yields 2 molecules of ATP per molecule of glucose, whereas oxidative phosphorylation yields 36 molecules<sup>92</sup>. As aerobic glycolysis is less efficient in generating ATP, it is significantly upregulated in cancers<sup>93,94</sup>. Metabolic differences in cancer and normal tissues can be used as a biochemical basis for developing therapeutic strategies that specifically target cancer cells. A wide range of cancers show increased expression of glucose transporters (GLUTs) on their cell membranes<sup>95,96</sup>. GLUT1 is commonly overexpressed in several cancers including hepatic, pancreatic, breast, ovarian and lung cancers<sup>97</sup>. Several studies have also found a close relationship between the overexpression of GLUT1 transporters and an unfavourable prognosis of many cancers<sup>98</sup>. These observations by Warburg and colleagues have had a profound influence on our understanding of cancer biology, clinical diagnosis, and cancer treatment<sup>99,100</sup>.

## **1.5 Glutamine targeting in cancers**

### **1.5.1 Glutamine**

Glutamine is the most abundant amino acid in the body with 0.6 to 0.9 mmol/L concentration circulating in the bloodstream<sup>101,102</sup>. It comprises approximately 20% of the total circulating free amino acid in the body<sup>103</sup>, making it a non-essential amino acid<sup>100</sup>. Glutamine is primarily obtained from the diet<sup>103</sup> but is also synthesised in many organs, predominately the skeletal muscles<sup>104,105</sup>. During times of catabolic stress such as healing of surgical, traumatic, and burn wounds, the body consumes glutamine at large rates that exceed maximal glutamine production<sup>106</sup>. It is also suggested that glutamine consumption increases during cancer<sup>105,107</sup>. Cancers often display increased demands for certain nutrients to support their rapid proliferation<sup>108</sup> which is one of the hallmarks of cancers<sup>107</sup>. In these cases, glutamine becomes a conditionally essential amino acid<sup>105,109</sup>. Some cancers experience “glutamine addiction”<sup>110</sup> and can undergo cell death without an exogenous supply of glutamine<sup>111,112</sup>. Glutamine is a major carbon source that replenishes intermediates of the tricarboxylic acid (TCA) cycle<sup>111,113</sup>

as it can undergo glutaminolysis. Glutaminolysis involves the conversion of glutamine to glutamate which maintains TCA cycle ATP, and NADPH production<sup>114</sup>. It is also a nitrogen source for the synthesis of nucleotides, amino acids and hexosamines<sup>115</sup>. The importance of glutamine in cancers was first discovered by Eagle who found that HeLa cells consumed 10 to 100 times more glutamine compared to other amino acids<sup>113</sup>.

### **1.5.2 Glutamine metabolism in cancers**

Glutamine is essential for anaplerosis which refers to the replenishment of TCA cycle intermediates<sup>116,117</sup>. Cancers rely on glutamine metabolism for anaplerosis as the function of the TCA cycle is downregulated in cancers due to the Warburg effect. Free glutamine enters cells via glutamine transporters<sup>108</sup>. In the cell cytoplasm, it undergoes glutaminolysis via glutaminase enzymes and is converted to glutamate. Glutamate then enters the mitochondria where it is converted to alpha-ketoglutarate by glutamate dehydrogenase. Alpha-ketoglutarate enters the TCA cycle where it is primarily converted to isocitrate and subsequently to citrate. A considerable portion of citrate is exported to the cytoplasm where it is converted to acetyl-CoA for lipid biosynthesis<sup>92, 108</sup>. Malate also leaves the TCA cycle to form pyruvate via malic enzymes<sup>111</sup>. Additionally, malic enzymes can form acetyl-CoA, contributing to the TCA cycle<sup>118</sup>. This reaction produced NADPH which is essential for fatty acid synthesis<sup>92</sup> and nucleotide biosynthesis<sup>119</sup>.

Glutamine is also an important source of nitrogen. It can donate its amino and amide nitrogens for the synthesis of purine and pyrimidine nucleotides needed for RNA/DNA synthesis. This synthesis supports the rapid growth and proliferation of cancer cells<sup>120</sup>. Increased glycine levels lead to an increase in glutathione, an essential antioxidant<sup>121</sup>, to drive many biosynthetic pathways, including the synthesis of nucleotides and non-essential amino acids (NEAA)<sup>116,122</sup>. Glutamine is involved in the *de novo* synthesis of nucleotides essential for cellular proliferation<sup>122,123</sup>. Glutamine-derived glutamate can also be catalysed by aminotransferases, GPT, GOT, and PSAT1 to produce alpha-ketoglutarate and different amino acids, alanine, aspartate, and phosphoserine respectively. These enzymes are upregulated in cancers and have been shown to reduce cell proliferation when inhibited. Phosphoserine is essential for cancer survival as it is converted to serine and subsequently to glycine. Serine catabolism which produces glycine generates a large pool of one-carbon units (1C)<sup>124</sup>, essential for nucleotide biosynthesis.

Glutamine-derived glutamate can be exchanged for cysteine, a glutathione precursor, via the SLC7A11 transporter<sup>108</sup>. Cancers are exposed to high levels of reactive oxygen species (ROS) generated by the mitochondrial electron transport chain during disease progression. In excess, ROS can damage DNA and other cellular components<sup>116</sup>. Glutathione is an endogenous antioxidant that lowers ROS levels and allows cells to resist oxidative stress, preventing their death<sup>121</sup>. Increased glutathione levels have also been shown to increase resistance to chemotherapy in many cancer types<sup>125</sup>.

### **1.5.3 Glutamine transporters**

As glutamine is hydrophilic and water-soluble, it cannot diffuse into cells across the plasma membrane without the aid of specific transporters<sup>126</sup>. 14 transporters that accept glutamine as a substrate have been identified in mammalian cells<sup>127</sup>. These transporters belong to four distinct gene families, Solute Carrier (SLC) 1, SLC6, SLC7, and SLC38. None of these transporters are exclusively selective for glutamine and can transport different types of amino acids. Most of these transporters mediate extracellular glutamine influx into cells, but some mediate the efflux of intracellular glutamine under normal physiological conditions<sup>128</sup>. Of these transporters, the Alanine, Serine, and Cysteine Transporter 2 (ASCT2) belonging to the SLC1 family has been receiving increasing attention for its potential role in cancer<sup>129</sup>. There has been interest in targeting ASCT2 to starve cancer cells of glutamine<sup>130</sup> as it is overexpressed in many cancer types<sup>130</sup> including triple-negative breast cancer, colon cancer, and lung cancers<sup>129</sup>.

### **1.5.4 Mechanism of ASCT2**

ASCT2 is a sodium (Na<sup>+</sup>) dependent, electroneutral, obligatory exchanger that transports neutral amino acids such as alanine, serine, cysteine, threonine, and glutamine across the cell membrane<sup>131</sup>. It sits on the plasma membrane of cells and exists as a homotrimer consisting of three identical protomers (Figure 1.5). ASCT2, like SLC1A members, uses an elevator mechanism of transport where each identical protomer is composed of a static scaffold domain and a mobile transport domain. The scaffold domain forms the trimer interface and remains embedded into the plasma membrane during transport. It also consists of two helical hairpin loops 1 and 2 (HP1 and HP2) and three transmembrane domains which contain the binding site for the substrates and coupled Na<sup>+</sup> ions<sup>132</sup>. ASCT2 is believed to function using a one-gate transport mechanism. Upon the binding of 3 Na<sup>+</sup> ions and a substrate at HP2, the transport domain moves down the lipid bilayer in an elevator-like manner and transports the substrate in



a fully occluded state. HP2 then opens at the cytoplasmic side to release the 3 Na<sup>+</sup> ions and substrate into the cell. As ASCT2 is an obligatory exchanger, this is followed by the transport of 3 Na<sup>+</sup> ions and another neutral amino acid from the intracellular face to the extracellular face. The binding of 3 Na<sup>+</sup> ions and a substrate to ASCT2 activates an uncoupled anion conductance which allows the flow of anions through the transporter, creating a charge movement across the membrane (Figure 1.6). This allows the use of electrophysiology to measure transporter activity despite ASCT2 being an electroneutral transporter. The magnitude of currents elicited varies with the type and concentration of substrate transported and the permeability of the anion present in the buffer. Increasing permeability of anions, elicits a greater magnitude of currents in decreasing order, nitrate (NO<sub>3</sub><sup>-</sup>), > iodide (I<sup>-</sup>) > bromide (Br<sup>-</sup>) > chloride (Cl<sup>-</sup>)<sup>133,134</sup>. In the absence of substrates, ASCT2 elicits a small magnitude conductance referred to as “leak anion conductance”. This occurs due to the permeability of some anions through the anion-gated channel at the resting state when Na<sup>+</sup> ions are present<sup>135</sup>.

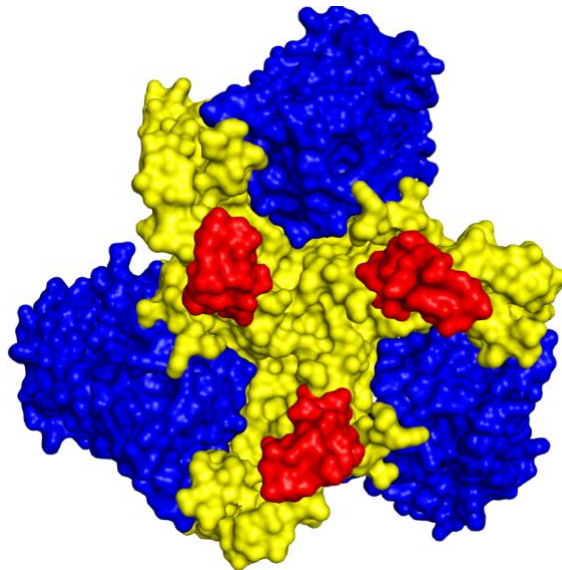


**Figure 1.5: Structural model of ASCT2.** ASCT2 exists as a trimeric structure where three identical protomers come together. Each protomer is made up of a scaffold domain (yellow), a transport domain in an inward-orientated state (blue), and a protruding loop (red) which acts as a docking area for retroviruses<sup>132</sup>. This figure was created by Dr. Lachlan Adamson and is used with permission.

### 1.5.5 Targeting ASCT2 for anticancer therapy

ASCT2 has been identified as a promising target for anticancer therapy. Studies have shown that blocking ASCT2 activity using inhibitors such as L- $\gamma$ -Glutamyl-p-nitroanilide (GPNA) and benzylserine can reduce cancer cell proliferation<sup>136</sup>. Van Geldermalsen *et al.* found that inhibiting the expression of ASCT2 significantly reduced glutamine uptake in triple-negative breast cancer lines which led to suppression of cell growth<sup>137</sup>. Additionally, a similar finding was observed by Wang *et al.* in pancreatic cells<sup>138</sup>. However, there is concern that inhibiting ASCT2 alone may not be sufficient due to the presence of SNAT1 and SNAT2, which also accept glutamine as a substrate. Broer *et al.* observed that ASCT-deficient cancer cells can display normal growth due to increased expression of SNAT1 and SNAT2<sup>139</sup>. ASCT2 may also be potentially used for the targeted delivery of anticancer drugs. A series of platinum(IV) prodrugs containing glutamine-like ligands were designed by Ravera *et al.* and their accumulation in human lung adenocarcinoma cells (A549) was investigated. A platinum(IV)-glutamine complex with glutamine linked via its  $\alpha$ -carboxylic group, was found to act as a trojan horse and enter ASCT2-overexpressing cells<sup>140</sup>.

### 1.6 Objectives of project

The aim is to synthesise biologically inert platinum(IV)-glutamine complexes and to study their transport via ASCT2. *Xenopus laevis* oocytes will be used as a model to isolate ASCT2 and conduct transport studies. First, bis(amino acid)platinum(II) complexes will be synthesised as precursors and their cytotoxicity will be determined using A549 cells. Biologically inert complexes will be used to prevent cell death to accurately study the transport of complexes into cells. The complexes will then be oxidised into their platinum(IV) state and coupled with a modified L-glutamine compound. This modified L-glutamine compound will be synthesised by attaching a 2-(2-aminoethoxy)ethanol linker at the  $\alpha$ -carboxylic acid of L-glutamine. This platinum(IV)-glutamine complex design was chosen as Ravera *et al.* investigated a platinum(IV)-glutamine complex with glutamine linked via its  $\alpha$ -carboxylic group and found that the complex enters ASCT2-overexpressing cells<sup>140</sup>. The linker was selected based on its hydrophilic property which reduces the occurrence of the platinum(IV)-glutamine complex entering cells via passive diffusion. It has also been identified that a longer linker is required to prevent the platinum from interfering with glutamine binding at its receptors<sup>141</sup>. As the platinum(IV)-glutamine complexes are being synthesised, it will be concurrently investigated if the modification of L-glutamine affects its transport via ASCT2. The modified glutamine

compound consisting of the 2-(2-aminoethoxy)ethanol linker will be applied to oocytes expressing human ASCT2 to study their transport.

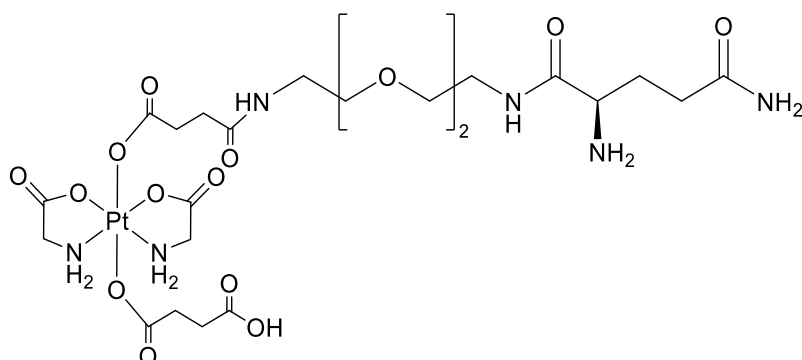


**Figure 1.6: Proposed design of platinum(IV)-glutamine complexes.** A platinum(IV) complex will be coupled with a modified L-glutamine compound which will be synthesised by attaching a 2-(2-aminoethoxy)ethanol linker at the  $\alpha$ -carboxylic acid of L-glutamine.

*CHAPTER 2: THE SYNTHESIS  
OF PLATINUM(II)  
PRECURSORS*

## 2.1. Introduction

The work described in this chapter aims to synthesise biologically inert, square-planar platinum(II) complexes consisting of a bis(amino acid)platinum core as precursors to synthesise platinum(IV)-glutamine complexes. Two amino acids were attached to the platinum core in a bidentate manner at the carboxyl and amine groups. The cytotoxicity of the platinum(II) complexes synthesised was measured using human lung adenocarcinoma cells (A549). The complexes were then oxidised into their more stable platinum(IV) state. A glutamine molecule can then be attached to the platinum(IV) complexes via a hydrophilic linker to form platinum(IV)-glutamine complexes.

### 2.1.1. Synthesis of *trans*-bis(amino acid)platinum(II) complexes

Potassium tetrachloroplatinate(II) ( $K_2PtCl_4$ ) was used as a starting material to synthesise *trans*-bis(amino acid)platinum(II) complexes. Difficulties were experienced during attempts to oxidise *trans*-[Pt(glycine)<sub>2</sub>] due to the poor solubility of these complexes in water and organic solvents. Geometric isomers were also formed at each synthesis step of *trans*-[Pt(L-alanine)<sub>2</sub>], which made purification difficult.

### 2.1.2. Synthesis of *cis*-platinum(II) complexes

To overcome these challenges, the design of the platinum(II) complexes was modified. *cis*-bis(amino acid)platinum(II) complexes that are more soluble in water and organic solvents were investigated. The use of *cis*-platinum(II) complexes should also prevent the formation of geometric isomers. *cis*-[PtCl<sub>2</sub>(DMSO)<sub>2</sub>] was explored as a starting material to synthesise these complexes. It was hypothesised that reactions of 1 mole [mol] of *cis*-[PtCl<sub>2</sub>(DMSO)<sub>2</sub>] with 2 mol of amino acid in the presence of a base would result in the synthesis of *cis*-bis(amino acid)platinum(II) complexes in high purity.

## 2.2 Materials and Instrumentation

All solvents used were purchased from Sigma-Aldrich (Merck) unless stated otherwise.

### 2.2.1 Infrared spectroscopy (IR)

All IR spectra were obtained using a Frontier FT-IR Spectrometer UATR (Perkin Elmer) over a range of 4000–400 cm<sup>-1</sup>. Data were processed using Spectrum 10™ (Version 10.5.0) (Perkin Elmer).

### 2.2.2 $^1\text{H}$ NMR spectroscopy

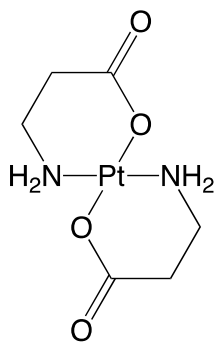
All NMR spectra were obtained using a NEO 300 MHz NMR Spectrometer (Bruker) equipped with a 5 mm multinuclear probehead ( $^{19}\text{F}$ - $^{15}\text{N}$ ) at 300 K.  $^1\text{H}$  NMR chemical shifts were internally referenced to the residual solvent peaks:  $\text{D}_2\text{O}$  ( $\delta = 4.79$ ).<sup>2</sup>  $^1\text{H}$  NMR data are reported as chemical shifts (in ppm), multiplicity, coupling constants, relative integrals, and chemical assignment. The multiplicities were reported as the following: s = singlet, d = doublet, t = triplet, q = quartet and m = multiplet. The coupling constants ( $J$ ) are reported in Hz, and denote hydrogen-hydrogen spin coupling, unless indicated by a subscript. All NMR data were processed using TopSpin® (Version 4.2.0) (Bruker).

### 2.2.3 Mass spectrometry

All mass spectrometry data were obtained using an amaZon SL mass spectrometer (Bruker). Low resolution ionisation mode (ESI) was used in both positive and negative modes. The spectrometer was connected to an Agilent 1100 HPLC with a binary pump.

## 2.3 Synthesis of *trans*-platinum complexes from $\text{K}_2\text{PtCl}_4$

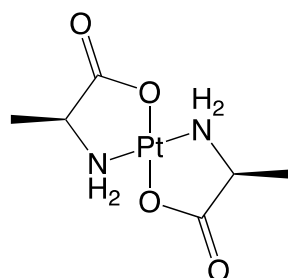
### 2.3.1 Synthesis of *trans*-[Pt( $\beta$ -alanine) $_2$ ]



$\text{K}_2\text{PtCl}_4$  (2 g, 4.82 mmol) was dissolved in 100 mL of distilled water.  $\beta$ -alanine (1 g, 11.22 mmol) was added. The reaction mixture was stirred in the dark at room temperature and a clear and bright red solution was formed. A 1 M NaOH solution was prepared by dissolving NaOH powder (0.80 g, 20 mmol) in 20 mL of distilled water. The solution (10 mL, 10 mmol) was periodically added to maintain the pH in the 5 to 6 range. The reaction mixture was stirred overnight in the dark at room temperature. The

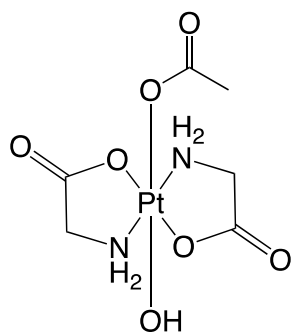
following day, a black solution was seen. The reaction mixture was left under a stream of nitrogen to completely remove the solvent. A black solid remained in the flask, indicating that the platinum(II) complex had decomposed.

### 2.3.2 Synthesis of *trans*-[Pt(L-alanine)<sub>2</sub>]



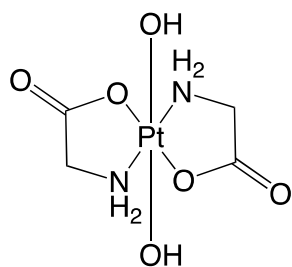
$\text{K}_2\text{PtCl}_4$  (0.50 g, 1.20 mmol) was dissolved in 25 mL of distilled water. KI (0.66 g, 3.98 mmol) was dissolved in 25 mL of distilled water and added to the reaction. L-alanine (0.18 g, 2.02 mmol) was also added. The reaction mixture was stirred at room temperature in the dark overnight. A light-yellow solution with blue solids was seen. The blue solids were removed by filtration, and the reaction mixture was left under a stream of nitrogen to reduce the volume of the solvent. A white precipitate was observed which was collected, washed with ethanol, and dried. A sample of the precipitate was analysed using IR spectroscopy. An O-H bond band was detected at  $3096.93\text{cm}^{-1}$  and a N-H bond band was detected at  $3392.47\text{cm}^{-1}$ . (Appendix 1)  $^1\text{H NMR}$  ( $\text{D}_2\text{O}$ , 400 MHz, ppm):  $\delta$  1.46 (d,  $J = 7.3$  Hz, 3H,  $\text{CH}_3$ ),  $\delta$  3.68 (q,  $J = 7.3$  Hz, H, CH). X-ray crystallography was used by Prof. Trevor Hambley to confirm that the  $^1\text{H NMR}$  chemical shifts corresponded to the *trans* isomer. (Appendix 2)

### 2.3.3 Synthesis of *trans*-[Pt(glycine)<sub>2</sub>(OH)(CH<sub>3</sub>COO<sup>-</sup>)]



*trans*-[Pt(glycine)<sub>2</sub>] was synthesised by Prof. Trevor Hambley. *trans*-[Pt(glycine)<sub>2</sub>] (0.19 g, 0.55 mmol) was suspended in an excess of glacial acetic acid ( $\text{CH}_3\text{COOH}$ ). 3 drops of hydrogen peroxide 30% solution ( $\text{H}_2\text{O}_2$ ) were added using a 1 mL glass pipette. The reaction mixture was stirred at room temperature in the dark overnight. A white, cloudy solution was seen. Infrared (IR) spectroscopy was used to monitor the progress of the reaction. No change was seen in the IR spectrum when compared to the starting material, *trans*-[Pt(glycine)<sub>2</sub>], indicating that the reaction had not occurred yet. (Appendix 3) An additional 6 drops of a 30%  $\text{H}_2\text{O}_2$  solution were added, and the reaction mixture was stirred in the dark at room temperature for 3 days. The reaction mixture was left under a stream of nitrogen to remove the solvent. A white solid remained in the flask, which was collected and analysed using IR spectroscopy. No change was seen in the IR spectrum when compared to the spectrum of *trans*-[Pt(glycine)<sub>2</sub>]. This indicates that the synthesis of *trans*-[Pt(glycine)<sub>2</sub>(OH)(CH<sub>3</sub>COO<sup>-</sup>)] was unsuccessful.

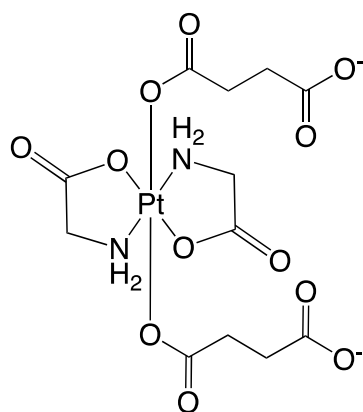
### 2.3.4 Synthesis of *trans*-[Pt(glycine)<sub>2</sub>(OH)<sub>2</sub>]



*trans*-[Pt(glycine)<sub>2</sub>] (0.19 g, 0.55 mmol) was dissolved in 10 mL of distilled water. 6.5 mL of a 30% H<sub>2</sub>O<sub>2</sub> solution was added. After 1 hour, the reaction mixture was heated at 70 °C for 3 hours, then stirred at room temperature in the dark for 4 days. The reaction mixture was left under a stream of nitrogen to remove the solvent. A white solid was collected, washed with ethanol, and dried. A sample of the solid was analysed using IR spectroscopy. An O-H bond band was detected at 3206.22 cm<sup>-1</sup>. (Appendix 4)

### 2.3.5 Synthesis of *trans*-[Pt(glycine)<sub>2</sub>(succinate)<sub>2</sub>]

#### *Using DMA as a solvent*



*trans*-[Pt(glycine)<sub>2</sub>] (0.19 g, 0.55 mmol) was suspended in 20 mL of DMA. Succinic anhydride (0.30 g, 3 mmol) was added. The reaction mixture was stirred at room temperature in the dark for 5 days. Additional succinic anhydride (0.13 g, 1.30 mmol) was added. A dark orange solution containing a white precipitate was seen, which was transferred into centrifuge tubes and centrifuged. The solid was collected and washed twice with ethanol, once with acetone, and dried under a stream of nitrogen. A sample of the solid was analysed using IR spectroscopy. No change was seen in the IR spectrum when compared to the spectrum of *trans*-[Pt(glycine)<sub>2</sub>(OH)<sub>2</sub>]. This indicates that the synthesis of *trans*-[Pt(glycine)<sub>2</sub>(succinate)<sub>2</sub>] was unsuccessful.

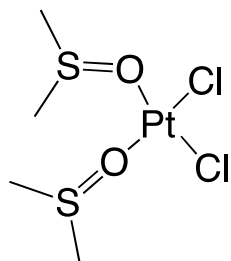
#### *Using DMSO as a solvent*

*trans*-[Pt(glycine)<sub>2</sub>(OH)<sub>2</sub>] (0.19 g, 0.55 mmol) was suspended in 20 mL of DMSO. Succinic anhydride (0.30 g, 3 mmol) was added. The reaction mixture was stirred at room temperature in the dark overnight. An additional (0.1 g, 1 mmol) of succinic anhydride was added. A white, cloudy solution was formed, which was heated at 70 °C for 3 hours, then stirred at room temperature overnight in the dark. The solution was transferred into centrifuge tubes and centrifuged. The solid was dried under a stream of nitrogen. IR spectroscopy was performed to analyse the product. No change was seen in the IR spectrum when compared to the spectrum of *trans*-[Pt(glycine)<sub>2</sub>(OH)<sub>2</sub>], indicating that the synthesis of *trans*-[Pt(glycine)<sub>2</sub>(succinate)<sub>2</sub>] was unsuccessful.



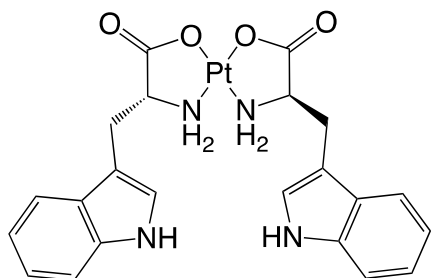
## 2.4 Synthesis of platinum(II) complexes from *cis*-[PtCl<sub>2</sub>(DMSO)<sub>2</sub>]

### 2.4.1 Synthesis of *cis*-[PtCl<sub>2</sub>(DMSO)<sub>2</sub>]



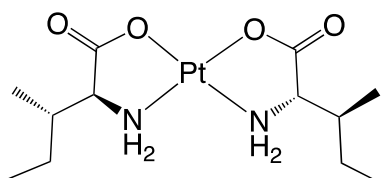
$K_2PtCl_4$  (2 g, 4.82 mmol) was dissolved in 100 mL of distilled water. A clear, bright red solution was formed. DMSO (0.75 g, 9.60 mmol) was added to the reaction mixture, which changed the colour of the solution from red to yellow. The reaction mixture was left at room temperature and crystals formed. The crystals were collected, washed with ethanol, and dried under a stream of nitrogen. The crystals were analysed using IR spectroscopy, which detected bands at  $3008.66\text{ cm}^{-1}$  and  $2918.20\text{ cm}^{-1}$ , as reported in the literature.<sup>8</sup> (Appendix 5)

### 2.4.2 Synthesis of *cis*-[Pt(L- tryptophan)<sub>2</sub>]



*cis*-[PtCl<sub>2</sub>(DMSO)<sub>2</sub>] (0.52 g, 1.23 mmol) was suspended in 50 mL of 1-butanol. L-Tryptophan (0.50 g, 2.45 mmol) was added. The reaction mixture was heated to 70 °C in the dark for 15 minutes. A dark brown solution with a white precipitate was formed. Triethylamine (2.40 mmol) and an additional 150 mL of 1-butanol were added. The reaction mixture was stirred at room temperature in the dark for 5 days. The reaction mixture remained a dark brown solution with a white precipitate and was transferred into centrifuge tubes and centrifuged. The solid was collected, washed twice with ethanol, and dried under a stream of nitrogen. IR spectroscopy was performed to analyse the product. No change was seen between the solid and *cis*-[PtCl<sub>2</sub>(DMSO)<sub>2</sub>] spectra, indicating that the synthesis of *cis*-[Pt(L-tryptophan)<sub>2</sub>] was unsuccessful.

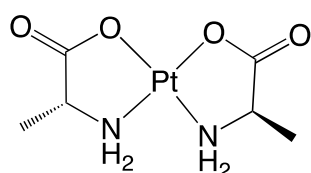
### 2.4.3 Synthesis of *cis*-[Pt(L-isoleucine)<sub>2</sub>]



*cis*-[PtCl<sub>2</sub>(DMSO)<sub>2</sub>] (0.50 g, 1.18 mmol) was suspended in 50 mL of 1-butanol. L-isoleucine (0.33 g, 2.52 mmol) was added. The reaction was stirred at room temperature in the dark for two days. A yellow solution with a white precipitate was formed. The reaction was heated at 70 °C in the dark for 5 hours, then stirred at room temperature for 3 days. Triethylamine (2.50 mmol) was added. The reaction mixture remained

as a yellow solution with a white precipitate and was transferred into centrifuge tubes. The tubes were centrifuged, and the supernatant was collected and dried under a stream of nitrogen, forming an oil. Mass spectrometry ESI (+): ( $m/z$ ) revealed peaks at 461.97 and 541.07. ESI (-): ( $m/z$ ) revealed peaks at 473.99, 525.08, and 563.06. (Appendix 6) The precipitate collected was analysed using IR spectroscopy, which determined that the precipitate was L-isoleucine. The oil was dissolved in 50 mL of 1-butanol and heated at 70 °C in the dark for 4 days. The reaction was left under a stream of nitrogen to remove the solvent. A yellow oil formed. The oil was dissolved in water and a yellow solution with a white precipitate was formed. Both fractions were separated, washed with methanol, and dried. Mass spectrometry ESI (-): ( $m/z$ ) revealed peaks at 525.11 and 638.10 in the solid fraction. (Appendix 7) Mass spectrometry ESI (-): ( $m/z$ ) revealed peaks at 474.05, 525.17, 561.10, and 639.17 in the solution fraction. (Appendix 8) The oil was dissolved again in 100 mL of 1-butanol. Additional L-isoleucine (0.16 g, 1.22 mmol) and triethylamine (1.20 mmol) were added to the reaction mixture and heated at 70 °C for 2 days. A yellow solution with a white precipitate was seen. The precipitate was collected and analysed using IR spectroscopy, which determined that the precipitate was L-isoleucine. The solution was left under a stream of nitrogen to remove the solvent. Mass spectrometry ESI (-): ( $m/z$ ) revealed peaks at 525.11, and 639.10. (Appendix 9) Expected mass calculated for  $C_{12}H_{24}N_2O_4Pt$ , at 455.14.

#### 2.4.4 Synthesis of *cis*-[Pt(L-alanine)<sub>2</sub>] in 1-butanol



##### *cis*-[PtCl<sub>2</sub>(DMSO)<sub>2</sub>]: L-alanine in a 1:2 ratio

*cis*-[PtCl<sub>2</sub>(DMSO)<sub>2</sub>] (0.61 g, 1.44 mmol) was suspended in 50 mL of 1-butanol. L-Alanine (0.23 g, 2.58 mmol) was added to the reaction. The reaction mixture was heated at 70 °C and stirred in the dark for 5 hours, then left to cool overnight at room temperature. A clear, bright yellow solution with a white precipitate was seen. Triethylamine (2.60 mmol) was added. An additional 100 mL of 1-butanol was added, and the reaction mixture was heated at 70 °C and left stirring in the dark for another 5 hours. The reaction mixture was left under a stream of nitrogen at 40 °C to remove the solvent. A yellow, oily substance was left behind. The oil was washed with hexane and dried. Mass spectrometry ESI (-): ( $m/z$ ) revealed peaks 395.95 and 440.97. (Appendix 10) The oil was redissolved in 50 mL of 1-butanol and heated at 70 °C for 5 hours, then overnight for 2 days. The reaction formed a yellow solution with a white precipitate. The precipitate was collected, dissolved in water, and dried under a stream of nitrogen. Mass

spectrometry ESI (+): ( $m/z$ ) revealed peaks at 418.92, and ESI (-): ( $m/z$ ) revealed peaks at 395.95 and 423.85. (Appendix 11) The remaining solution was left under a stream of nitrogen to remove the solvent. Mass spectrometry ESI (-): ( $m/z$ ) revealed peaks at 406.00. Expected mass calculated for  $C_6H_{12}N_2O_4Pt$ , [M+Cl] at 406.01.

#### ***cis*-[PtCl<sub>2</sub>(DMSO)<sub>2</sub>]: L-alanine in a 1:3 ratio**

*cis*-[PtCl<sub>2</sub>(DMSO)<sub>2</sub>] (0.50 g, 1.18 mmol) was suspended in 50 mL of 1-butanol. L-Alanine (0.21 g, 2.36 mmol) was added. The reaction mixture was heated at 70 °C and stirred in the dark for 5 hours then cooled overnight at room temperature. Additional L-alanine (0.11 g, 1.23 mmol) and triethylamine (2.40 mmol) were added. The reaction mixture was stirred overnight at room temperature. A cloudy solution with a white solid was observed at the bottom of the flask. A sample of the solid was taken and washed twice with ethanol and once with acetone. The sample was then analysed using IR spectroscopy which revealed that the solid was L-alanine. (Appendix 12) The flask was left under a stream of nitrogen for 1 hour. More precipitate was seen as the solvent volume was reduced. The solution was transferred into centrifuge tubes and centrifuged. The solid was collected and washed twice with ethanol, once with acetone and dried under nitrogen. A small amount of the solid was transferred into a vial. Water and ethanol were added to fill half the vial in a 1:2 ratio. The vial was placed in a dark bottle that was half filled with ethanol which was placed in a dark cupboard for 2 weeks. White crystals were present in the vial. Mass spectrometry and <sup>1</sup>H NMR spectroscopy analysis were performed on the crystals. Mass spectrometry ESI (-): ( $m/z$ ) revealed peaks at 370.0. (Appendix 13) Mass spectrometry ESI (-) calculated for  $C_6H_{12}N_2O_4Pt$ , [M-H] at 370.04. <sup>1</sup>H NMR (D<sub>2</sub>O, 300 MHz, ppm): δ 1.44 (d,  $J$  = 7.2 Hz, 3H, CH<sub>3</sub>), δ 1.48 (d,  $J$  = 7.2 Hz, 3H, CH<sub>3</sub>), δ 3.66 (q,  $J$  = 7.2 Hz, H, CH), δ 3.77 (q,  $J$  = 7.2 Hz, H, CH). (Appendix 14)

#### ***cis*-[PtCl<sub>2</sub>(DMSO)<sub>2</sub>]: L-alaninate**

L-alanine (0.08 g, 0.90 mmol) and sodium hydroxide (0.04 g, 1 mmol) were dissolved in 50 mL of distilled water. The solution was stirred at room temperature for 5 days. A clear solution was seen, which was left under a stream of nitrogen to remove the solvent. A white solid was collected, which was then dissolved in 50 mL of butanol. *cis*-[PtCl<sub>2</sub>(DMSO)<sub>2</sub>] (0.21 g, 0.50 mmol) was added to the reaction. The reaction mixture was heated at 70 °C and stirred in the dark for 6 hours, then at room temperature for 1 week. A clear, yellow solution was observed, which was dried under a stream of nitrogen. Mass spectrometry ESI (+): ( $m/z$ ) revealed peaks at 419.92, and ESI (-): ( $m/z$ ) revealed peaks at 431.95. (Appendix 16)

## 2.4.5 Synthesis of *cis*-[Pt(L-alanine)<sub>2</sub>] in methanol

### *cis*-[PtCl<sub>2</sub>(DMSO)<sub>2</sub>] : lithium L-alaninate

L-alanine (5.80 g, 0.065 mol) and lithium hydroxide (LiOH·H<sub>2</sub>O) (1.56 g, 0.037 mol) were dissolved in 50 mL of distilled water to form lithium L-alaninate. The reaction mixture was stirred at room temperature and dried under a stream of nitrogen. A white solid was collected and washed with ethanol. *cis*-[PtCl<sub>2</sub>(DMSO)<sub>2</sub>] (0.23 g, 0.54 mmol) was suspended in 100 mL of methanol. Lithium L-alaninate (0.13 g, 1.37 mmol) was added to the reaction. The reaction mixture was heated at 40 °C and stirred in the dark for 2 days. The reaction mixture was dried under a stream of nitrogen and a yellow, sticky solid was formed. Mass spectrometry ESI (+): (*m/z*) revealed peaks at 401.97. Additional lithium L-alaninate (0.06 g, 0.63 mmol) was added and the reaction mixture was heated at 40 °C and stirred in the dark for 6 hours, then at room temperature for 1 week. A clear solution with a white precipitate was seen. The reaction was dried under a stream of nitrogen to remove half of the solvent and was then transferred into centrifuge tubes. The tubes were centrifuged, and the solid was collected and washed with ethanol. Mass spectrometry ESI (-): (*m/z*) revealed peaks at 370.02. (Appendix 17) Mass spectrometry ESI (-) calculated for C<sub>6</sub>H<sub>12</sub>N<sub>2</sub>O<sub>4</sub>Pt, [M-H] at 370.04.

### *cis*-[PtCl<sub>2</sub>(DMSO)] : L-alanine in a 1:2 ratio

*cis*-[PtCl<sub>2</sub>(DMSO)<sub>2</sub>] (2.03 g, 4.81 mmol) was suspended in 100 mL of methanol. L-Alanine (0.85 g, 9.54 mmol) was added to the reaction. The reaction mixture was heated at 40 °C and stirred in the dark, then cooled at room temperature overnight. Lithium hydroxide (0.41 g, 9.77 mmol) was added, and the reaction mixture was stirred in the dark at room temperature. A clear solution with a white precipitate was observed. The reaction mixture was dried under a stream of nitrogen to remove half of the solvent and centrifuged. The solid was collected and dissolved in 5 mL of water, and the solution was transferred into a vial. The vial was placed under a stream of nitrogen to remove the solvent. White crystals were present in the vial. Mass spectrometry ESI (+): (*m/z*) revealed peaks at 393.98. Mass spectrometry ESI (-): (*m/z*) revealed peaks at 370.01. (Appendix 18) Mass spectrometry ESI (+) was calculated for C<sub>6</sub>H<sub>12</sub>N<sub>2</sub>O<sub>4</sub>Pt, [M+Na] at 394.03. Mass spectrometry ESI (-) calculated for C<sub>6</sub>H<sub>12</sub>N<sub>2</sub>O<sub>4</sub>Pt, [M-H] at 370.04. <sup>1</sup>H NMR (D<sub>2</sub>O, 300 MHz, ppm): δ 1.46 (d, *J* = 7.2 Hz, 3H, CH<sub>3</sub>), δ 1.50 (d, *J* = 7.3 Hz, 3H, CH<sub>3</sub>), δ 2.26 (s, 6H, CH<sub>3</sub>), δ 3.68 (q, *J* = 7.4 Hz, H, CH), δ 3.80 (q, *J* = 7.2 Hz, H, CH). (Appendix 19) Additional L-alanine (0.44 g, 4.94 mmol) was added to the remaining supernatant. The reaction was heated at 40 °C and stirred in the dark, then cooled at room temperature overnight. A cloudy solution was observed, which was transferred into centrifuge

tubes and centrifuged. The solid was collected and dissolved in 2 mL of water and was dried under a stream of nitrogen to remove the water. The solid was collected and washed with ethanol. Mass spectrometry ESI (+): ( $m/z$ ) revealed peaks at 394.00. Mass spectrometry ESI (+) calculated for  $C_6H_{12}N_2O_4Pt$ , [M+Na] at 394.03. Mass spectrometry ESI (-): ( $m/z$ ) revealed peaks at 406.03 and 459.07. (Appendix 20) Mass spectrometry ESI (-) calculated for  $C_6H_{12}N_2O_4Pt$ , [M+Cl] at 406.01. 5 mL of acetone was added to the solid and a cloudy solution was formed. The solution was centrifuged, and the solid fraction was collected and dried under a stream of nitrogen.  $^1H$  NMR ( $D_2O$ , 300 MHz, ppm):  $\delta$  1.50 (d,  $J = 7.3$  Hz, 3H,  $CH_3$ ),  $\delta$  2.26 (s, 6H,  $CH_3$ ),  $\delta$  3.80 (q,  $J = 7.3$  Hz, H, CH). (Appendix 21) The supernatant fraction was dried under a stream of nitrogen.  $^1H$  NMR ( $D_2O$ , 300 MHz, ppm):  $\delta$  3.82 (q,  $J = 7.4$  Hz, CH), 3.80 (q,  $J = 7.4$  Hz, CH), 3.77 (q,  $J = 7.4$  Hz, CH), 3.75 (q,  $J = 7.4$  Hz, CH), 3.57 (q,  $J = 7.3$  Hz, CH), 3.55 (q,  $J = 7.3$  Hz, CH), 3.52 (q,  $J = 7.3$  Hz, CH), 3.50 (q,  $J = 7.3$  Hz, CH), 1.50 (d,  $J = 7.2$  Hz,  $CH_3$ ), 1.48 (d,  $J = 7.2$  Hz,  $CH_3$ ). (Appendix 22)

#### 2.4.6 Synthesis of *cis*-[Pt(L-alanine)<sub>2</sub>] in acetone

*cis*-[PtCl<sub>2</sub>(DMSO)<sub>2</sub>] (1.05 g, 2.49 mmol) was suspended in 100 mL of acetone. L-alanine (0.44 g, 4.94 mmol) was added. The reaction mixture was heated at 40 °C and stirred in the dark, then at room temperature for 2 days. A light-yellow solution with a yellow precipitate was formed. Lithium hydroxide (0.41 g, 9.77 mmol) was added. A bright yellow solution with a white precipitate was observed. The precipitate was collected and dissolved in 2 mL of distilled water. The solution was left under a stream of nitrogen to remove the solvent. The white solid formed was collected and analysed using  $^1H$  NMR spectrometry.  $^1H$  NMR ( $D_2O$ , 300 MHz, ppm):  $\delta$  1.26 (d,  $J = 7.2$  Hz, 3H,  $CH_3$ ),  $\delta$  1.30 (d,  $J = 7.1$  Hz, 3H,  $CH_3$ ),  $\delta$  1.45 (d,  $J = 7.0$  Hz, 3H,  $CH_3$ ),  $\delta$  2.72 (s, 6H,  $CH_3$ ),  $\delta$  3.45 (q,  $J = 7.1$  Hz, H, CH),  $\delta$  3.91 (q,  $J = 7.2$  Hz, H, CH). (Appendix 23) Additional lithium hydroxide (0.23 g, 5.48 mmol) was added to the solution. The reaction was stirred overnight at room temperature in the dark. A yellow solution with a white precipitate was observed. The precipitate was separated and collected. The remaining solution was collected and dried under a stream of nitrogen to remove the solvent, forming a solid. Mass spectrometry ESI (+): ( $m/z$ ) revealed peaks at 419.93 and ESI (-): ( $m/z$ ) revealed peaks at 431.95. (Appendix 24)

## **2.5 Cytotoxicity studies**

### **2.5.1 Materials**

A549 cells were purchased from the American Type Culture Collection (ATCC, Cat. No. CCL-185). A549 cells were incubated at 37 °C and 5% CO<sub>2</sub> atmosphere. Cells were cultured in Advanced Dulbecco's modified Eagle's medium (DMEM, Thermo Fisher Scientific) supplemented with 2.5 mM L-glutamine and 2% Fetal Bovine Serum (Thermo Fisher Scientific). Cells were passaged for a maximum of 20 times for cell culture studies.

### **2.5.2 Cell passaging**

Cell passaging was performed when cells were at 70 to 80% confluency. Cell culture media, trypsin, and Phosphate Buffered Saline (PBS) were warmed up in a 37 °C water bath. The following steps were performed in a biohazard biological cabinet class II. The media from the cell culture flask was removed and discarded. The cells were washed with 3 mL of PBS which was then discarded. 2 mL of trypsin was added to the flask. The flask was placed in the 37 °C incubator for 3-5 minutes until the cells detached from the flask. 2 mL of media was added to the flask to deactivate the trypsin. The cells were broken apart using a pipette and were transferred into a 15 mL centrifuge tube. The tube was centrifuged at 3000 rpm for 2 minutes. After the centrifugation was completed, the media was discarded, and the pellet was resuspended with 2 mL of media. 0.2 mL of cell suspension was added to a new cell culture flask containing 5 mL of media.

### **2.5.3 Isolation of cells**

After cell passaging, 15 µL of the cell suspension was transferred into a clean Eppendorf tube. 15 µL of trypan blue was added and mixed well. 10 µL of the solution was placed into a cell counting chamber slide and cell counting was performed (Countess 3 Automated Cell Counter, Thermo Fisher Scientific). 100 µL of PBS was added into the outer wells of a 96-well plate.  $1 \times 10^{-5}$  cells were suspended in 8 mL of medium. 100 µL of medium + cell suspension was added into the remaining wells of the 96-well plate. The plate was incubated for a 24-hour period to allow the suspended cells to adhere to the surface of the 96-well plate.

#### **2.5.4 Dosing A549 cells with platinum**

The following steps were performed in a cytotoxic drug safety cabinet. *trans*-[Pt(L-alanine)<sub>2</sub>] and oxaliplatin were dissolved in media (1 mM concentration) and filtered using a sterile 0.2 μM filter. A 12-well plate was obtained, and 700 μL of media was pipetted into 10 of the 12 wells. 700 μL of the *trans*-[Pt(L-alanine)<sub>2</sub>] solution was added to well 1. Serial dilution was performed by pipetting 700 μL of solution from well 1 into well 2. This was repeated until well 9. The previously prepared 96-well plate containing cells was taken from the incubator. All media in the 96-well plate were removed. 100 μL of solution from the 12-well plate was pipetted into the columns of the 96-well plate in increasing platinum concentration. These steps were repeated with oxaliplatin. The 96-well plates were incubated for 72 hours at 37 °C.

#### **2.5.5 MTT Assay**

The following steps were performed in the cytotoxic drug safety cabinet. Triazolyl blue tetrazolium bromide (MTT) (8 mg) was dissolved in 8 mL of media, forming a solution (1 mg/mL concentration). The solution was filtered with a 0.2 μM sterile filter. The previously prepared 96-well plates containing cells that had been dosed with *trans*-[Pt(L-alanine)<sub>2</sub>] and oxaliplatin were taken from the incubator. The media in the wells were removed using a multichannel pipette and discarded. 100 μL of MTT + media solution was added to the wells. The plate was incubated at 37 °C for 72 hours. The MTT + media solution was removed from the wells and discarded. 100 μL DMSO was added to the wells. Cell viability was measured with a plate reader (Perkin Elmer). Wallal 420 manager software with protocol absorbance @ 600 nm (1.0 s with shake) to analyse the data.

#### **2.5.6 Data analysis**

Data was normalised and analysed using GraphPad Prism Version 9.5.1. XY analyses, non-regression (curve fit) was used. The data was plotted as dose-response inhibition log(inhibitor) vs. response.

## 2.6 Results and Discussion

### 2.6.1 Platinum(IV)-glutamine complex synthesis

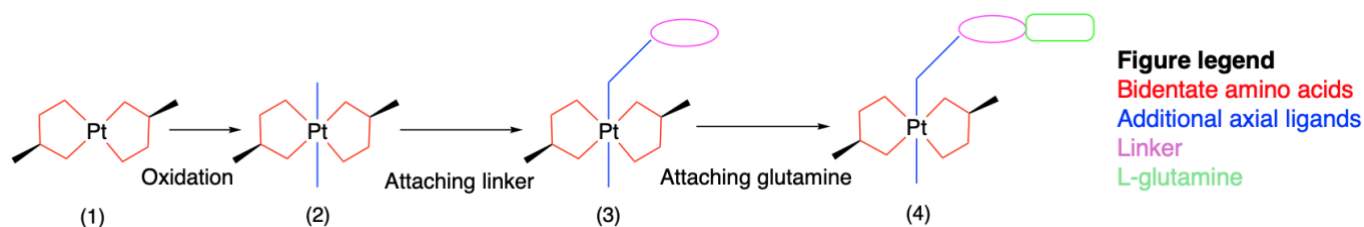


**Figure 2.1: Proposed synthetic pathway of platinum(IV)-glutamine complexes.**

Biologically inert platinum(IV)-glutamine complexes are essential to study the transport and behaviour of these complexes in cancer cells. To achieve this, a suitable platinum(II) complex (1) must be synthesised as a precursor for the subsequent synthesis of a platinum(IV)-glutamine complex. The precursor can be synthesised by attaching amino acids such as L-alanine and L-isoleucine in a bidentate manner (red) to the platinum core. *In vitro*, cytotoxicity studies must be performed to confirm that the complex is biologically inert. The platinum(II) complex can then be oxidised to its more inert platinum(IV) state (2). This results in the addition of two axial ligands (blue), which can be used to modify the properties of the platinum(IV) complex. A hydrophilic linker (purple) can be attached to the platinum(IV) complex (3) to increase the overall hydrophilicity of the complex. This is important to reduce the non-specific entry of the complexes into cells via passive diffusion. The linker must also be long enough to prevent the platinum from interfering with the glutamine binding at its receptor<sup>141</sup>. Glutamine (green) can then be attached to the platinum(IV) complex via the linker (purple) to form the platinum(IV)-glutamine complex (4).

### 2.6.2 Platinum(II) complex design

The platinum(II) complexes were designed to consist of a bis(amino acid)platinum core to form complexes that are square-planar and neutral. The complex was designed to be inert analogues of oxaliplatin. Amino acids were selected as it has been shown that complexes with two amine and four carboxylate donors allow the preparation of platinum(IV) complexes that are stable in cell growth media and blood plasma. The complexes are also readily reduced in cells and are not cytotoxic to cells<sup>142</sup>.



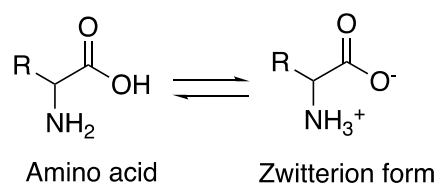


**Figure 2.2: Amino acids at neutral pH.**

Amino acids exist as zwitterions at neutral pH (Figure 2.2). At neutral pH, the carboxylate group ( $\text{COO}^-$ ) can displace ligands on the platinum to form a coordinate bond with the platinum core. When a base is added, the pH of the solution is increased. At a basic pH,  $\text{NH}_3^+$  becomes deprotonated forming  $\text{NH}_2$ . The amine group can then form a coordinate bond with the platinum core. Bidentate binding of the amino acids to the platinum increases the inertness of the platinum(II) complex. This is because if one donor arm of the amino acid becomes detached from the platinum, the other donor arm remains attached, making it likely for the detached donor arm to reattach to the platinum. This is important to prevent the displacement of ligands and the formation of reactive platinum(II) species that can form DNA adducts and cause cellular apoptosis. All synthetic procedures will be performed in dark conditions as platinum complexes are photosensitive. Unexpected changes may occur during light exposure, such as changes in oxidation number of metal, changes in the composition of the coordination shell without any change in oxidation number of metal and ligands, and changes in the coordination arrangement of ligands may occur<sup>143</sup>.

### 2.6.3 Synthesis of *trans*-platinum(II) complexes

The synthesis of *trans*-[Pt( $\beta$ -alanine)<sub>2</sub>] was unsuccessful as a black solid was formed, indicating that  $\text{K}_2\text{PtCl}_4$  and its reaction products had decomposed. *trans*-[Pt(L-alanine)<sub>2</sub>] was synthesised using a similar synthetic pathway (Figure 2.3) widely used to synthesise cisplatin, which was reported by Dhara in 1970<sup>144</sup>. L-alanine was chosen as a better option for the synthesising [Pt(alanine)<sub>2</sub>] as it forms a thermodynamically favourable five-membered ring, compared to the six-membered ring formed by  $\beta$ -alanine.

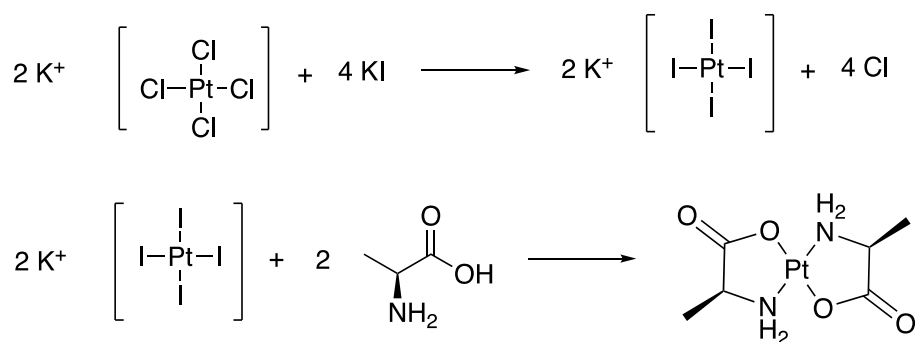


**Figure 2.3: Synthetic scheme of *trans*-[Pt(L-alanine)<sub>2</sub>].**

#### 2.6.4 Cytotoxicity studies of *trans*-[Pt(L-alanine)<sub>2</sub>]

The cytotoxicity of *trans*-[Pt(L-alanine)<sub>2</sub>] was studied in A549 cells using an MTT assay. MTT assay measures the cellular metabolic activity as an indicator of cell viability and cell proliferation<sup>145</sup>. The cells dosed with *trans*-[Pt(L-alanine)<sub>2</sub>] were incubated with MTT and media (1 mg/ mL concentration) for 72 hours. The MTT assays revealed that *trans*-[Pt(L-alanine)<sub>2</sub>] is biologically inert in A549 cells if administered to cells at a concentration below 1 mM (Figure 2.4).

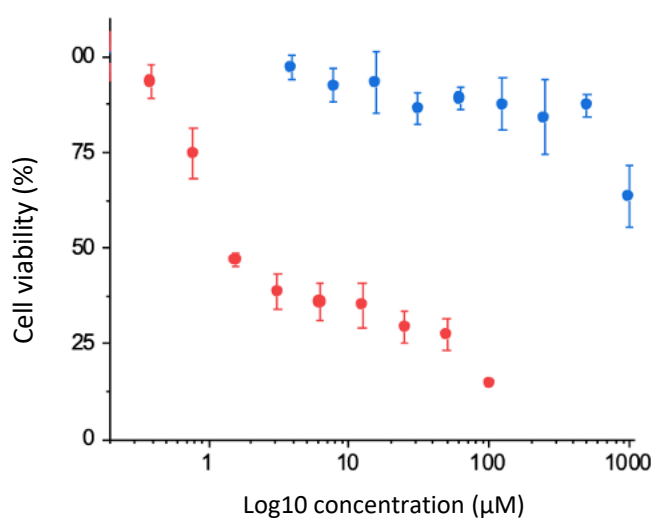


**Figure 2.4: Cytotoxicity studies of *trans*-[Pt(L-alanine)<sub>2</sub>] in A549 cells using MTT assay (72 hours).** Cytotoxicity of *trans*-[Pt(L-alanine)<sub>2</sub>] at different concentrations (blue dots) was measured with oxaliplatin (red dots) which was used as a control. The cytotoxicity of *trans*-[Pt(L-alanine)<sub>2</sub>] is almost negligible and decreased cell viability is only seen at 1 mM concentration. Oxaliplatin, a known cytotoxic drug, shows a biphasic dependence curve with lower cell viability (IC<sub>50</sub> = 1.4 ± 0.1 µM).

### 2.6.5 Synthesis of *trans*-platinum(IV) complexes

*trans*-[Pt(glycine)<sub>2</sub>] was synthesised by Prof. Trevor Hambley. The oxidation of *trans*-[Pt(glycine)<sub>2</sub>] into its platinum(IV) state was attempted using an excess of acetic acid and hydrogen peroxide (H<sub>2</sub>O<sub>2</sub>). The attempts were unsuccessful, as *trans*-[Pt(glycine)<sub>2</sub>] had poor solubility in acetic acid. The oxidation was attempted in water and H<sub>2</sub>O<sub>2</sub> instead. The oxidation was successful, and an O-H bond band was detected at 3206.22 cm<sup>-1</sup> when analysed with IR spectroscopy. However, *trans*-[Pt(glycine)<sub>2</sub>(OH)<sub>2</sub>] does not meet the design criteria of four carboxylate groups being attached to the platinum. Meeting the design criteria is essential to ensure that the platinum(IV) complexes synthesised are stable in media and blood plasma. To resolve this, *trans*-[Pt(glycine)<sub>2</sub>(OH)<sub>2</sub>] was reacted in DMA and DMSO with an excess of succinic anhydride to form *trans*-[Pt(glycine)<sub>2</sub>(succinate)<sub>2</sub>] complexes. However, the complexes had poor solubility in both solvents, and the synthesis of *trans*-[Pt(glycine)<sub>2</sub>(succinate)<sub>2</sub>] was unsuccessful.

### 2.6.6 Challenges encountered during the synthesis of *trans*-platinum(IV) complexes

Challenges were experienced during the attempts to synthesise *trans*-platinum(IV) complexes due to the poor solubility of the *trans*-[Pt(glycine)<sub>2</sub>(OH)<sub>2</sub>] in water and organic solvents. It is common practice to dissolve platinum(II) complexes with poor aqueous solubility in organic solvents such as DMSO and DMF<sup>146</sup>. The poor solubility of these complexes is concerning as it could lead to further difficulty when synthesising platinum(IV)-glutamine complexes. The complexes must also be soluble in aqueous solutions or media to perform cell culture and biological studies successfully. The formation of geometric isomers during the synthesis of platinum(IV)-glutamine complexes was also a concern. The *trans*-platinum(IV) complexes synthesised have methyl groups that are both oriented in the same direction relative to the platinum plane. During oxidation of these complexes, the platinum centre loses 2 electrons, allowing the addition of two axial ligands to be added to the platinum core<sup>68</sup>. The linker (purple) and subsequent glutamine molecule (green) (Figure 2.5) will only be added as one of the additional axial ligand. It cannot be certain if the linker will bind to the platinum core in the same orientation as the methyl groups (A) or in the opposite direction (B) (Figure 2.5). This will lead to the formation of isomers during the oxidation and addition of the linker to *trans*-platinum(IV) complexes, complicating the purification process.

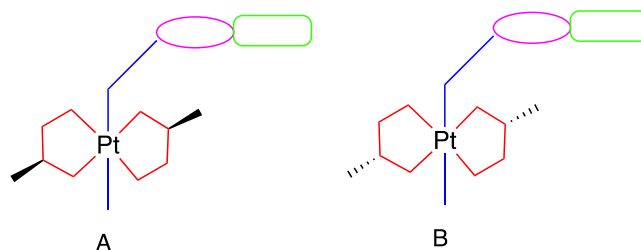


**Figure 2.5. Formation of geometric isomers during oxidation and subsequent linker attachment of *trans*-platinum(IV) complexes.** A: Both methyl groups of the amino acid are orientated in the upward direction to the platinum core. B: Both methyl groups of the amino acid are orientated in the downward direction to the platinum core.

## 2.7 Synthesis of *cis*-platinum(II) complexes

To overcome these challenges, the synthesis of *cis*-platinum(II) complexes was investigated. *cis* Complexes are expected to be more soluble than their *trans* isomers due to the differences in their molecular geometry. This is because *cis* isomers are less symmetrical and more polar and have a greater potential for dipole-dipole interactions with polar solvents, increasing their solubility in aqueous solutions compared to their *trans* isomers. Cisplatin is roughly eight times more soluble than its geometric *trans* isomer, transplatin<sup>147</sup>. Substituents of the *cis*-platinum(II) complexes have methyl groups that are oriented in the opposite directions from each other relative to the platinum core (Figure 2.6). The oxidation of *cis*-platinum(II) complexes and subsequent attachment of a linker and glutamine to one methyl group of the complex will reduce the formation of geometric isomers.

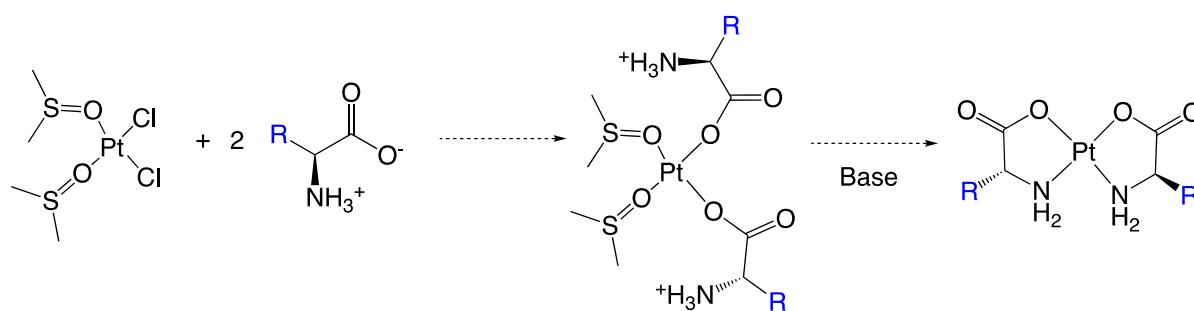


**Figure 2.6. Hypothesised synthetic pathway of *cis*-bis(amino acid)platinum(II) complexes using *cis*-[PtCl<sub>2</sub>(DMSO)<sub>2</sub>] as a starting material.** R represents a specific side chain of amino acids. The final product, *cis*-platinum(II) complexes have both its methyl groups oriented in opposite directions from each other relative to the platinum core.

It was hypothesised that when 1 mol of *cis*-[PtCl<sub>2</sub>(DMSO)<sub>2</sub>] is suspended in a solvent and 2 mol of amino acids (zwitterion state), the carboxylate group of the amino acids will displace the weaker chloride (Cl<sup>-</sup>) ligands on the platinum core first. This will decrease the pH of the reaction mixture to acidic levels due to the release of protons. When 2 mol of base is added, the amine (NH<sub>3</sub><sup>+</sup>) will be deprotonated and displace the dimethyl sulfoxide (DMSO) ligands (Figure 2.6). This will lead to the formation of *cis*-platinum(II) complexes in high purity.

This is a new approach to synthesising *cis*-bis(amino acid)platinum(II) complexes. Different reaction conditions, including solvent, temperature, duration of reaction, and the molarity of base and amino acid used, were studied to develop a new synthetic procedure. Amino acids such as L-alanine, L-isoleucine, and L-tryptophan (Figure 2.7) were selected to investigate the synthesis of *cis*-bis(amino acid)platinum(II) complexes.

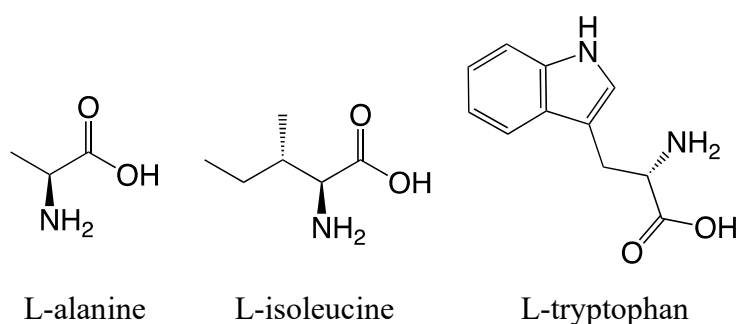


**Figure 2.7: Various amino acids were investigated to synthesise *cis*- bis(amino acid)platinum(II) complexes.**

### 2.7.1 Synthesis of *cis*-[Pt(L-tryptophan)<sub>2</sub>]

This synthetic procedure was first designed with 1-butanol as the solvent and triethylamine as the base. *cis*-[PtCl<sub>2</sub>(DMSO)<sub>2</sub>] and L-tryptophan in 1-butanol in a 1:2 ratio to attempt to synthesise *cis*-[Pt(L-tryptophan)<sub>2</sub>]. The reaction mixture turned dark brown after being heated at 70 °C for 15 minutes in the dark. The heat was turned off and the reaction mixture was stirred at room temperature for five days. A dark brown solution with a white precipitate was observed. The precipitate in the reaction mixture was collected and analysed using IR spectroscopy and was identified as *cis*-[PtCl<sub>2</sub>(DMSO)<sub>2</sub>]. It is possible that the synthesis did not take place due to the degradation of L-tryptophan. L-tryptophan has been identified to be sensitive to many factors including light, heat, solvent, presence of air, and the presence of other compounds<sup>148</sup>. This could explain why the reaction mixture turned dark brown. It was determined that L-

tryptophan is not a suitable amino acid for the synthesis of *cis*-bis(amino acid)platinum(II) complexes due to its sensitivity.

### 2.7.2 Synthesis of *cis*-[Pt(L-isoleucine)<sub>2</sub>]

*cis*-[PtCl<sub>2</sub>(DMSO)<sub>2</sub>] and L-isoleucine were reacted in 1-butanol in a 1:2 ratio to attempt to synthesise *cis*-[Pt(L-isoleucine)<sub>2</sub>]. A yellow solution with a white precipitate was observed. The fractions were separated for analysis. The white precipitate was identified as L-isoleucine through IR spectrometry. The solvent was removed, which formed an oil, that was analysed using mass spectrometry. Mass spectrometry revealed that [Pt(L-isoleucine)<sub>2</sub>] was not present, indicating that the synthesis had not occurred. Only intermediates (Figure 2.8) of the synthesis were present. To identify if a longer reaction time was required for the synthesis of [Pt(L-isoleucine)<sub>2</sub>], the oil was redissolved in 1-butanol and the solution was heated for 4 days. Then, the solvent was removed, and the oil formed was dissolved in water and the precipitate was collected to attempt to obtain pure *cis*-[Pt(L-isoleucine)<sub>2</sub>] that may have formed. [Pt(L-isoleucine)<sub>2</sub>] was not detected in both precipitate and oil fractions when analysed using mass spectrometry while the intermediates (Figure 2.8) previously detected remained. It is possible that removing the suspended L-isoleucine from the reaction mixture earlier resulted in insufficient L-isoleucine being present to displace the ligands on the platinum to form *cis*-[Pt(L-isoleucine)<sub>2</sub>] complexes. The fractions were combined and resuspended in 1-butanol. An additional equivalent of L-isoleucine and triethylamine base were added to the reaction mixture and heated for two days to allow the reaction to take place. White precipitate was observed in the solution which was collected and analysed using IR spectroscopy. Analysis showed the precipitate was L-isoleucine that had remained suspended in the reaction mixture. The solvent from the solution was removed and analysed using mass spectrometry which did not detect [Pt(L-isoleucine)<sub>2</sub>]. It is possible that L-isoleucine was not sufficiently soluble in 1-butanol to displace the ligands on the platinum and form *cis*-[Pt(L-isoleucine)<sub>2</sub>].

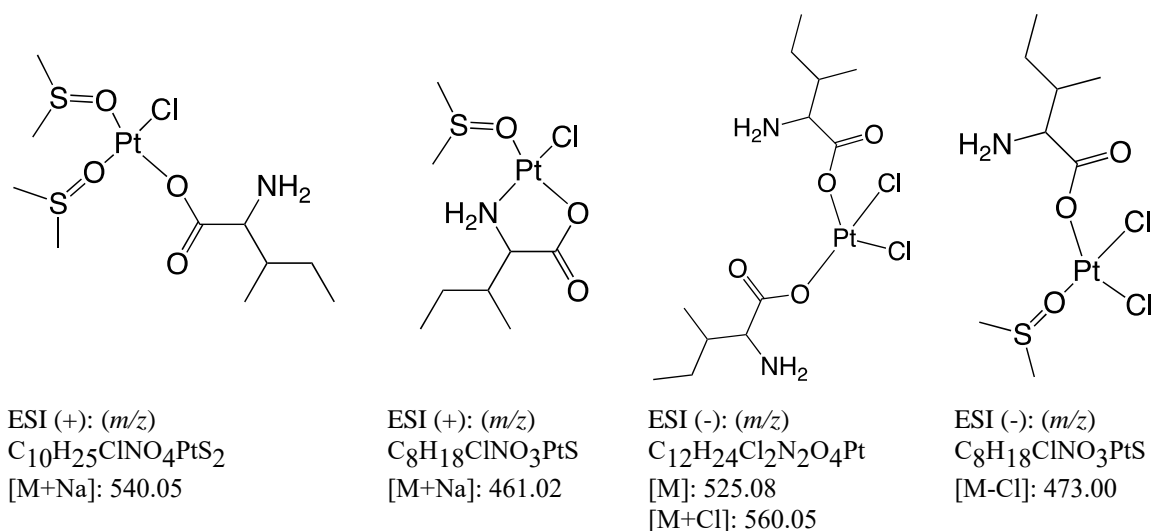


**Figure 2.8: Intermediates of *cis*-[Pt(L-isoleucine)<sub>2</sub>] synthesis.**

Although the synthesis of *cis*-[Pt(L-isoleucine)<sub>2</sub>] was unsuccessful, many insights into the synthetic process were gained through the mass spectrometry analysis. It was hypothesised (Figure 2.6) that the synthesis of *cis*-[Pt(amino acid)<sub>2</sub>] will take place in a systematic manner where the carboxylate group of an amino acid (zwitterion state) will displace the weaker chloride ligands (Cl<sup>-</sup>) on the platinum. The addition of a base will then deprotonate the amine (NH<sub>3</sub><sup>+</sup>) group which can then displace the dimethyl sulfoxide (DMSO) ligands on the platinum. This would result in the synthesis of *cis*-platinum(II) complexes in high purity. However, mass spectrometry analysis disproves this hypothesis as it indicates the presence of different various intermediates. The detection of complexes such as C<sub>12</sub>H<sub>24</sub>Cl<sub>2</sub>N<sub>2</sub>O<sub>4</sub>Pt (Figure 2.8) suggests that L-isoleucine displaced the DMSO ligands before the chloride ligands. These different intermediates can present challenges, as they could lead to the formation of both *cis* and *trans* isomers, affecting the synthesis of *cis*-bis(amino acid)platinum(II) complexes in terms of yield and purity.

### 2.7.3 Synthesis of *cis*-[Pt(L-alanine)<sub>2</sub>] in 1-butanol

*cis*-[PtCl<sub>2</sub>(DMSO)<sub>2</sub>] and L-alanine were reacted in a 1:2 ratio to attempt to synthesise *cis*-[Pt(L-alanine)<sub>2</sub>]. It was predicted that an excess of L-alanine was not required and that *cis*-[Pt(L-alanine)<sub>2</sub>] would be synthesised within 3 days. The precipitate from the reaction mixture was collected and analysed using mass spectrometry after 3 days. The mass spectrometry results showed that *cis*-[Pt(L-alanine)<sub>2</sub>] had not been synthesised yet. Instead, intermediates of the reaction (Figure 2.9) were present in the reaction mixture (Appendix 11). Similar to what was

observed during the synthesis of *cis*-[Pt(L-isoleucine)<sub>2</sub>], different variations of intermediates were present in the reaction mixture (Figure 2.9). This confirms that the ligands of *cis*-[PtCl<sub>2</sub>(DMSO)<sub>2</sub>] are unpredictably displaced from the platinum. It was predicted that the reaction mixture needed to be stirred for a longer duration to allow the synthesis of *cis*-[Pt(L-alanine)<sub>2</sub>] to be completed. The reaction mixture was stirred for an additional 2 days. The precipitate from the reaction mixture was collected and analysed again using mass spectrometry. However, the intermediates (Figure 2.9) were still present in the reaction mixture, and *cis*-[Pt(L-alanine)<sub>2</sub>] had not been synthesised. This suggests that the duration for which the reaction mixture is stirred may not affect the synthesis of *cis*-[Pt(L-alanine)<sub>2</sub>]. Additional factors, such as the presence of excess L-alanine and base in the reaction mixture, may also affect the synthesis of *cis*-[Pt(L-alanine)<sub>2</sub>].

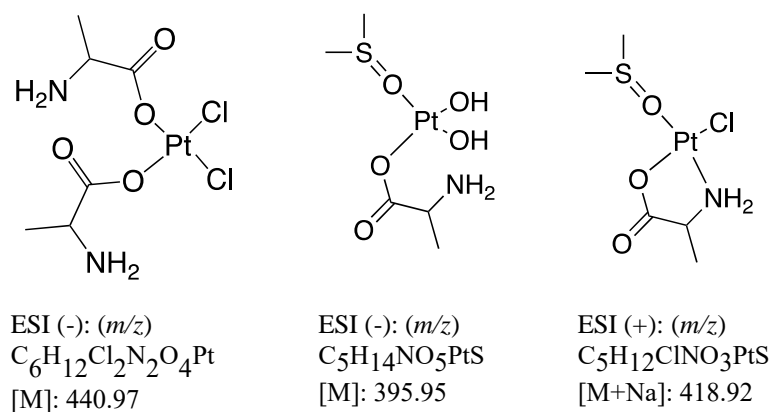
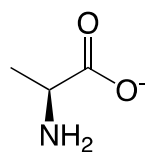


**Figure 2.9: Intermediates of *cis*-[Pt(L-alanine)<sub>2</sub>] synthesis.**

The synthesis of *cis*-[Pt(L-alanine)<sub>2</sub>] may have been unsuccessful due to insufficient L-alanine in the reaction mixture. The synthetic procedure was repeated in the same conditions but with *cis*-[PtCl<sub>2</sub>(DMSO)<sub>2</sub>] and L-alanine present in a 1:3 ratio. The precipitate in the reaction mixture was collected and analysed using mass spectrometry. The mass expected for [Pt(L-alanine)<sub>2</sub>] was detected, indicating that the synthesis was successful. <sup>1</sup>H NMR spectrometry was used to determine if the *cis* or *trans* isomer was present and the purity of the sample. The chemical shifts seen in the sample (Appendix 14) were different from the chemical shifts of *trans*-[Pt(L-alanine)<sub>2</sub>] previously detected (Appendix 2). However, the spectrum showed that large amounts of L-alanine were present in the sample. This suggests that *cis*-[Pt(L-alanine)<sub>2</sub>] was successfully synthesised but that the synthetic procedure can be further optimised to yield *cis*-[Pt(L-alanine)<sub>2</sub>] in greater purity.





L-alaninate

**Figure 2.10: Structure of L-alaninate.**

An alternative approach to synthesising *cis*-[Pt(L-alanine)<sub>2</sub>] was attempted by reacting *cis*-[PtCl<sub>2</sub>(DMSO)<sub>2</sub>] and L-alaninate (Figure 2.10) in a 1:2 ratio. This was performed to investigate if deprotonating the amine group prior to the addition of *cis*-[PtCl<sub>2</sub>(DMSO)<sub>2</sub>] would allow the displacement of ligands to occur more effectively. The use of triethylamine as a base was also reconsidered. Its addition to the acidic reaction mixture results in the formation of triethylammonium chloride, which precipitates out of the solution together with the intermediates. This salt interferes with <sup>1</sup>H NMR spectroscopy and mass spectrometry analysis as triethylammonium chloride can produce additional signals in the <sup>1</sup>H NMR spectrum that may overlap with the signals of *cis*-[Pt(L-alanine)<sub>2</sub>]. Triethylammonium chloride also forms adduct ions with the product during mass spectrometry, which can interfere with the interpretation of the data. L-alanine was first reacted with sodium hydroxide to form Na<sup>+</sup> L-alaninate. The precipitate in the reaction mixture was collected and analysed using mass spectrometry. The mass spectrometry results showed that the synthesis of *cis*-[Pt(L-alanine)<sub>2</sub>] was unsuccessful. Intermediates of the reaction were present in the reaction mixture.

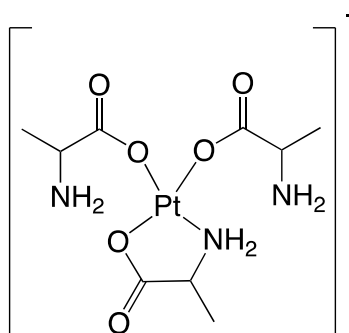
The attempts to synthesise *cis*-[Pt(L-alanine)<sub>2</sub>] in high purity using 1-butanol as a solvent were unsuccessful. The intermediates formed were insoluble in 1-butanol and precipitated out of the solution. The early precipitation of these intermediates could be affecting the synthesis of *cis*-[Pt(L-alanine)<sub>2</sub>]. Methanol was investigated as an alternative solvent to explore as it is more polar than 1-butanol. The intermediates were also found to be soluble in methanol.

#### **2.7.4 Synthesis of *cis*-[Pt(L-alanine)<sub>2</sub>] in methanol**

L-Alanine was reacted with lithium hydroxide to form lithium L-alaninate. *cis*-[PtCl<sub>2</sub>(DMSO)<sub>2</sub>] was reacted with lithium L-alaninate in a 1:2 ratio to attempt to synthesise *cis*-[Pt(L-alanine)<sub>2</sub>]. A clear solution was observed. A sample of the solution was taken and analysed using mass spectrometry, which determined that only intermediates of the synthesis were present. Additional lithium L-alaninate was added to the reaction mixture. A clear solution with a white precipitate was observed. The precipitate was separated and analysed

using mass spectrometry, which determined that  $[\text{Pt}(\text{L-alanine})_2]$  was present. However, the  $^1\text{H}$  NMR spectroscopy spectrum had multiple peaks, indicating that impurities were present in the complexes.

The deprotonation of L-alanine prior to the addition of  $\text{cis-}[\text{PtCl}_2(\text{DMSO})_2]$  was reconsidered. The synthesis was repeated with  $\text{cis-}[\text{PtCl}_2(\text{DMSO})_2]$  and L-alanine added in a 1:2 ratio, and the base was added when the pH of the reaction mixture became acidic. A clear solution with a white precipitate was observed. The precipitate was separated and dissolved in water. The water was removed slowly which produced white crystals. The crystals were analysed using mass spectrometry which identified the crystals as  $[\text{Pt}(\text{L-alanine})_2]$ .  $^1\text{H}$  NMR spectroscopy was also performed which showed that the crystals had similar chemical shifts (Appendix 19) as the previously identified  $\text{trans-}[\text{Pt}(\text{L-alanine})_2]$  (Appendix 2). This indicates that the crystals were  $\text{trans-}[\text{Pt}(\text{L-alanine})_2]$ . The  $\text{cis}$  isomer might require more time to synthesise. Additional L-alanine and lithium hydroxide were added to the reaction mixture and heated. A clear solution with a white precipitate was observed. The precipitate was collected and dissolved in water, as done previously to form crystals. The crystals formed were analysed using mass spectrometry, which detected complexes,  $[\text{Pt}(\text{L-alanine})_2]$  and  $[\text{Pt}(\text{L-alanine})_3]^-$  (Appendix 20). The crystals were then dissolved in acetone, which formed a solution with a white precipitate. The precipitate was separated and analysed using mass spectrometry which detected  $[\text{Pt}(\text{L-alanine})_2]$ .  $^1\text{H}$  NMR spectroscopy was used to determine the isomer of  $[\text{Pt}(\text{L-alanine})_2]$  present. The chemical shifts detected in the spectrum were different from the chemical shifts of  $\text{trans-}[\text{Pt}(\text{L-alanine})_2]$  complexes previously establish. This indicates that  $\text{cis-}[\text{Pt}(\text{L-alanine})_2]$  complexes had been synthesised (Appendix 21). The presence of  $[\text{Pt}(\text{L-alanine})_3]^-$  (Appendix 22) complexes indicates that too much L-alanine had been added to the reaction mixture.



Exact Mass: 459.08

**Figure 2.11: Structure of  $[\text{Pt}(\text{L-alanine})_3]^-$**

The addition of amino acids in excess had a different reaction in 1-butanol compared to methanol. In 1-butanol, an excess of L-alanine and L-isoleucine remained suspended in the reaction mixture. However, in methanol, the excess L-alanine was soluble in methanol and displaced ligands on the platinum to form  $[\text{Pt}(\text{L-alanine})_3]^-$  (Figure 2.11). This could lead to further challenges, as it may be difficult to remove the additional L-alanine bound to the platinum to form *cis*- $[\text{Pt}(\text{L-alanine})_2]$ .

The synthetic procedure was repeated with a smaller amount of L-alanine added to the reaction mixture. L-alanine was added to *cis*- $[\text{PtCl}_2(\text{DMSO})_2]$  in a 2:1 ratio. The precipitate was collected for analysis. The mass spectrometry analysis determined that  $[\text{Pt}(\text{L-alanine})_2]$  was present.  $^1\text{H}$  NMR spectroscopy was performed, which revealed that both *cis* and *trans* isomers were present. The chemical shifts seen in the spectrum were similar to *trans*- $[\text{Pt}(\text{L-alanine})_2]$  and *cis*- $[\text{Pt}(\text{L-alanine})_2]$ . An additional base was added to the remaining solution in an attempt to increase the yield of  $[\text{Pt}(\text{L-alanine})_2]$ . A clear solution with a white precipitate was formed. The precipitate was separated for analysis.  $^1\text{H}$  NMR spectroscopy revealed that the precipitate was *trans*- $[\text{Pt}(\text{L-alanine})_2]$ . Traces of acetone and DMSO were also seen in the spectrum. To determine if a higher yield of *cis*- $[\text{Pt}(\text{L-alanine})_2]$  could be synthesised from the reaction mixture, additional lithium hydroxide was added to the remaining solution. A clear solution with a white precipitate was formed. The precipitate was separated and analysed using mass spectrometry. However, only intermediates of the synthesis and  $[\text{Pt}(\text{L-alanine})_3]^-$  were detected. The solution was also collected and dried for mass spectrometry analysis which detected that only intermediates of the synthesis. The synthesis of  $[\text{Pt}(\text{L-alanine})_3]^-$  was unexpected as an excess of L-alanine had not been added to the reaction mixture. An excess of L-alanine may be required to synthesise *cis*- $[\text{Pt}(\text{L-alanine})_2]$ . However, the amount of L-alanine added must be carefully monitored to minimise the synthesis of  $[\text{Pt}(\text{L-alanine})_3]^-$ .

### 2.7.5 Synthesis of *cis*- $[\text{Pt}(\text{L-alanine})_2]$ in acetone

From the previous attempts, it was identified that the intermediates of the synthesis and  $[\text{Pt}(\text{L-alanine})_3]^-$  are soluble in acetone. However, *cis*- $[\text{Pt}(\text{L-alanine})_2]$  was found to be insoluble in acetone. Acetone was investigated as a solvent choice as it is predicted that *cis*- $[\text{Pt}(\text{L-alanine})_2]$  as it would precipitate out of the reaction mixture to collect a pure sample.

It was suggested that acetone could be a suitable solvent choice to obtain pure *cis*-[Pt(L-alanine)<sub>2</sub>] as it would precipitate out of the reaction mixture. *cis*-[PtCl<sub>2</sub>(DMSO)<sub>2</sub>] and L-alanine were reacted in a 1:2 ratio to attempt to synthesise *cis*-[Pt(L-alanine)<sub>2</sub>]. A yellow solution with a white precipitate was observed. The precipitate was separated and analysed using <sup>1</sup>H NMR spectroscopy. The synthesis did not occur as expected. <sup>1</sup>H NMR spectroscopy revealed many impurities present, which made the spectrum difficult to read. Additional lithium hydroxide was added to the solution. The precipitate was separated and analysed using both mass spectrometry and <sup>1</sup>H NMR spectroscopy. However, platinum complexes were not detected in either spectrum. The solvent in reaction mixture solution was removed, and the oil formed was analysed using mass spectrometry. Only intermediates of the synthesis were present. It was determined that acetone may not be a suitable solvent for the synthesis of *cis*-[Pt(L-alanine)<sub>2</sub>].

### **2.8 Reaction conditions for optimal synthesis of *cis*-[Pt(L-alanine)<sub>2</sub>]**

The synthetic procedures were performed in different conditions to determine the best conditions to optimise the synthesis of *cis*-[Pt(L-alanine)<sub>2</sub>]. It was determined that the synthesis must be performed in the dark as light exposure may lead to the platinum degradation. The reaction mixture must be heated and stirred to increase the rate of the reaction. The reaction mixture was heated to 70 °C without any traces of decomposition seen. Methanol was determined to be a suitable solvent for the synthesis of *cis*-[Pt(L-alanine)<sub>2</sub>] over 1-butanol and acetone. Other solvents should be investigated when developing synthetic procedures involving different amino acids based on their polarities. After the first batch of *cis*-[Pt(L-alanine)<sub>2</sub>] is collected, it is possible to increase the yield by adding more L-alanine and base to the reaction mixture. However, the addition of L-alanine should be performed carefully to reduce the formation of [Pt(L-alanine)<sub>3</sub>]<sup>-</sup>. It is also recommended to monitor the pH of the reaction mixture as an indicator if an additional base or L-alanine is required. Future experiments can be performed to identify reaction conditions to optimise the synthesis of *cis*-[Pt(L-alanine)<sub>2</sub>].

### **2.9 Conclusion**

*trans*-bis(amino acid)platinum(II) complexes were identified as unsuitable precursors for the synthesis of platinum(IV)-glutamine complexes due to their poor solubility and formation of geometric isomers during oxidation. *cis*-[PtCl<sub>2</sub>(DMSO)<sub>2</sub>] was explored as a starting material for the synthesis of *cis*-bis(amino acid)platinum(II) complexes. A new synthetic scheme to

synthesise *cis*-[Pt(L-alanine)<sub>2</sub>] in high purity was explored. It was hypothesised that only one intermediate and the *cis* isomer would be synthesised due to the systematic displacement of *cis*-[PtCl<sub>2</sub>(DMSO)<sub>2</sub>] ligands (Figure 2.1) Various reaction conditions were evaluated to design an appropriate synthetic pathway. Although *cis*-[Pt(L-alanine)<sub>2</sub>] was successfully synthesised, various intermediates were also present. Future steps involve the 2 to ensure that it is suitable for cytotoxicity studies to determine the biological inertness of *cis*-[Pt(L-alanine)<sub>2</sub>]. If found to be inert, the complex can be used as a precursor for the synthesis of platinum (IV)-glutamine complexes.

*CHAPTER 3: TRANSPORT OF  
MODIFIED GLUTAMINE  
COMPLEXES VIA ASCT2*

### 3.1 Introduction

ASCT2 is overexpressed in various cancer types to accommodate their increased glutamine needs. This makes ASCT2 a potential target for anticancer therapy. The aim was to study the transport of modified glutamine compounds in oocytes expressing human ASCT2 (hASCT2). This study was conducted prior to synthesising platinum(IV)-glutamine complexes to first elucidate if modification of glutamine impacts its recognition and transport via ASCT2. This is essential to identify if ASCT2 is a suitable transporter to selectively deliver platinum(IV)-glutamine complexes into cancer cells.

#### 3.1.1 Mechanism of amino acid transport of ASCT2

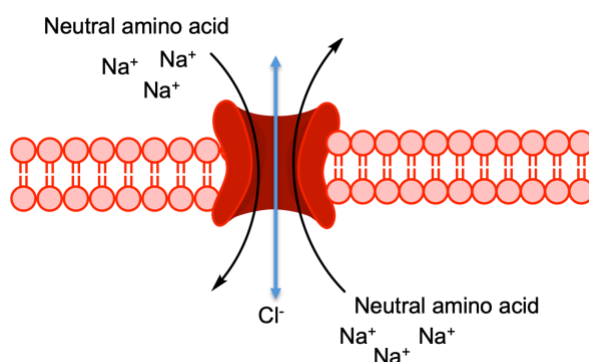


**Figure 3.1: Mechanism of amino acid transport of ASCT2.**

A substrate and 3 Na<sup>+</sup> ions bind at the helical hairpin (HP) 2 of the transport domain which allows the translocation of the domain through the plasma membrane. The HP2 gate opens at the cytoplasmic environment allowing the release of the substrate and 3 Na<sup>+</sup> ions into the cell. As ASCT2 functions as an obligatory exchanger, another neutral amino acid and 3 Na<sup>+</sup> ions will be transported from the intracellular to the extracellular environment<sup>132</sup>. This transport process activates the flow of anions through the transporter, which creates a charge movement across the membrane<sup>133,134</sup>. The figure was created using BioRender.com.

### 3.1.2 Compound 1

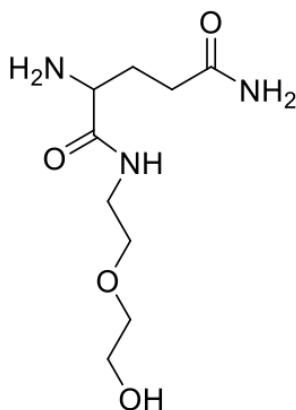


**Figure 3.2: Structure of Compound 1**

Compound 1 (C<sub>9</sub>H<sub>12</sub>N<sub>3</sub>O<sub>4</sub>) was used to study the transport of modified glutamine compounds via ASCT2. 2-(2-aminoethoxy)ethanol was attached to the  $\alpha$ -carboxylic acid of L-glutamine via peptide coupling reaction. This compound was synthesised by Dr. Adnan Bani-Saad.

### 3.1.3 Compound 2 (L-theanine)

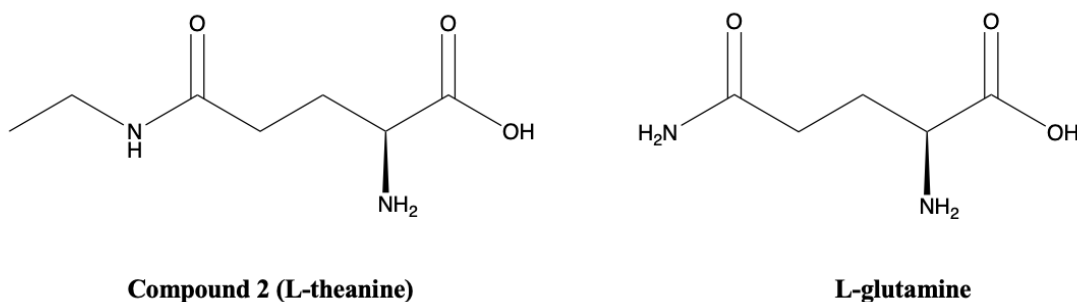


**Figure 3.3: L-theanine, an analogue of L-glutamine**

Compound 2 (L-theanine) was also used to study the transport of modified glutamine compounds via ASCT2. L-theanine is an analog of glutamine which has an additional ethyl group on the amide nitrogen. L-theanine used was purchased from Chem Supply Pty Ltd.

## 3.2 Methods and Materials

All materials used were purchased from Sigma-Aldrich (Merck) unless stated otherwise.

### 3.2.1 Harvesting of *Xenopus laevis* oocytes

*Xenopus laevis* oocytes were supplied by the Victor Chang Cardiac Research Institute and approved by the Garvan Institute/St Vincents Hospital Animal Ethics Committee (Animal



Research Authority 23\_11) under the Australian Code of Practice for the Care and Use of Animals for Scientific Purposes. Stage. Oocytes were defolliculated by agitation with 1.5-1.7 mg/mL collagenase A (Roche) at 18 °C for 30 to 60 minutes. Isolated oocytes were then given a series of rinses as follows; five rinses in OR-2, 10 rinses in ND96 (96 mM NaCl, 2 mM KCl, 1 mM MgCl<sub>2</sub>, 1.8 mM CaCl<sub>2</sub>, 5 mM hemisodium-HEPES, pH 7.5) and two rinses in ND96 storage buffer (ND96 supplemented with 50 µg/ml gentamycin, 2.5 mM sodium pyruvate, 50 µg/ml tetracycline and 0.5 mM theophylline).

### **3.2.2 Production of human ASCT2 RNA**

The hASCT2 clone in the vector pcDNA3.1+C-eGFP was subcloned into pOTV by Dr. Natasha Freidman. Plasmid DNA was obtained and transformed into NEB<sup>®</sup> 5- alpha Competent E. coli cells (New England BioLabs Inc), following manufacturer's instructions then purified using GeneJET Plasmid Miniprep Kit (Thermo Fisher Scientific). The plasmid DNA was linearised using restriction enzyme Spe1 (New England BioLabs Inc) and purified with Phenol Chloroform Isoamyl-Alcohol and Phenol Isoamyl-Alcohol. The sequence of the complementary DNA (cDNA) products was confirmed by the Australian Genome Research Facility. Linear DNA was transcribed using T7 RNA polymerase with AMBION mMACHINE<sup>™</sup> T7 transcription kit (Invitrogen<sup>™</sup>, Thermo Fisher Scientific). Messenger RNA (mRNA) was diluted with RNase-free water (Thermo Fisher Scientific) to form 300 ng/µL hASCT2 mRNA.

### **3.2.3 Oocytes microinjection**

Healthy stage V defolliculated oocytes that were spherical and lacking follicular membrane were selected and microinjected with 23 nL hASCT2 mRNA. Injection needles were made with 3.5' Drummond glass capillaries (Drummond Scientific Company) using a PC-100 microelectrode puller (Narishige). Injected oocytes were stored at 18 °C in ND96 buffer and shaken for three days to allow the expression of hASCT2 on the oocytes cell membrane.

### **3.2.4 Electrophysiology studies**

Current recordings were measured using two-electrode voltage clamp electrophysiology with a Geneclamp 500 amplifier (Axon Instruments) and a MacLab 2e chart recorder (ADInstruments). LabChart (version 8) (ADInstruments) and Digidata 1322A (Axon Instruments) controlled by an IBM-compatible computer with pClamp (version 10.6)

(Molecular Devices) were used. Compounds of interest were dissolved in NO<sub>3</sub><sup>-</sup> buffer (96 mM NaNO<sub>3</sub>, 2 mM KNO<sub>3</sub>, 1 mM Mg(NO<sub>3</sub>)<sub>2</sub>, 6H<sub>2</sub>O, 1.8 mM Ca(NO<sub>3</sub>)<sub>2</sub>, and 5 mM hemisodium HEPES, pH 7.5). The solutions were applied to oocytes through perfusion into the recording bath where they are held and washed out with NO<sub>3</sub><sup>-</sup> buffer between applications. The magnitude of current activated by a compound was measured as the conductance recorded during application subtracted by the conductance recorded immediately before application. The recording bath was grounded using a salt bridge containing 3 M KCl and 3% agarose gel which was connected to a 3 M KCl reservoir to minimise offset potentials. Oocytes expressing hASCT2 were clamped at -30 mV. Voltage pulses at 10 mV intervals between -100 mV to +60 mV were applied to oocytes every 150 milliseconds to generate current-voltage (IV) plots.

### 3.2.5 Substrate dose-response relationship

Dose-response relationships were measured by applying a range of concentrations of a single compound to oocytes expressing hASCT2. IV plots were generated as described above and the currents measured at +60 mV were taken from each plot. Currents measured at +60 mV were used to plot the dose-response curves as the largest amplitude of currents was measured at that voltage. Data was processed using GraphPad Prism (Version 9.5.1). The data was fitted to the Michaelis-Menten equation using the least square fit:

$$I / I_{max} = [S] / (K_m + [S])$$

$I$  = substrate-elicited current at +60 mV,  $I_{max}$  = maximum response,  $S$  = substrate concentrations, and  $K_m$  = substrate concentration required to reach half-maximum response.

Data was normalised to the predicted maximal current for each substrate ( $I_{max}$ ).

## 3.3 Results

### 3.3.1 Substrate dose-response curve

The dose-response of known substrates of ASCT2 - L-glutamine and L-serine was measured. The substrates were applied to oocytes expressing hASCT2 clamped at -30 mV. The substrates were applied in a range of concentrations (1 to 1000  $\mu$ M) and voltage pulses at 10 mV intervals between -100 to +60 mV were applied to oocytes every 150 milliseconds to generate current-voltage (IV) plots. The currents measured at +60 mV were taken and normalised to the predicted maximal current ( $I_{max}$ ). The data must be normalised to the  $I_{max}$  as the expression of

transporters in the oocytes can change over time after their injection, affecting the observed current magnitudes. Application of both L-glutamine and L-serine generated outward currents, elicited by the activation of an uncoupled anion conductance (Figure 3.4). Increased currents were measured as higher concentrations of the substrates were applied until the saturating concentration was reached. L-Serine was also identified to have a lower affinity for ASCT2 than L-glutamine (Table 3.1). No current was observed when L-glutamine was applied to uninjected oocytes at identical concentrations (Figure 3.5). This confirms that the currents elicited are a direct result of the expression of hASCT2 on the oocyte cell membrane and further verifies that the uncoupled anion conductance is activated by the exchange of 3 Na<sup>+</sup> ions and the substrate from the intracellular to the extracellular environment.

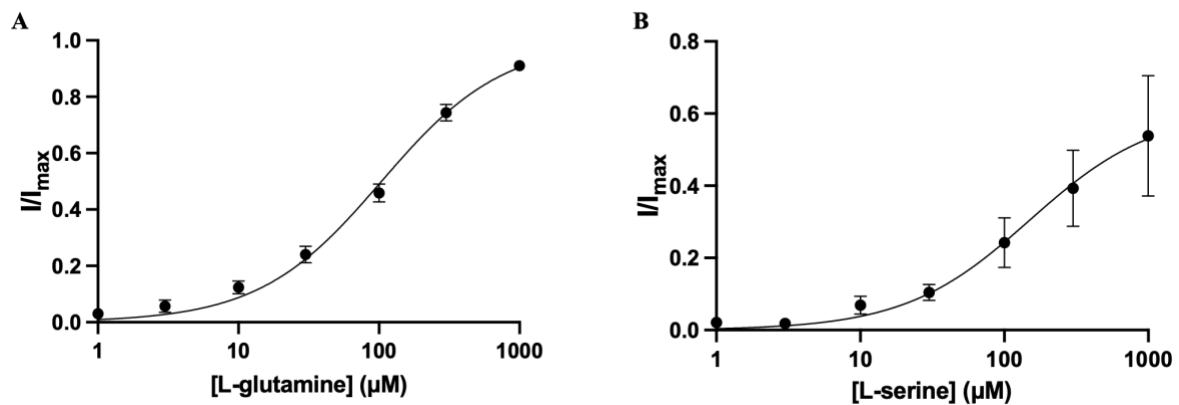


**Figure 3.4: Dose-response relationship of known substrates.** Dose-response relationships were measured by currents elicited during the application of L-glutamine (A) and L-serine (B) in oocytes expressing hASCT2 at +60 mV in  $\text{NO}_3^-$  buffer. Data for each cell were normalised to the  $I_{max}$  for each substrate. Data analysis was performed using GraphPad Prism (Version 9.5.1). Each dot point represents the mean signal response from 5 individual cells ( $n = 5$ ). Data are presented as mean  $\pm$  SEM. Experiments were replicated three times, across two different batches of oocytes. Both substrates show increased currents elicited as increased concentrations of the substrates were applied.

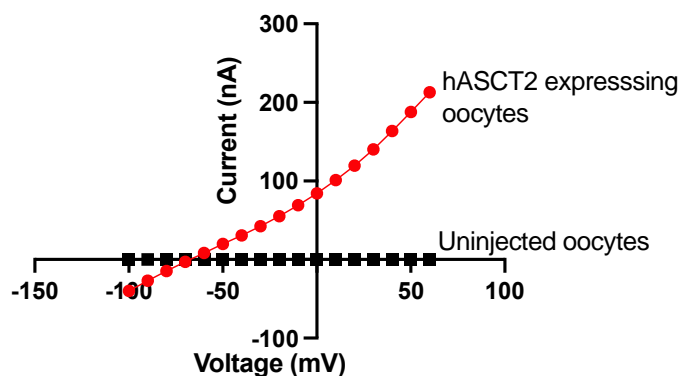


**Figure 3.5: Current-voltage relationship elicited by L-glutamine.** L-glutamine (100  $\mu\text{M}$ ) was applied to oocytes expressing hASCT2 (red) and to uninjected oocytes (black) clamped at -30 mV. Outward currents that reversed in direction at approximately -60 mV were measured when L-glutamine was applied to oocytes expressing hASCT2. No measurable current was detected when L-glutamine was applied to uninjected oocytes. Data analysis was performed using GraphPad (Version 9.5.1).

**Table 3.1: Calculated substrate  $K_m$  and  $I_{max}$  values and  $\pm$  SEM at +60 mV for ASCT2.**

Substrate	$K_m$ ( $\mu\text{M}$ )	$I_{max}$ ( $\mu\text{M}$ )
L-glutamine	$62 \pm 16$	$357 \pm 34$
L-serine	$177 \pm 20$	$707 \pm 46$

Application of both L-glutamine and L-serine generated outward currents when applied to oocytes expressing hASCT2. L-Serine has a lower affinity for ASCT2 ( $K_m = 177 \pm 20 \mu\text{M}$ ) compared to L-glutamine ( $K_m = 62 \pm 16 \mu\text{M}$ ). Increased currents were elicited as increased concentrations of L-glutamine and L-serine were applied to oocytes until the saturating concentrations of L-glutamine ( $I_{max} = 357 \pm 34 \mu\text{M}$ ) and L-serine ( $I_{max} = 700 \pm 46 \mu\text{M}$ ) were reached.

### 3.2.2 Compound 1 transport studies

Compound 1 (300  $\mu\text{M}$ , 1mM) was applied to oocytes expressing hASCT2 with known substrates, L-glutamine (100  $\mu\text{M}$ ) and L-serine (100  $\mu\text{M}$ ), and a known inhibitor benzylserine (1 mM) used as control compounds. The compounds were applied to oocytes clamped at -30 mV for approximately 60 seconds. Oocytes were washed with  $\text{NO}_3^-$  buffer for approximately 60 seconds between each application. Data was obtained from LabChart (version 8), and the

trace was plotted in GraphPad Prism (Version 9.5.1). IV plots were also generated and plotted in GraphPad Prism (Version 9.5.1). Current-voltage relationships of compound 1 (300  $\mu\text{M}$ ) + L-serine (100  $\mu\text{M}$ ) were recorded with L-serine (100  $\mu\text{M}$ ) used as a control. No measurable current was detected when compound 1 was applied to oocytes (Figure 3.6A). Current-voltage relationship elicited by compound 1 was also measured which consistently showed no measurable currents (Figure 3.6B) being elicited across 5 oocytes. This indicates that compound 1 is not a substrate or inhibitor of ASCT2. To confirm that compound 1 is not an inhibitor of ASCT2, compound 1 (300  $\mu\text{M}$ ) + L-serine (100  $\mu\text{M}$ ) was applied to oocytes expressing hASCT2. A decrease in currents elicited was not seen compared to the currents elicited during the application of L-serine (100  $\mu\text{M}$ ) (Figure 3.6C). This further shows that compound 1 is not an inhibitor of ASCT2.

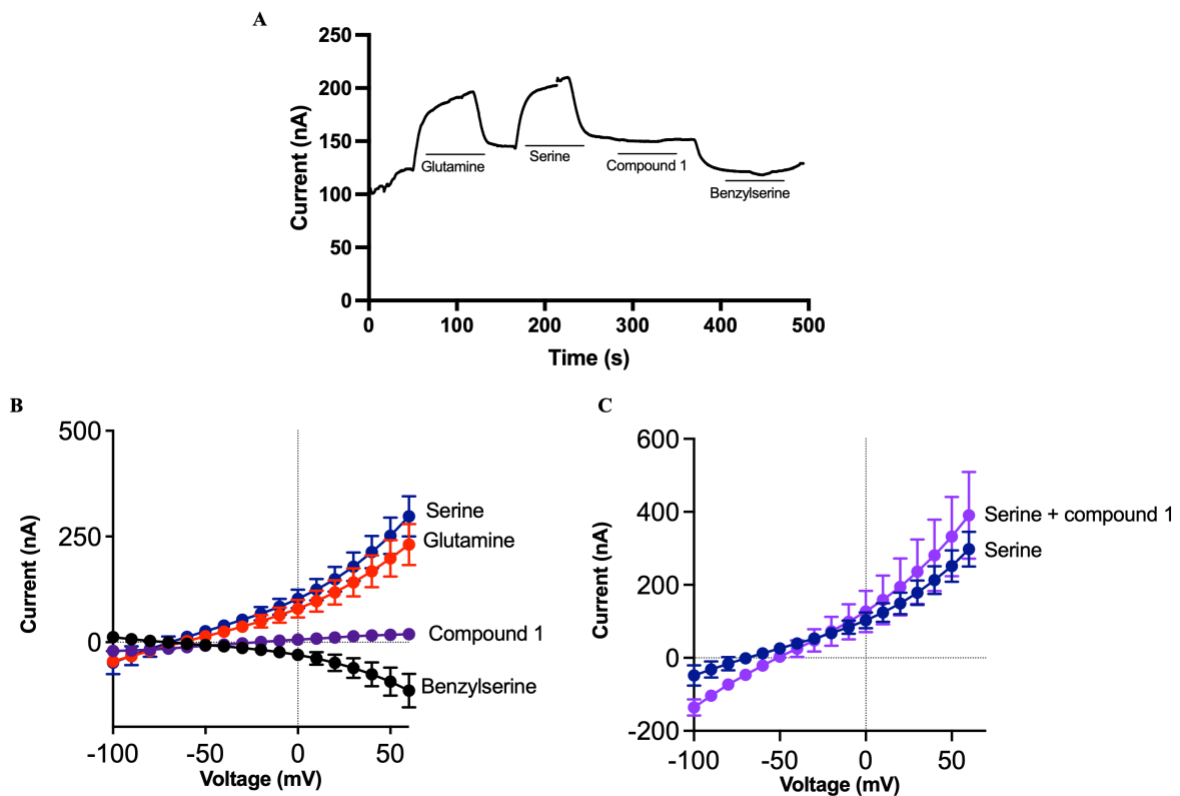


**Figure 3.6: Transport of compound 1 in oocytes expressing hASCT2 clamped at -30 mV in  $\text{NO}_3^-$  buffer.** (A) Representative traces of currents elicited during the application of L-glutamine (100  $\mu\text{M}$ ), L-serine (100  $\mu\text{M}$ ), compound 1 (1 mM) and benzylserine (1 mM) as labelled in the figure. The trace was obtained by measuring currents elicited by a single oocyte at 0.25 seconds intervals. (B) Current-voltage relationship elicited by L-serine (100  $\mu\text{M}$ ) (blue), L-glutamine (100  $\mu\text{M}$ ) (red), compound 1 (300  $\mu\text{M}$ ) (purple), and benzylserine (1 mM) (black).

(C) Current-voltage relationship elicited by L-serine (100  $\mu$ M) + compound 1 (300  $\mu$ M) (purple) and L-serine (100  $\mu$ M) (blue). (B and C) Each dot point represents the mean signal response from 5 individual cells ( $n = 5$ ). Data are presented as mean  $\pm$  SEM. Experiments were replicated three times, across two different batches of oocytes. Data analysis was performed using GraphPad (Version 9.5.1). Compound 1 is neither a substrate nor an inhibitor of ASCT2. Scale of each figure is different.

### **3.33 L-theanine transport studies**

L-Theanine (1 mM) was applied to oocytes expressing hASCT2 clamped at -30 mV with known substrates L-glutamine (100  $\mu$ M) and L-serine (100  $\mu$ M) and a known inhibitor benzylserine (1 mM) used as control compounds. IV plots were generated and plotted in GraphPad Prism (Version 9.5.1). Current-voltage relationships of L-theanine (1 mM) + L-serine (100  $\mu$ M) and L-theanine (1 mM) + L-glutamine (100  $\mu$ M) were recorded with L-glutamine (100  $\mu$ M) and L-serine (100  $\mu$ M) used as controls. Application of L-glutamine and L-serine to oocytes expressing hASCT2 produced outward currents (Figure 3.7A) while application of L-theanine produced inward currents similar to those produced by the inhibitor benzylserine (Figure 3.7D). This suggests that L-theanine is an inhibitor of ASCT2. Further studies were performed to confirm that L-theanine is an inhibitor of ASCT2. L-theanine (1 mM) + L-serine (100  $\mu$ M) was applied to oocytes expressing hASCT2. A decrease in currents elicited was observed compared to the application of L-serine (100  $\mu$ M) alone (Figure 3.7C). A decrease in currents elicited was also observed when L-theanine (1 mM) + L-glutamine (100  $\mu$ M) was applied compared to L-glutamine (100  $\mu$ M) alone (Figure 3.7B). This confirms that L-theanine is an inhibitor of ASCT2, inhibiting the transport of its substrates.

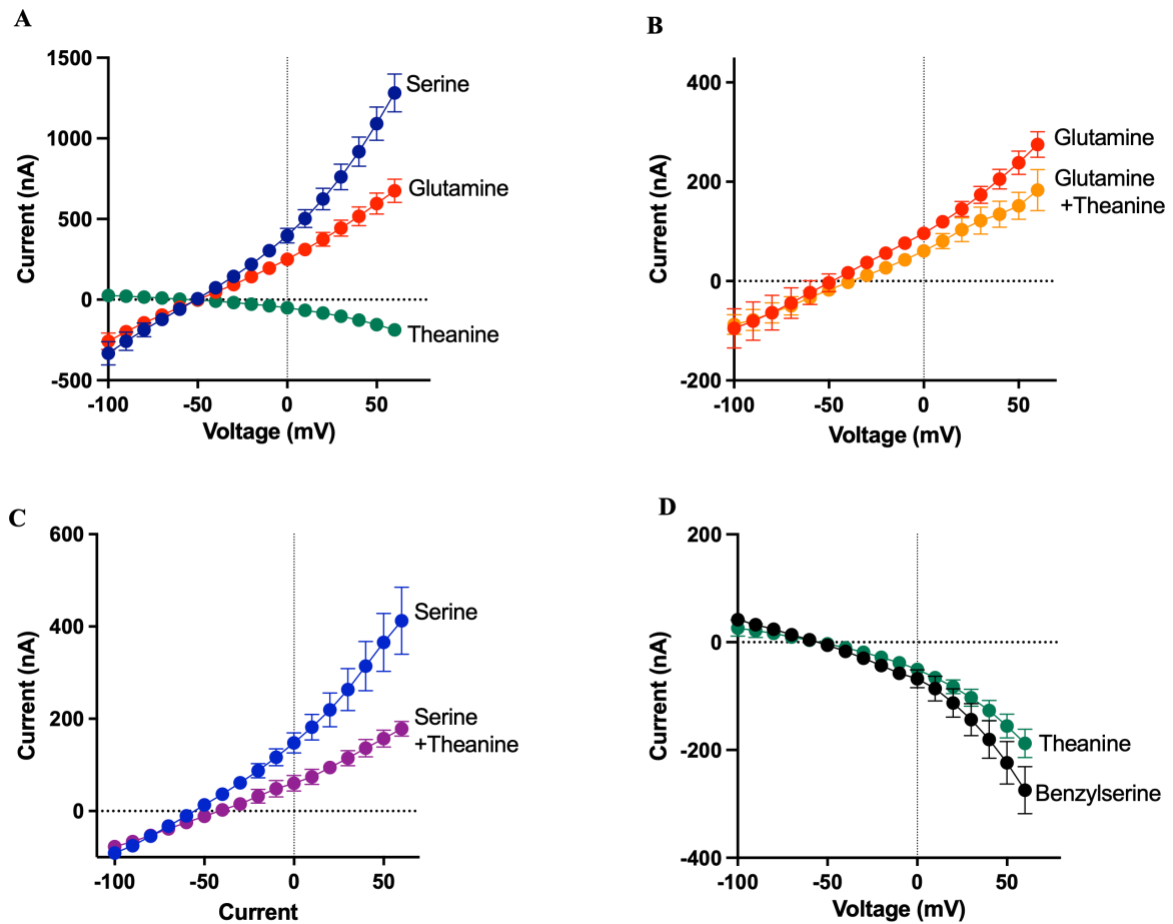


**Figure 3.7: Transport of theanine in oocytes expressing hASCT2 clamped at -30 mV in  $\text{NO}_3^-$  buffer.** (A) Current-voltage relationship elicited by L-serine (1 mM) (blue), L-glutamine (1 mM) (red), and L-theanine (1 mM) (green). (B) Current-voltage relationship elicited by L-glutamine (100  $\mu\text{M}$ ) (red) and L-glutamine (100  $\mu\text{M}$ ) + L-theanine (1 mM) (orange). (C) Current-voltage relationship elicited by L-serine (100  $\mu\text{M}$ ) (blue) and L-serine (100  $\mu\text{M}$ ) + L-theanine (1 mM) (purple). (D) Current-voltage relationship elicited by benzylserine (1 mM) (black) and L-theanine (1 mM) (green). (A-D) Each dot point represents the mean signal response from 5 individual cells ( $n = 5$ ). Data are presented as mean  $\pm$  SEM. Experiments were replicated three times, across two different batches of oocytes. Data analysis was performed using GraphPad (Version 9.5.1). Scale of each figure is different.

### 3.4 Discussion

*Xenopus laevis* oocytes were used as a model to study the transport of modified glutamine compounds (compound 1, L-theanine) in ASCT2. *Xenopus laevis* oocytes have been used in research for decades to perform electrophysiology experiments using two-electrode voltage clamps to study membrane transport. Oocytes are used to isolate transporters to effectively

study their behaviours. Oocytes are a suitable choice as mature oocytes are fairly large (1-1.2 mm), allowing them to be prepared, injected, and tested easily<sup>149</sup>. Electrophysiology experiments are also conducted with stage V oocytes as they have the lowest number of endogenous transport systems present in their membrane at this stage. This allows transporters to be studied background-free in many cases<sup>150</sup>. Oocytes also have a fully equipped translational machinery and can effectively translate heterologous mRNA and cDNA-derived cRNA. This allows the high expression of recombinant proteins at the cell surface needed for transport studies<sup>151</sup>.

Dose-response relationships were obtained using known substrates of ASCT2, L-glutamine and L-serine.  $\text{NO}_3^-$  buffer was used for the experiments as it has a higher permeability through the anion-gated channel, allowing more robust currents to be measured<sup>133,134</sup>. The currents measured are not directly produced by the movement of substrates and  $\text{Na}^+$  ions in ASCT2. They are produced by the influx of  $\text{NO}_3^-$  ions in the anion-gated channel which occurs during substrate transport<sup>133,152</sup>. Increased currents were measured as increasing concentrations of the substrates were applied to oocytes expressing hASCT2 (Figure 3.4). A similar pattern was seen by Scopelliti *et al.* who studied the dose-response relationships of L-glutamine and L-serine in oocytes expressing hASCT2 at +60 mV in  $\text{NO}_3^-$  buffer<sup>134</sup>.

L-Serine ( $K_m = 177 \pm 20 \mu\text{M}$ ) has a lower affinity to ASCT2 than L-glutamine ( $K_m = 62 \pm 16 \mu\text{M}$ ). The predicted maximal current for each substrate ( $I_{max}$ ) was also calculated, L-glutamine ( $I_{max} = 357 \pm 34 \mu\text{M}$ ) and L-serine ( $I_{max} = 707 \pm 46 \mu\text{M}$ ) (Table 3.1). The  $I_{max}$  indicates the saturating substrate concentrations of ASCT2. This information may be valuable when applying platinum(IV)-glutamine complexes to cells to prevent overdosing cells which may have toxic side effects.

Compound 1 was applied to oocytes expressing hASCT2 with known substrates, L-glutamine and L-serine and a known inhibitor, benzylserine used as controls. It was hypothesised that compound 1 would be readily transported by ASCT2 as it has a hydrophilic side chain which prevents its transport into cells via passive diffusion. It was also believed that compound 1 was structurally similar enough to L-glutamine to allow its recognition at ASCT2. Compound 1 consistently elicited no currents during its application to oocytes and remained at  $\text{NO}_3^-$  baseline levels ( $n = 5$ ) (Figure 3.6A, 3.6B). Compound 1 + L-serine was applied to oocytes expressing



hASCT2. A decrease in currents elicited was not measured when compound 1 was present (Figure 3.6C), confirming that compound 1 is not an inhibitor of L-serine transport via ASCT2. Compound 1 is neither a substrate nor an inhibitor of ASCT2. This suggests that compound 1 may be unable to bind on the transport domain of ASCT2, preventing the translocation of the transport domain down the lipid bilayer required for the exchange of substrates and Na<sup>+</sup> ions to take place. Garaeva *et al.* suggested that bulkier substrates may prevent the closure of HP2 affecting their transport in ASCT2<sup>132</sup>. This is supported by Albers *et al.* who suggest that the activity of transporter substrates decreases strongly as the side chain volume reaches or threshold or if the compound has a bulky hydrophobic group<sup>152</sup>. Despite 2-(2-aminoethoxy)ethanol being hydrophilic, attaching it to glutamine may have made compound 1 too large for transport via ASCT2. These results were an important finding as they facilitated the redesign of the platinum(IV)-glutamine complex. The complex must be transported in ASCT2 to selectively deliver drugs to cancer cells overexpressing ASCT2.

Based on the results obtained from compound 1, modification of L-glutamine at its side chain with a decreased length of the linker was explored. L-theanine was selected for transport studies in ASCT2 as it is a structural analog of L-glutamine and met the criteria of our new design. L-theanine is a non-essential amino acid that is not produced by the human body. It is abundantly present in green tea leaves<sup>153</sup>.

L-theanine was applied to oocytes expressing hASCT2 with known substrates, L-glutamine and L-serine and a known inhibitor, benzylserine, were used as controls. It was hypothesised that L-theanine would be transported in ASCT2 as it is structurally similar to L-glutamine and its  $\alpha$ -carboxylic acid and amine group were unmodified. Application of L-theanine elicited inward currents similar to those measured during the application of benzylserine (Figure 3.7D). Inward currents are observed when inhibitors are applied to ASCT2 as they block the tonic leak anion conductance. Freidman *et al.* also observed inward currents when benzylserine (1 mM) was applied to oocytes expressing hASCT2 clamped at -30 mV in NO<sub>3</sub><sup>-</sup> buffer<sup>131</sup>. This suggests that L-theanine is acting as an inhibitor of ASCT2 and blocks the leak of NO<sub>3</sub><sup>-</sup> conductance. The application of substrates L-glutamine and L-serine in the presence of L-theanine to oocytes expressing hASCT2 revealed a decrease in currents elicited. A greater decrease in currents was also measured when L-theanine was applied with L-serine compared to L-glutamine. The results suggest that L-theanine binds to ASCT2, inhibiting the transport of L-glutamine and L-serine.

L-theanine was found to be an inhibitor of ASCT2 which is still an important finding. Inhibitors can be used to starve cancer cells of glutamine, impacting their growth. This behaviour was observed in endometrial carcinoma overexpressing ASCT2 by Marshall *et al.* where certain endometrial cell lines showed reduced growth when treated with known ASCT2 inhibitors, benzylserine and L- $\gamma$ -Glutamyl-p-nitroanilide (GPNA)<sup>154</sup>. The literature also states that L-theanine has anti-cancer properties. Liu *et al.* observed a significant inhibitory effect on the migration of non-small cell lung cancer cells (A549) after treating them with theanine for 6 hours<sup>155</sup>. Xin *et al.* also found that the application of L-theanine induced human hepatoblastoma (HepG2) cell death under glutamine-restricted conditions via the caspase-9-dependent and caspase-independent mitochondrial pathways<sup>156</sup>. The identification of L-theanine as an inhibitor of ASCT2 could provide a further understanding of the mechanism of its anticancer effects.

### **3.5 Conclusion**

It was identified that the modification of L-glutamine impacts its transport in ASCT2. Compound 1 is neither a substrate nor an inhibitor of ASCT2. Attaching a 2-(2-aminoethoxy)ethanol linker at the  $\alpha$ -carboxylic acid of L-glutamine could have made compound 1 too large for transport in ASCT2. Modification of the  $\alpha$ -carboxylic acid of L-glutamine could also have affected its recognition at the transporter. L-Theanine (compound 2) was used as it has a shorter side chain and is unmodified at the  $\alpha$ -carboxylic acid and amine groups. L-theanine was identified as an inhibitor of ASCT2, which could potentially explain its anticancer effects reported in literature.

*CHAPTER 4: SUMMARY OF  
PROJECT*

#### 4.1 Summary of project

The primary objective was to study the transport of biologically inert platinum(IV)-glutamine complexes into cancer cells to investigate if platinum(II) drugs can be selectively delivered to cancer cells by exploiting the overexpression of certain glutamine transporters on cancer cells, which occurs to meet the increased glutamine demands of cancer cells<sup>130</sup>. This study is essential to overcome the challenges of current platinum(II) drugs used in clinics such as cisplatin, carboplatin, and oxaliplatin. These drugs are toxic and enter cells non-specifically via passive diffusion, which results in the death of both cancerous and healthy cells<sup>19</sup>. They can also lead to severe side effects<sup>12,21,23</sup> and the development of drug resistance<sup>17</sup>. To study the transport of platinum(IV)-glutamine complexes into cancer cells, biologically inert platinum(II) complexes were synthesised to effectively study their transport and behaviour in cancer cells while avoiding cellular apoptosis. These platinum(II) complexes can subsequently be oxidised into their platinum(IV) state and attached to L-glutamine via a hydrophilic linker. The synthesis of bis(amino acid)platinum(II) complexes that are analogs of oxaliplatin was prioritised. It was hypothesised that attaching amino acids to the platinum in a bidentate manner would prevent the displacement of the ligands inside the cell, preventing the formation of reactive and toxic platinum(II) species. *trans*-[Pt(L-alanine)<sub>2</sub>] was synthesised using the Dhara method first reported in 1970, which is widely used to synthesise cisplatin<sup>144</sup>. Cytotoxicity studies were performed which confirmed that *trans*-[Pt(L-alanine)<sub>2</sub>] is not significantly cytotoxic when administered to A549 cells at a concentration below 1 mM. However, *trans*-[Pt(L-alanine)<sub>2</sub>] had poor solubility in water and many organic solvents, making oxidation challenging. A similar pattern was observed with *trans*-[Pt(glycine)<sub>2</sub>]. Although it was successfully synthesised into its platinum(IV) state, *trans*-[Pt(glycine)<sub>2</sub>(OH)<sub>2</sub>] was insoluble in water and organic solvents, preventing the synthesis of platinum(IV)-glutamine complexes using *trans*-[Pt(glycine)<sub>2</sub>] as a precursor. Additionally, the possibility of geometric isomer formation at each step of the platinum(IV)-glutamine complex synthesis when using *trans* complexes as precursors was also a concern. The presence of these isomers can make the purification of *trans*-platinum(IV) complexes challenging and result in a lower yield of products. Thus, *trans*-bis(amino acid)platinum(II) complexes were deemed unsuitable precursors of the synthesis of platinum(IV)-glutamine complexes due to their poor solubility and formation of geometric isomers during oxidation. A new procedure to synthesis *cis*-bis(amino acid)platinum(II) complexes using *cis*-[PtCl<sub>2</sub>(DMSO)<sub>2</sub>] as a starting material was attempted. It was hypothesised that suspending *cis*-[PtCl<sub>2</sub>(DMSO)<sub>2</sub>] in a solvent with two equivalents of amino acid and a

base, will lead to the synthesis of *cis*-bis(amino acid)platinum(II) complexes in high purity. This synthetic procedure was first explored using different amino acids such as L-isoleucine, L-tryptophan, and L-alanine. L-Tryptophan was deemed unsuitable for the synthesis of *cis*-bis(amino acid)platinum(II) complexes due to its instability in reaction mixtures. L-Alanine was selected to refine and optimise the synthetic procedures as it is a small amino acid with a non-bulky side chain, which may allow for easier and more effective complexation compared to L-isoleucine. It was found that using *cis*-[PtCl<sub>2</sub>(DMSO)<sub>2</sub>] as a starting material led to the synthesis of both *cis* and *trans* isomers. Although *trans*-bis(amino acid)platinum(II) complexes are unsuitable for the synthesis of the platinum(IV)-glutamine complexes, this synthetic procedure could still be valuable for researchers aiming to synthesise both *cis* and *trans*-bis(amino acid)platinum(II) complexes. This synthetic procedure is also beneficial as it prevents the decomposition of the platinum and requires a shorter reaction time. The Dhara method requires the conversion of K<sub>2</sub>PtCl<sub>4</sub> to K<sub>2</sub>PtI<sub>4</sub> in situ<sup>157</sup> while *cis*-[PtCl<sub>2</sub>(DMSO)<sub>2</sub>] can be directly reacted with amino acids, expediting the synthesis process. *cis*-[Pt(L-alanine)<sub>2</sub>] was successfully synthesised but the purification process was challenging due to the presence of various intermediates with similar solubility in water and solvents. Further exploration is needed to obtain pure *cis*-[Pt(L-alanine)<sub>2</sub>] complexes. While developing an optimal synthetic procedure of *cis*-[Pt(L-alanine)<sub>2</sub>] complexes, it was concurrently investigated if the modification of L-glutamine would still allow its recognition by ASCT2 transporters. The transport of modified L-glutamine compounds into ASCT2 was studied using *Xenopus laevis* oocyte as a model using two-electrode voltage clamp electrophysiology. ASCT2 was explored, as the transporter is overexpressed in many different types of cancers and has been identified as a potential target for anticancer therapy<sup>130</sup>. Compound 1 was synthesised by attaching a 2-(2-aminoethoxy)ethanol linker to the  $\alpha$ -carboxylic acid of L-glutamine. Compound 1 was found to neither be a substrate nor an inhibitor of ASCT2 as no measurable currents were elicited when applied to *Xenopus laevis* oocytes expressing ASCT2. It is possible that compound 1 is too large for transport via ASCT2 or that the modification of the  $\alpha$ -carboxylic acid of L-glutamine affected its recognition at the transporter. The transport of L-theanine (compound 2) was explored as it is an analog of glutamine with a shorter side chain and is unmodified at the  $\alpha$ -carboxylic acid and amine groups. L-theanine was identified as an inhibitor of ASCT2, eliciting inward currents when applied to *Xenopus laevis* oocytes expressing ASCT2, similar to benzylserine a known ASCT2 inhibitor. This could explain its potential anticancer effects discussed in literature<sup>154,155,156</sup> as it inhibits the transport of L-glutamine via ASCT2, reducing L-glutamine intake by cancer cells. The studies of compound 1 and L-

theanine found that modification of L-glutamine either at its  $\alpha$ -carboxylic acid or R group, prevents it from acting as a substrate of ASCT2. This leads to challenges as platinum(IV)-glutamine complexes must be readily transported via glutamine transporters to selectively deliver these complexes to cancer cells. Further studies are essential to identify if glutamine transporters are a suitable target for the selective delivery of anticancer drugs.

#### **4.2 Future work**

Further research is crucial to design a modified glutamine compound that is transported via ASCT2. If any modification to L-glutamine still prevents its transport via ASCT2, alternative glutamine transporters that are overexpressed in cancer cells should be investigated. The Sodium-Dependent Neutral Amino Acid Transporters (SNATs) 1 and 2 are suitable alternatives as these transporters are overexpressed in cancer cells as well. Further studies are also required to optimise the synthesis of *cis*-bis(amino acid)platinum(II) complexes using *cis*-[PtCl<sub>2</sub>(DMSO)<sub>2</sub>] as a starting material. Although the synthesis of *cis*-[Pt(L-alanine)<sub>2</sub>] was successful, its purification process must be further explored to effectively separate it from *trans*-[Pt(L-alanine)<sub>2</sub>] and intermediates of the synthesis present. Different experimental conditions such as the solvents used, or the ratio of amino acids and base used can be further explored to develop a synthetic procedure that can yield *cis*-[Pt(L-alanine)<sub>2</sub>] in high purity and yield. Cytotoxic studies should also be performed on *cis*-[Pt(L-alanine)<sub>2</sub>] to confirm its biological inertness. The complexes should also be oxidised into their platinum(IV) state to confirm that they are suitable for the synthesis of platinum(IV)-glutamine complexes. These additional studies should be performed to meet the objectives of studying the transport of biologically inert platinum(IV)-glutamine complexes into glutamine transporters that are overexpressed in cancer cells.

## REFERENCES

1. Ma, X.; Yu, H., Cancer issue: global burden of cancer. *The Yale journal of biology and medicine* **2006**, *79* (3-4), 85.
2. von Meyenfeldt, M., Cancer-associated malnutrition: an introduction. *European Journal of Oncology Nursing* **2005**, *9*, S35-S38.
3. Hanahan, D.; Weinberg, R. A., The hallmarks of cancer. *Cell* **2000**, *100* (1), 57-70.
4. Weinberg, R. A., How cancer arises. *Sci.Am.* **1996**, *275* (3), 62-70.
5. Aldossary, S. A., Review on pharmacology of cisplatin: clinical use, toxicity and mechanism of resistance of cisplatin. *Biomedical and Pharmacology Journal* **2019**, *12* (1), 7-15.
6. Oppenheimer, S. B., Cellular basis of cancer metastasis: A review of fundamentals and new advances. *Acta Histochemica* **2006**, *108* (5), 327-334.
7. Floor, S. L.; Dumont, J. E.; Maenhaut, C.; Raspe, E., Hallmarks of cancer: of all cancer cells, all the time? *Trends Mol. Med* **2012**, *18* (9), 509-515.
8. Pilleron, S.; Sarfati, D.; Janssen-Heijnen, M.; Vignat, J.; Ferlay, J.; Bray, F.; Soerjomataram, I., Global cancer incidence in older adults, 2012 and 2035: A population-based study. *Int. J. Cancer* **2019**, *144* (1), 49-58.
9. Gonzalez, V. M.; Fuertes, M. A.; Alonso, C.; Perez, J. M., Is cisplatin-induced cell death always produced by apoptosis? *Mol. Pharmacol.* **2001**, *59* (4), 657-663.
10. Cohen, S. M.; Lippard, S. J., Cisplatin: From DNA damage to cancer chemotherapy. In *Progress in Nucleic Acid Research and Molecular Biology*, Moldave, K., Ed. Elsevier Academic Press Inc: San Diego, **2001**; Vol. 67, pp 93-130.
11. Tsvetkova, D.; Ivanova, S., Application of Approved Cisplatin Derivatives in Combination Therapy against Different Cancer Diseases. *Molecules* **2022**, *27* (8), 2466.
12. Johnstone, T. C.; Suntharalingam, K.; Lippard, S. J., The Next Generation of Platinum Drugs: Targeted Pt(II) Agents, Nanoparticle Delivery, and Pt(IV) Prodrugs. *Chemical Reviews* **2016**, *116* (5), 3436-3486.
13. Krieger, M. L.; Eckstein, N.; Schneider, V.; Koch, M.; Royer, H. D.; Jaehde, U.; Bendas, G., Overcoming cisplatin resistance of ovarian cancer cells by targeted liposomes in vitro. *International Journal of Pharmaceutics* **2010**, *389* (1-2), 10-17.
14. Wheate, N. J.; Walker, S.; Craig, G. E.; Oun, R., The status of platinum anticancer drugs in the clinic and in clinical trials. *Dalton Trans.* **2010**, *39* (35), 8113-8127.
15. Santabarbara, G.; Maione, P.; Rossi, A.; Gridelli, C., Pharmacotherapeutic options for treating adverse effects of Cisplatin chemotherapy. *Expert Opinion on Pharmacotherapy* **2016**, *17* (4), 561-570.
16. Petrović, M.; Todorović, D., Biochemical and Molecular Mechanisms of Action of Cisplatin in Cancer Cells. *Facta Universitatis, Series: Medicine & Biology* **2016**, *18* (1).
17. Klein, A. V.; Hambley, T. W., Platinum Drug Distribution in Cancer Cells and Tumors. *Chemical Reviews* **2009**, *109* (10), 4911-4920.
18. Makovec, T., Cisplatin and beyond: molecular mechanisms of action and drug resistance development in cancer chemotherapy. *Radiol. Oncol.* **2019**, *53* (2), 148-158.
19. Kelland, L., The resurgence of platinum-based cancer chemotherapy. *Nat. Rev. Cancer* **2007**, *7* (8), 573-584.
20. Alderden, R. A.; Hall, M. D.; Hambley, T. W., The discovery and development of cisplatin. *Journal of Chemical Education* **2006**, *83* (5), 728-734.
21. Ivanov, A. I.; Christodoulou, J.; Parkinson, J. A.; Barnham, K. J.; Tucker, A.; Woodrow, J.; Sadler, P. J., Cisplatin binding sites on human albumin. *J. Biol. Chem.* **1998**, *273* (24), 14721-14730.

22. Messori, L.; Merlino, A., Cisplatin binding to proteins: A structural perspective. *Coord. Chem. Rev.* **2016**, *315*, 67-89.
23. Urien, S.; Lokiec, F., Population pharmacokinetics of total and unbound plasma cisplatin in adult patients. *British Journal of Clinical Pharmacology* **2004**, *57* (6), 756-763.
24. Kool, M.; deHaas, M.; Scheffer, G. L.; Scheper, R. J.; vanEijk, M. J. T.; Juijn, J. A.; Baas, F.; Borst, P., Analysis of expression of cMOAT (MRP2), MRP3, MRP4, and MRP5, homologues of the multidrug resistance-associated protein gene (MRP1), in human cancer cell lines. *Cancer Res.* **1997**, *57* (16), 3537-3547.
25. Zhang, C. Y.; Xu, C.; Gao, X. Y.; Yao, Q. Q., Platinum-based drugs for cancer therapy and anti-tumor strategies. *Theranostics* **2022**, *12* (5), 2115-2132.
26. Browning, R. J.; Reardon, P. J. T.; Parhizkar, M.; Pedley, R. B.; Edirisinghe, M.; Knowles, J. C.; Stride, E., Drug Delivery Strategies for Platinum-Based Chemotherapy. *ACS Nano* **2017**, *11* (9), 8560-8578.
27. Yu, C. Q.; Wang, Z. B.; Sun, Z. R.; Zhang, L.; Zhang, W. W.; Xu, Y. G.; Zhang, J. J., Platinum-Based Combination Therapy: Molecular Rationale, Current Clinical Uses, and Future Perspectives. *Journal of Medicinal Chemistry* **2020**, *63* (22), 13397-13412.
28. Wang, D.; Lippard, S. J., Cellular processing of platinum anticancer drugs. *Nat. Rev. Drug Discov.* **2005**, *4* (4), 307-320.
29. Ventura, G.; Nardella, M. I.; Panella, A.; Arnesano, F.; Calvano, C. D.; Losito, I.; Palmisano, F.; Cataldi, T. R. I., Structural Elucidation of Cisplatin and Hydrated cis-Diammineplatinum(II) Complex Conjugated with Cyanocobalamin by Liquid Chromatography with Electrospray Ionization-Mass Spectrometry and Multistage Mass Spectrometry. *ASC Omega* **2018**, *3* (10), 12914-12922.
30. Tchounwou, P. B.; Dasari, S.; Noubissi, F. K.; Ray, P.; Kumar, S., Advances in our understanding of the molecular mechanisms of action of cisplatin in cancer therapy. *Journal of experimental pharmacology* **2021**, *13*, 303.
31. Lilley, D. M. J., Cisplatin adducts in DNA: Distortion and recognition. *J. Biol. Inorg. Chem.* **1996**, *1* (3), 189-191.
32. Florea, A.-M.; Büsselberg, D., Cisplatin as an anti-tumor drug: cellular mechanisms of activity, drug resistance and induced side effects. *Cancers* **2011**, *3* (1), 1351-1371.
33. Wong, E.; Giandomenico, C. M., Current status of platinum-based antitumor drugs. *Chemical Reviews* **1999**, *99* (9), 2451-2466.
34. Reedijk, J., Improved understanding in platinum antitumor chemistry. *Chemical Communications* **1996**, (7), 801-806.
35. Cubeddu, L. X.; Hoffmann, I. S.; Fuenmayor, N. T.; Finn, A. L., Efficacy of Ondansetron (Gr-38032f) and the Role of Serotonin in Cisplatin-Induced Nausea and Vomiting. *New England Journal of Medicine* **1990**, *322* (12), 810-816.
36. Cohen, L.; de Moor, C. A.; Eisenberg, P.; Ming, E. E.; Hu, H., Chemotherapy-induced nausea and vomiting-incidence and impact on patient quality of life at community oncology settings. *Support. Care Cancer* **2007**, *15* (5), 497-503.
37. Malik, I. A.; Khan, W. A.; Qazilbash, M.; Ata, E.; Butt, A.; Khan, M. A., Clinical efficacy of lorazepam in prophylaxis of anticipatory, acute, and delayed nausea and vomiting induced by high doses of cisplatin. A prospective randomized trial. *Am. J. Clin. Oncol.-Cancer Clin. Trials* **1995**, *18* (2), 170-175.
38. Kris, M. G.; Gralla, R. J.; Clark, R. A.; Tyson, L. B.; Oconnell, J. P.; Wertheim, M. S.; Kelsen, D. P., Incidence, course, and severity of delayed nausea and vomiting following the administration of high-dose cisplatin. *J. Clin. Oncol.* **1985**, *3* (10), 1379-1384.



39. Troy, L.; McFarland, K.; Littman-Power, S.; Kelly, B. J.; Walpole, E. T.; Wyld, D.; Thomson, D., Cisplatin-based therapy: A neurological and neuropsychological review. *Psycho-Oncol.* **2000**, *9* (1), 29-39.
40. Kearsley, J. H.; Williams, A. M.; Fiumara, A. M., Antiemetic superiority of lorazepam over oxazepam and methylprednisolone as premedicants for patients receiving cisplatin-containing chemotherapy. *Cancer* **1989**, *64* (8), 1595-1599.
41. Almanric, K.; Marceau, N.; Cantin, A.; Bertin, E., Risk Factors for Nephrotoxicity Associated with Cisplatin. *Can. J. Hosp. Pharm.* **2017**, *70* (2), 99-106.
42. Yao, X.; Panichpisal, K.; Kurtzman, N.; Nugent, K., Cisplatin nephrotoxicity: A review. *Am. J. Med. Sci.* **2007**, *334* (2), 115-124.
43. Zazuli, Z.; Vijverberg, S.; Slob, E.; Liu, G.; Carleton, B.; Veltman, J.; Baas, P.; Masereeuw, R.; Maitland-van der Zee, A. H., Genetic Variations and Cisplatin Nephrotoxicity: A Systematic Review. *Front. Pharmacol.* **2018**, *9*, 17.
44. Hanigan, M. H.; Devarajan, P., Cisplatin nephrotoxicity: molecular mechanisms. *Cancer therapy* **2003**, *1*, 47.
45. Karasawa, T.; Steyger, P. S., An integrated view of cisplatin-induced nephrotoxicity and ototoxicity. *Toxicology Letters* **2015**, *237* (3), 219-227.
46. Cornelison, T. L.; Reed, E., Nephrotoxicity and hydration management for cisplatin, carboplatin, and ormaplatin. *Gynecol. Oncol.* **1993**, *50* (2), 147-158.
47. Astolfi, L.; Ghiselli, S.; Guaran, V.; Chicca, M.; Simoni, E.; Olivetto, E.; Lelli, G.; Martini, A., Correlation of adverse effects of cisplatin administration in patients affected by solid tumours: A retrospective evaluation. *Oncol. Rep.* **2013**, *29* (4), 1285-1292.
48. Wolf, S.; Barton, D.; Kottschade, L.; Grothey, A.; Loprinzi, C., Chemotherapy-induced peripheral neuropathy: Prevention and treatment strategies. *Eur. J. Cancer* **2008**, *44* (11), 1507-1515.
49. Ozols, R. F.; Young, R. C. In *High-dose cisplatin therapy in ovarian cancer*, Seminars in oncology, 1985; pp 21-30.
50. Thompson, S. W.; Davis, L. E.; Kornfeld, M.; Hilgers, R. D.; Standefer, J. C., Cisplatin neuropathy. Clinical, electrophysiologic, morphologic, and toxicologic studies. *Cancer* **1984**, *54* (7), 1269-1275.
51. Amptoulach, S.; Tsavaris, N., Neurotoxicity caused by the treatment with platinum analogues. *Chemotherapy research practice* **2011**, *2011*.
52. Von Hoff, D.; Schilsky, R.; Reichert, C.; Reddick, R.; Rozenzweig, M.; Young, R.; Muggia, F., Toxic effects of cis-dichlorodiammineplatinum (II) in man. *Cancer treatment reports* **1979**, *63* (9-10), 1527-1531.
53. Ohmichi, M.; Hayakawa, J.; Tasaka, K.; Kurachi, H.; Murata, Y., Mechanisms of platinum drug resistance. *Trends in pharmacological sciences* **2005**, *26* (3), 113-116.
54. Stewart, D. J., Mechanisms of resistance to cisplatin and carboplatin. *Crit. Rev. Oncol./Hematol.* **2007**, *63* (1), 12-31.
55. Mortensen, A. C. L.; Mohajershojai, T.; Hariri, M.; Pettersson, M.; Spiegelberg, D., Overcoming Limitations of Cisplatin Therapy by Additional Treatment With the HSP90 Inhibitor Onalespib. *Frontiers in Oncology* **2020**, *10*, 15.
56. Shimolina, L.; Gulin, A.; Ignatova, N.; Druzhkova, I.; Gubina, M.; Lukina, M.; Snopova, L.; Zagaynova, E.; Kuimova, M. K.; Shirmanova, M., The Role of Plasma Membrane Viscosity in the Response and Resistance of Cancer Cells to Oxaliplatin. *Cancers* **2021**, *13* (24), 18.
57. Preta, G., New Insights Into Targeting Membrane Lipids for Cancer Therapy. *Front. Cell. Dev. Biol.* **2020**, *8*, 10.
58. Holzer, A. K.; Howell, S. B., The internalization and degradation of human copper transporter 1 following cisplatin exposure. *Cancer Res.* **2006**, *66* (22), 10944-10952.

59. Kenny, R. G.; Chuah, S. W.; Crawford, A.; Marmion, C. J., Platinum(IV) Prodrugs - A Step Closer to Ehrlich's Vision? *Eur. J. Inorg. Chem.* **2017**, (12), 1596-1612.
60. Sliesoraitis, S.; Chikhale, P., Carboplatin hypersensitivity. *International Journal of Gynecologic Cancer* **2005**, *15* (1).
61. Desoize, B.; Madoulet, C., Particular aspects of platinum compounds used at present in cancer treatment. *Crit. Rev. Oncol./Hematol.* **2002**, *42* (3), 317-325.
62. Perego, P.; Robert, J., Oxaliplatin in the era of personalized medicine: from mechanistic studies to clinical efficacy. *Cancer Chemother. Pharmacol.* **2016**, *77*, 5-18.
63. Stordal, B.; Pavlakis, N.; Davey, R., Oxaliplatin for the treatment of cisplatin-resistant cancer: a systematic review. *Cancer treatment reviews* **2007**, *33* (4), 347-357.
64. Hector, S.; Bolanowska-Higdon, W.; Zdanowicz, J.; Hitt, S.; Pendyala, L., In vitro studies on the mechanisms of oxaliplatin resistance. *Cancer Chemother. Pharmacol.* **2001**, *48* (5), 398-406.
65. Saris, C.; van de Vaart, P. M.; Rietbroek, R.; Bloramaert, F., In vitro formation of DNA adducts by cisplatin, lobaplatin and oxaliplatin in calf thymus DNA in solution and in cultured human cells. *Carcinogenesis* **1996**, *17* (12), 2763-2769.
66. Raymond, E.; Chaney, S. G.; Taamma, A.; Cvitkovic, E., Oxaliplatin: A review of preclinical and clinical studies. *Ann. Oncol.* **1998**, *9* (10), 1053-1071.
67. Xu, Z.; Wang, Z.; Deng, Z.; Zhu, G., Recent advances in the synthesis, stability, and activation of platinum (IV) anticancer prodrugs. *Coordination Chemistry Reviews* **2021**, *442*, 213991.
68. Zhang, S. R.; Wang, X. Y.; Guo, Z. J., Rational design of anticancer platinum(IV) prodrugs. In *Medicinal Chemistry*, Sadler, P. J.; VanEldik, R., Eds. Elsevier Academic Press Inc: San Diego, 2020; Vol. 75, pp 149-182.
69. Wang, Z. G.; Deng, Z. Q.; Zhu, G. Y., Emerging platinum(IV) prodrugs to combat cisplatin resistance: from isolated cancer cells to tumor microenvironment. *Dalton Trans.* **2019**, *48* (8), 2536-2544.
70. Gibson, D., Platinum(IV) anticancer prodrugs - hypotheses and facts. *Dalton Trans.* **2016**, *45* (33), 12983-12991.
71. Wexselblatt, E.; Yavin, E.; Gibson, D., Platinum(IV) Prodrugs with Haloacetato Ligands in the Axial Positions can Undergo Hydrolysis under Biologically Relevant Conditions. *Angew. Chem.-Int. Edit.* **2013**, *52* (23), 6059-6062.
72. Jovanovic, S.; Petrovic, B.; Bugarcic, Z. D.; van Eldik, R., Reduction of some Pt(IV) complexes with biologically important sulfur-donor ligands. *Dalton Transactions* **2013**, *42* (24), 8890-8896.
73. Dilruba, S.; Kalayda, G. V., Platinum-based drugs: past, present and future. *Cancer Chemother. Pharmacol.* **2016**, *77* (6), 1103-1124.
74. Tolbatov, I.; Coletti, C.; Marrone, A.; Re, N., Insight into the Electrochemical Reduction Mechanism of Pt(IV) Anticancer Complexes. *Inorg. Chem.* **2018**, *57* (6), 3411-3419.
75. Wexselblatt, E.; Gibson, D., What do we know about the reduction of Pt (IV) prodrugs? *Journal of inorganic biochemistry* **2012**, *117*, 220-229.
76. Mi, Q.; Shu, S.; Yang, C.; Gao, C.; Zhang, X.; Luo, X.; Bao, C.; Zhang, X.; Niu, J., Current status for oral platinum (IV) anticancer drug development. *International Journal of Medical Physics, Clinical Engineering and Radiation Oncology* **2018**, *7* (02), 231.
77. Freeman, A. I.; Mayhew, E., Targeted drug delivery. *Cancer* **1986**, *58* (S2), 573-583.
78. Winau, F.; Westphal, O.; Winau, R., Paul Ehrlich - in search of the magic bullet. *Microbes Infect.* **2004**, *6* (8), 786-789.

79. Strebhardt, K.; Ullrich, A., Paul Ehrlich's magic bullet concept: 100 years of progress. *Nature Reviews Cancer* **2008**, *8* (6), 473-480.
80. Tewabe, A.; Abate, A.; Tamrie, M.; Seyfu, A.; Siraj, E. A., Targeted drug delivery—from magic bullet to nanomedicine: principles, challenges, and future perspectives. *Journal of Multidisciplinary Healthcare* **2021**, *14*, 1711.
81. Lewis, L., Editor's view Cancer pharmacotherapy: 21st century 'magic bullets' and changing paradigms. *Br. J. Clin. Pharmacol.* **2006**, *62* (1), 1.
82. Zhong, Y.; Jia, C.; Zhang, X.; Liao, X.; Yang, B.; Cong, Y.; Pu, S.; Gao, C., Targeting drug delivery system for platinum (IV)-Based antitumor complexes. *European Journal of Medicinal Chemistry* **2020**, *194*, 112229.
83. Bazak, R.; Hourri, M.; El Achy, S.; Hussein, W.; Refaat, T., Passive targeting of nanoparticles to cancer: A comprehensive review of the literature. *Mol. Clin. Oncol.* **2014**, *2* (6), 904-908.
84. Akhtar, M. J.; Ahamed, M.; Alhadlaq, H. A.; Alrokayan, S. A.; Kumar, S., Targeted anticancer therapy: Overexpressed receptors and nanotechnology. *Clinica Chimica Acta* **2014**, *436*, 78-92.
85. Zhao, J.; Hua, W.; Xu, G.; Gou, S., Biotinylated platinum (IV) complexes designed to target cancer cells. *Journal of Inorganic Biochemistry* **2017**, *176*, 175-180.
86. Huang, R.; Wang, Q.; Zhang, X.; Zhu, J.; Sun, B., Trastuzumab-cisplatin conjugates for targeted delivery of cisplatin to HER2-overexpressing cancer cells. *Biomedicine Pharmacotherapy* **2015**, *72*, 17-23.
87. Ma, J.; Liu, H. F.; Xi, Z. Q.; Hou, J. Z.; Li, Y. G.; Niu, J.; Liu, T.; Bi, S. N.; Wang, X.; Wang, C. J.; Wang, J. J.; Xie, S. Q.; Wang, P. G., Protected and De-protected Platinum(IV) Glycoconjugates With GLUT1 and OCT2-Mediated Selective Cancer Targeting: Demonstrated Enhanced Transporter-Mediated Cytotoxic Properties in vitro and in vivo. *Front. Chem.* **2018**, *6*, 15.
88. Wang, X. Y.; Wang, X. H.; Guo, Z. J., Functionalization of Platinum Complexes for Biomedical Applications. *Accounts Chem. Res.* **2015**, *48* (9), 2622-2631.
89. Warburg, O., The metabolism of carcinoma cells. *The Journal of Cancer Research* **1925**, *9* (1), 148-163.
90. Kim, J. W.; Dang, C. V., Cancer's molecular sweet tooth and the Warburg effect. *Cancer Res.* **2006**, *66* (18), 8927-8930.
91. Kim, H. H.; Joo, H.; Kim, T.-H.; Kim, E.-Y.; Park, S.-J.; Park, J.-K.; Kim, H.-J., The mitochondrial Warburg effect: a cancer enigma. *Interdisciplinary Bio Central* **2009**, *1* (2), 7.1-7.7.
92. Chambers, J. W.; Maguire, T. G.; Alwine, J. C., Glutamine Metabolism Is Essential for Human Cytomegalovirus Infection. *J. Virol.* **2010**, *84* (4), 1867-1873.
93. Chen, X. Z.; Qian, Y. R.; Wu, S. Y., The Warburg effect: Evolving interpretations of an established concept. *Free Radic. Biol. Med.* **2015**, *79*, 253-263.
94. Koppenol, W. H.; Bounds, P. L.; Dang, C. V., Otto Warburg's contributions to current concepts of cancer metabolism. *Nat. Rev. Cancer* **2011**, *11* (8), 618-618.
95. Macheda, M. L.; Rogers, S.; Best, J. D., Molecular and cellular regulation of glucose transporter (GLUT) proteins in cancer. *Journal of cellular physiology* **2005**, *202* (3), 654-662.
96. Fu, J. J.; Yang, J. X.; Seeberger, P. H.; Yin, J., Glycoconjugates for glucose transporter-mediated cancer-specific targeting and treatment. *Carbohydr. Res.* **2020**, *498*, 8.
97. Patra, M.; Johnstone, T. C.; Suntharalingam, K.; Lippard, S. J., A potent glucose-platinum conjugate exploits glucose transporters and preferentially accumulates in cancer cells. *Angewandte Chemie* **2016**, *128* (7), 2596-2600.

98. Pliszka, M.; Szablewski, L., Glucose transporters as a target for anticancer therapy. *Cancers* **2021**, *13* (16), 4184.
99. Chen, Z.; Lu, W. Q.; Garcia-Prieto, C.; Huang, P., The Warburg effect and its cancer therapeutic implications. *J. Bioenerg. Biomembr.* **2007**, *39* (3), 267-274.
100. Labow, B. I.; Souba, W. W., Glutamine. *World J.Surg.* **2000**, *24* (12), 1503-1513.
101. Smith, R. J.; Wilmore, D. W., Glutamine nutrition and requirements. *J. Parenter. Enter. Nutr.* **1990**, *14* (4), S94-S99.
102. Hensley, C. T.; Wasti, A. T.; DeBerardinis, R. J., Glutamine and cancer: cell biology, physiology, and clinical opportunities. *J. Clin. Invest.* **2013**, *123* (9), 3678-3684.
103. Pallett, L. J.; Dimeloe, S.; Sinclair, L. V.; Byrne, A. J.; Schurich, A., A glutamine ‘tug-of-war’: targets to manipulate glutamine metabolism for cancer immunotherapy. *Immunotherapy Advances* **2021**, *1* (1), Itab010.
104. Melis, G. C.; ter Wengel, N.; Boelens, P. G.; van Leeuwen, P. A. M., Glutamine: recent developments in research on the clinical significance of glutamine. *Curr. Opin. Clin. Nutr. Metab. Care* **2004**, *7* (1), 59-70.
105. Bott, A. J.; Maimouni, S.; Zong, W. X., The Pleiotropic Effects of Glutamine Metabolism in Cancer. *Cancers* **2019**, *11* (6), 16.
106. Ellinger, S., Micronutrients, arginine, and glutamine: does supplementation provide an efficient tool for prevention and treatment of different kinds of wounds? *Advances in wound care* **2014**, *3* (11), 691-707.
107. Ganapathy, V.; Thangaraju, M.; Prasad, P. D., Nutrient transporters in cancer: Relevance to Warburg hypothesis and beyond. *Pharmacology & Therapeutics* **2009**, *121* (1), 29-40.
108. Garcia-Bermudez, J.; Williams, R. T.; Guarecuco, R.; Birsoy, K., Targeting extracellular nutrient dependencies of cancer cells. *Mol. Metab.* **2020**, *33*, 67-82.
109. Patra, M.; Awuah, S. G.; Lippard, S. J., Chemical approach to positional isomers of glucose–platinum conjugates reveals specific cancer targeting through glucose-transporter-mediated uptake in vitro and in vivo. *J. Am. Chem. Soc.* **2016**, *138* (38), 12541-12551.
110. Scalise, M.; Pochini, L.; Galluccio, M.; Console, L.; Indiveri, C., Glutamine Transport and Mitochondrial Metabolism in Cancer Cell Growth. *Front. Oncol.* **2017**, *7*, 9.
111. Nguyen, T.-L.; Durán, R. V., Glutamine metabolism in cancer therapy. *Cancer Drug Resistance* **2018**, *1* (3), 126-138.
112. Vanhove, K.; Derveaux, E.; Graulus, G. J.; Mesotten, L.; Thomeer, M.; Noben, J. P.; Guedens, W.; Adriaensens, P., Glutamine Addiction and Therapeutic Strategies in Lung Cancer. *International Journal of Molecular Sciences* **2019**, *20* (2), 17.
113. De Vitto, H.; Perez-Valencia, J.; Radosevich, J. A., Glutamine at focus: versatile roles in cancer. *Tumor Biology* **2016**, *37* (2), 1541-1558.
114. Goldsmith, J.; Levine, B.; Debnath, J., Autophagy and cancer metabolism. *Methods in enzymology* **2014**, *542*, 25-57.
115. Choi, Y. K.; Park, K. G., Targeting Glutamine Metabolism for Cancer Treatment. *Biomol. Ther.* **2018**, *26* (1), 19-28.
116. Zhao, Y. Q.; Zhao, X.; Chen, V.; Feng, Y.; Wang, L.; Croniger, C.; Conlon, R. A.; Markowitz, S.; Fearon, E.; Puchowicz, M.; Brunengraber, H.; Hao, Y. J.; Wang, Z. H., Colorectal cancers utilize glutamine as an anaplerotic substrate of the TCA cycle in vivo. *Scientific Reports* **2019**, *9*, 9.
117. Alkan, H. F.; Bogner-Strauss, J. G., Maintaining cytosolic aspartate levels is a major function of the TCA cycle in proliferating cells. *Mol. Cell Oncol.* **2019**, *6* (5), 3.
118. Mitsch, M. J.; Cowie, A.; Finan, T. M., Malic enzyme cofactor and domain requirements for symbiotic N<sub>2</sub> fixation by *Sinorhizobium meliloti*. *Journal of bacteriology* **2007**, *189* (1), 160-168.

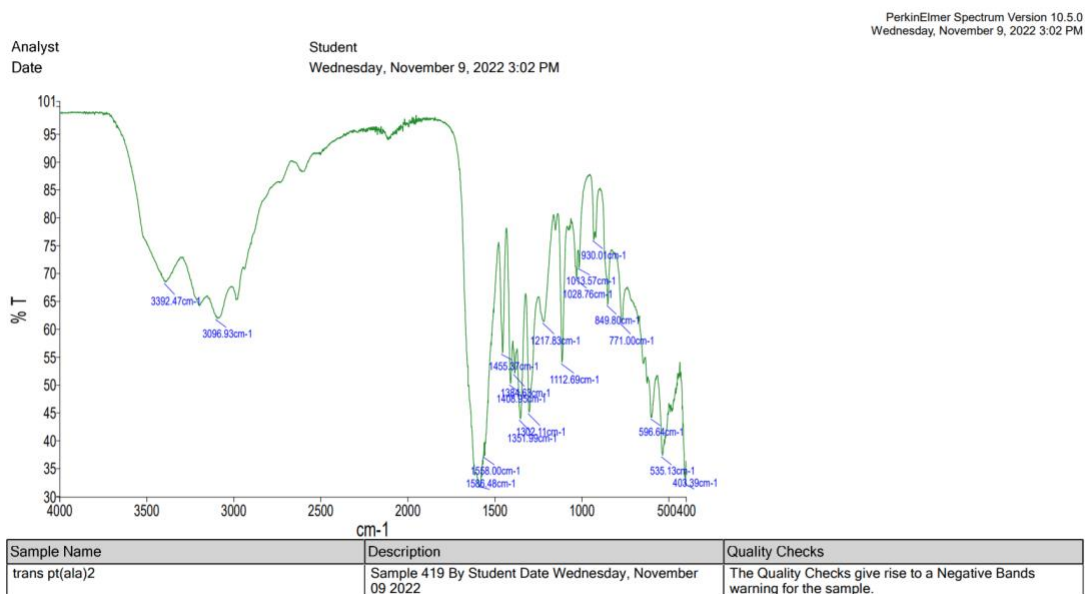
119. DeBerardinis, R. J.; Mancuso, A.; Daikhin, E.; Nissim, I.; Yudkoff, M.; Wehrli, S.; Thompson, C. B., Beyond aerobic glycolysis: Transformed cells can engage in glutamine metabolism that exceeds the requirement for protein and nucleotide synthesis. *Proc. Natl. Acad. Sci. U. S. A.* **2007**, *104* (49), 19345-19350.
120. Pan, S.; Fan, M.; Liu, Z.; Li, X.; Wang, H., Serine, glycine and one-carbon metabolism in cancer. *International Journal of Oncology* **2021**, *58* (2), 158-170.
121. Le, A., *The heterogeneity of cancer metabolism*. Springer Nature: 2021.
122. Natarajan, S. K.; Venneti, S., Glutamine metabolism in brain tumors. *Cancers* **2019**, *11* (11), 1628.
123. DeBerardinis, R. J.; Cheng, T., Q's next: the diverse functions of glutamine in metabolism, cell biology and cancer. *Oncogene* **2010**, *29* (3), 313-324.
124. Geeraerts, S. L.; Heylen, E.; De Keersmaecker, K.; Kampen, K. R., The ins and outs of serine and glycine metabolism in cancer. *Nature metabolism* **2021**, *3* (2), 131-141.
125. Balendiran, G. K.; Dabur, R.; Fraser, D., The role of glutathione in cancer. *Cell Biochem. Funct.* **2004**, *22* (6), 343-352.
126. Han, C., Glutamine Metabolism: A New Target Pathway for PET Imaging and Cancer Therapy. *Cancer* **2019**, *3*, 4.
127. Rubio-Aliaga, I.; Wagner, C. A., Regulation and function of the SLC38A3/SNAT3 glutamine transporter. *Channels* **2016**, *10* (6), 440-452.
128. Bhutia, Y. D.; Ganapathy, V., Glutamine transporters in mammalian cells and their functions in physiology and cancer. *Biochim. Biophys. Acta-Mol. Cell Res.* **2016**, *1863* (10), 2531-2539.
129. Wang, Q.; Hardie, R. A.; Hoy, A. J.; Van Geldermalsen, M.; Gao, D.; Fazli, L.; Sadowski, M. C.; Balaban, S.; Schreuder, M.; Nagarajah, R., Targeting ASCT2-mediated glutamine uptake blocks prostate cancer growth and tumour development. *The Journal of pathology* **2015**, *236* (3), 278-289.
130. Scalise, M.; Pochini, L.; Galluccio, M.; Console, L.; Indiveri, C., Glutamine transporters as pharmacological targets: From function to drug design. *Asian journal of pharmaceutical sciences* **2020**, *15* (2), 207-219.
131. Freidman, N. J.; Briot, C.; Ryan, R. M., Characterizing unexpected interactions of a glutamine transporter inhibitor with members of the SLC1A transporter family. *J. Biol. Chem.* **2022**, *298* (8).
132. Garaeva, A. A.; Oostergetel, G. T.; Gati, C.; Guskov, A.; Paulino, C.; Slotboom, D. J., Cryo-EM structure of the human neutral amino acid transporter ASCT2. *Nature Structural & Molecular Biology* **2018**, *25* (6), 515-521.
133. Broer, A.; Wagner, C.; Lang, F.; Broer, S., Neutral amino acid transporter ASCT2 displays substrate-induced Na<sup>+</sup> exchange and a substrate-gated anion conductance. *Biochemical Journal* **2000**, *346* (3), 705-710.
134. Scopelliti, A. J.; Font, J.; Vandenberg, R. J.; Boudker, O.; Ryan, R. M., Structural characterisation reveals insights into substrate recognition by the glutamine transporter ASCT2/SLC1A5. *Nature Communications* **2018**, *9* (1), 38.
135. Grewer, C.; Grabsch, E., New inhibitors for the neutral amino acid transporter ASCT2 reveal its Na<sup>+</sup>-dependent anion leak. *The Journal of physiology* **2004**, *557* (3), 747-759.
136. Liu, Y.; Zhao, T.; Li, Z.; Wang, L.; Yuan, S.; Sun, L., The role of ASCT2 in cancer: a review. *European journal of pharmacology* **2018**, *837*, 81-87.
137. Van Geldermalsen, M.; Wang, Q.; Nagarajah, R.; Marshall, A.; Thoeng, A.; Gao, D.; Ritchie, W.; Feng, Y.; Bailey, C.; Deng, N., ASCT2/SLC1A5 controls glutamine uptake and tumour growth in triple-negative basal-like breast cancer. *Oncogene* **2016**, *35* (24), 3201-3208.

138. Wang, W.; Pan, H.; Ren, F.; Chen, H.; Ren, P., Targeting ASCT2-mediated glutamine metabolism inhibits proliferation and promotes apoptosis of pancreatic cancer cells. *Bioscience Reports* **2022**, *42* (3), BSR20212171.
139. Broer, A.; Rahimi, F.; Broer, S., Deletion of amino acid transporter ASCT2 (SLC1A5) reveals an essential role for transporters SNAT1 (SLC38A1) and SNAT2 (SLC38A2) to sustain glutaminolysis in cancer cells. *Journal of biological chemistry* **2016**, *291* (25), 13194-13205.
140. Ravera, M.; Gabano, E.; Tinello, S.; Zanellato, I.; Osella, D., May glutamine addiction drive the delivery of antitumor cisplatin-based Pt (IV) prodrugs? *Journal of Inorganic Biochemistry* **2017**, *167*, 27-35.
141. Srinivasarao, M.; Low, P. S., Ligand-Targeted Drug Delivery. *Chemical Reviews* **2017**, *117* (19), 12133-12164.
142. Chen, C. K.; Zhang, J. Z.; Aitken, J. B.; Hambley, T. W., Influence of equatorial and axial carboxylato ligands on the kinetic inertness of platinum (IV) complexes in the presence of ascorbate and cysteine and within DLD-1 cancer cells. *Journal of medicinal chemistry* **2013**, *56* (21), 8757-8764.
143. Balzani, V.; Carassiti, V., Photochemistry of some square-planar and octahedral platinum complexes. *The Journal of Physical Chemistry* **1968**, *72* (2), 383-388.
144. Wilson, J. J.; Lippard, S. J., Synthetic methods for the preparation of platinum anticancer complexes. *Chemical reviews* **2014**, *114* (8), 4470-4495.
145. Tolosa, L.; Donato, M. T.; Gómez-Lechón, M. J., General cytotoxicity assessment by means of the MTT assay. *Protocols in in vitro hepatocyte research* **2015**, 333-348.
146. Marzano, C.; Sbovata, S. M.; Gandin, V.; Michelin, R. A.; Venzo, A.; Bertani, R.; Seraglia, R., Cytotoxicity of cis-platinum (II) cycloaliphatic amidine complexes: Ring size and solvent effects on the biological activity. *Journal of inorganic biochemistry* **2009**, *103* (8), 1113-1119.
147. Kalinowska-Lis, U.; Ochocki, J.; Matlawska-Wasowska, K., Trans geometry in platinum antitumor complexes. *Coord. Chem. Rev.* **2008**, *252* (12-14), 1328-1345.
148. Gérard, V.; Galopin, C.; Ay, E.; Launay, V.; Morlet-Savary, F.; Graff, B.; Lalevée, J., Photostability of L-tryptophan in aqueous solution: Effect of atmosphere and antioxidants addition. *Food Chemistry* **2021**, *359*, 129949.
149. Bhatt, M.; Di Iacovo, A.; Romanazzi, T.; Roseti, C.; Cinquetti, R.; Bossi, E., The “www” of *Xenopus laevis* oocytes: the why, when, what of *Xenopus laevis* oocytes in membrane transporters research. *Membranes* **2022**, *12* (10), 927.
150. Fastner, A.; Absmanner, B.; Hammes, U. Z. J. P. H. M.; Protocols, Use of *Xenopus laevis* oocytes to study auxin transport. **2017**, 259-270.
151. Bergeron, M. J.; Boggavarapu, R.; Meury, M.; Ucurum, Z.; Caron, L.; Isenring, P.; Hediger, M. A.; Fotiadis, D., Frog oocytes to unveil the structure and supramolecular organization of human transport proteins. *PLoS One* **2011**, *6* (7), e21901.
152. Albers, T.; Marsiglia, W.; Thomas, T.; Gameiro, A.; Grewer, C., Defining substrate and blocker activity of alanine-serine-cysteine transporter 2 (ASCT2) ligands with novel serine analogs. *Molecular pharmacology* **2012**, *81* (3), 356-365.
153. Mu, W.; Zhang, T.; Jiang, B., An overview of biological production of L-theanine. *Biotechnology advances* **2015**, *33* (3-4), 335-342.
154. Marshall, A. D.; Van Geldermalsen, M.; Otte, N. J.; Lum, T.; Vellozzi, M.; Thoeng, A.; Pang, A.; Nagarajah, R.; Zhang, B.; Wang, Q., ASCT2 regulates glutamine uptake and cell growth in endometrial carcinoma. *Oncogenesis* **2017**, *6* (7), e367-e367.

155. Liu, Q.; Duan, H.; Luan, J.; Yagasaki, K.; Zhang, G., Effects of theanine on growth of human lung cancer and leukemia cells as well as migration and invasion of human lung cancer cells. *Cytotechnology* **2009**, *59*, 211-217.
156. Xin, Y.; Ben, P.; Wang, Q.; Zhu, Y.; Yin, Z.; Luo, L., Theanine, an antitumor promoter, induces apoptosis of tumor cells via the mitochondrial pathway. *Molecular Medicine Reports* **2018**, *18* (5), 4535-4542.
157. Petruzzella, E.; Chiroasca, C. V.; Heidenga, C. S.; Hoeschele, J. D., Microwave-assisted synthesis of the anticancer drug cisplatin, cis-[Pt (NH<sub>3</sub>)<sub>2</sub> Cl<sub>2</sub>]. *Dalton Transactions* **2015**, *44* (7), 3384-3392.

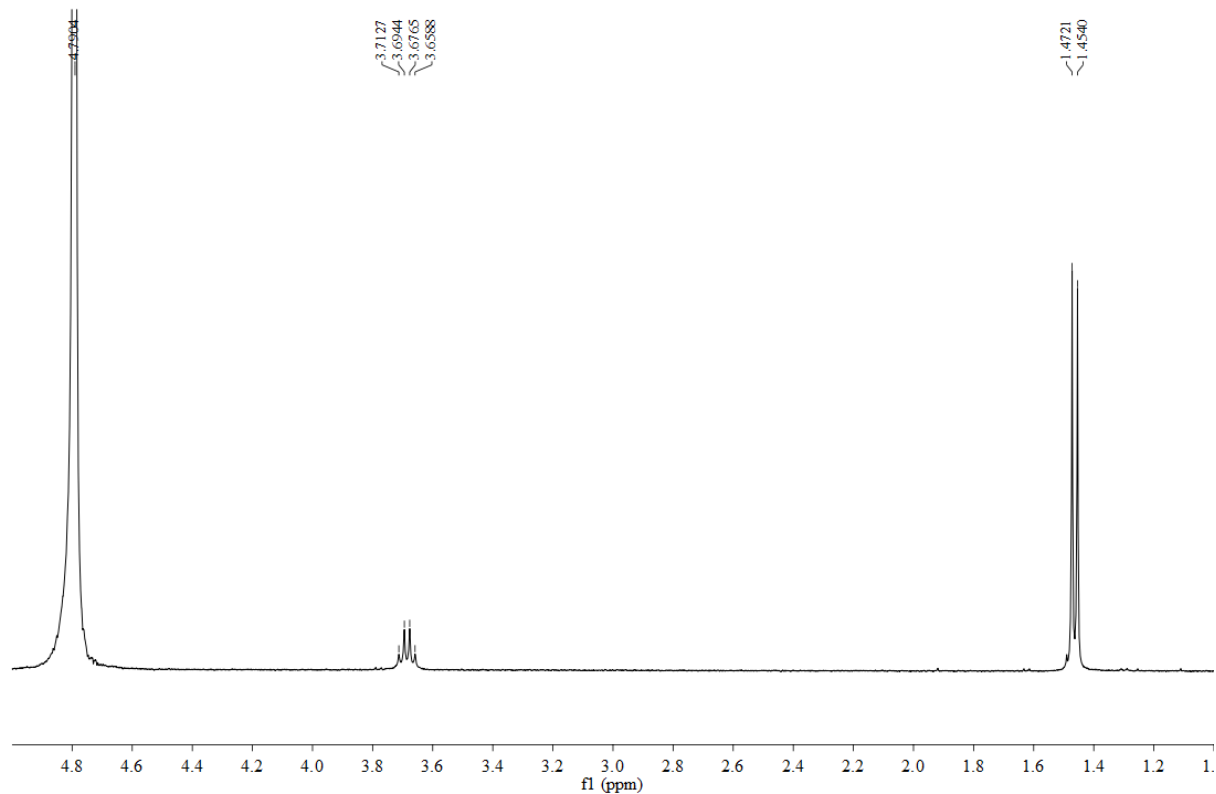
# APPENDICES

## Appendix 1: IR spectrum of *trans*-[Pt(L-alanine)<sub>2</sub>].



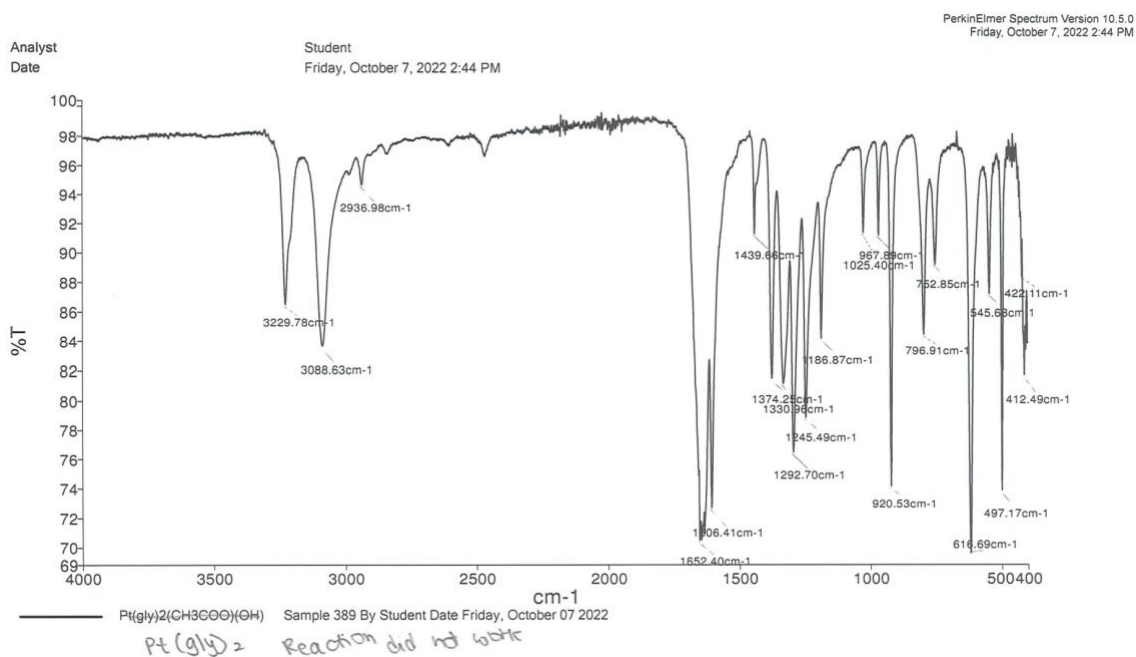
## Appendix 2: <sup>1</sup>H NMR spectrum of *trans*-[Pt(L-alanine)<sub>2</sub>].

20190523 [Pt(ala)<sub>2</sub>] NMR 400 MHz D<sub>2</sub>O-d<sub>2</sub>

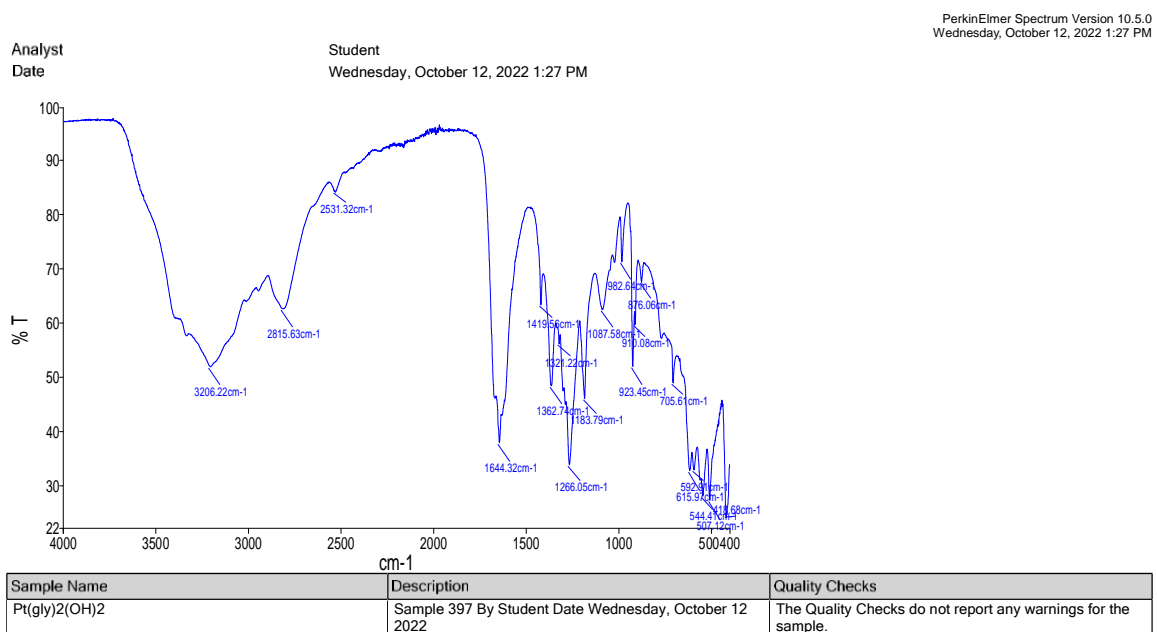




### Appendix 3: IR spectrum of *trans*-[Pt(glycine)<sub>2</sub>].

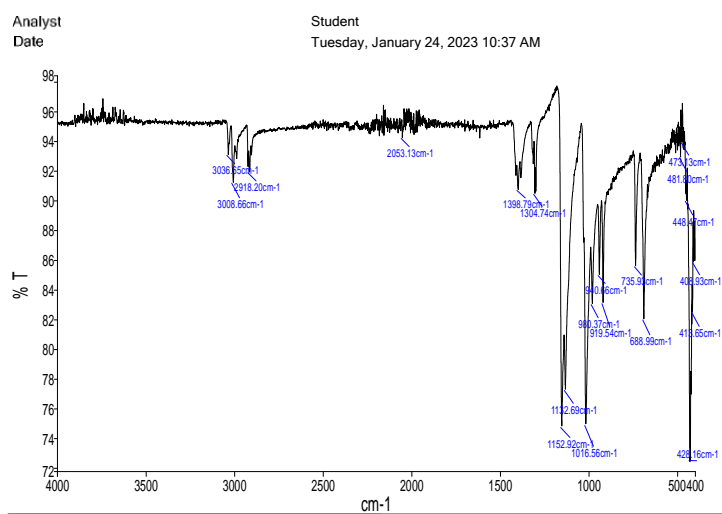


### Appendix 4: IR spectrum of *trans*-[Pt(glycine)<sub>2</sub>(OH)<sub>2</sub>].



## Appendix 5: IR spectrum of *cis*-[PtCl<sub>2</sub>(DMSO)<sub>2</sub>].

PerkinElmer Spectrum Version 10.5.0  
Tuesday, January 24, 2023 10:37 AM



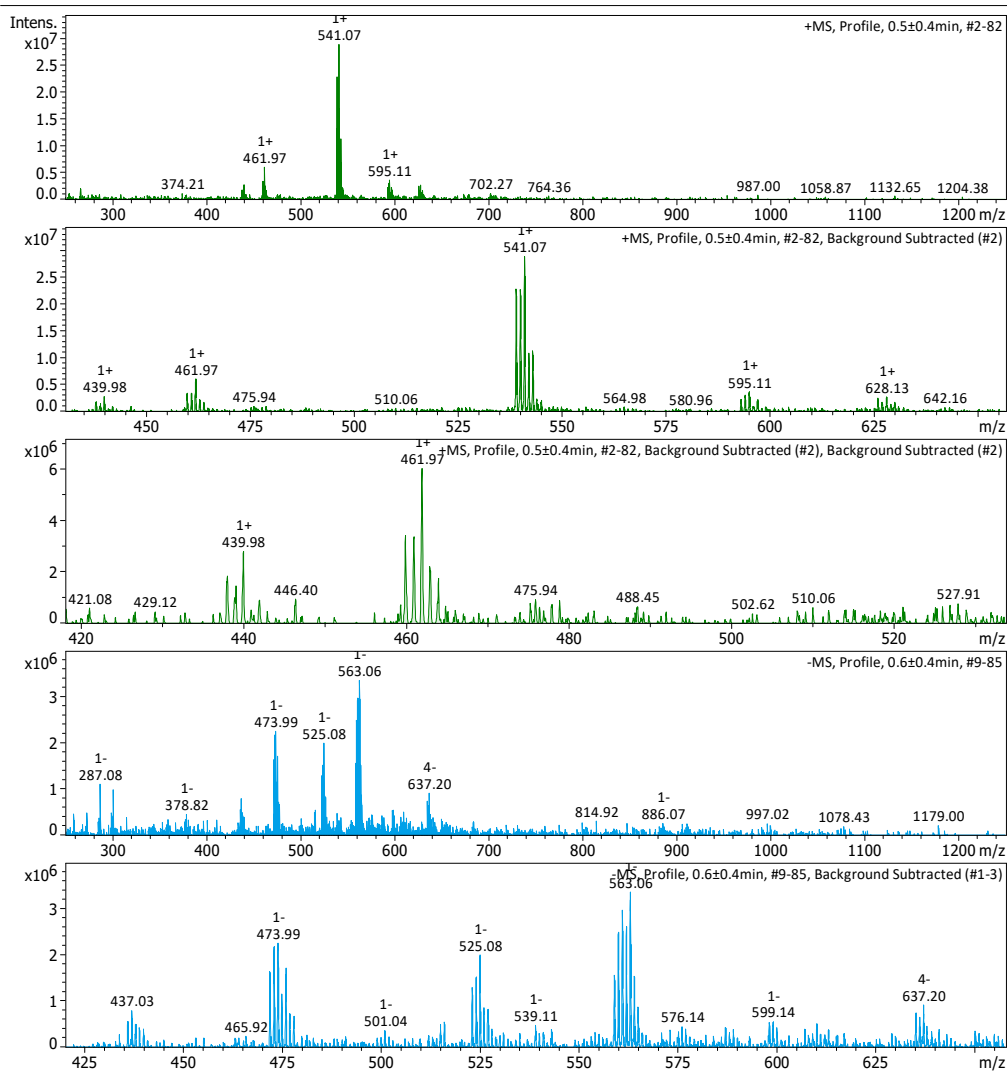
Sample Name	Description	Quality Checks
PtCl <sub>2</sub> (DMSO) <sub>2</sub> Crystals	Sample 481 By Student Date Tuesday, January 24 2023	The Quality Checks give rise to a Weak Bands warning for the sample.

# Appendix 6: Mass spectrometry ESI (+) and (-) analysis of oil

## (2.4.3 Synthesis of *cis*-[Pt(L-isoleucine)<sub>2</sub>])

### Generic Display Report

<b>Analysis Info</b>		Acquisition Date	10-Feb-23 10:54:40 AM
Analysis Name	D:\Data\OneDrive - The University of Sydney (Staff)\Instrument_Data\BrukerAmazonSL\Data\MS Facility\Billy\2023-02-10\20230210_Service_ESI_00015.d		
Method	DEF_MS-NP.M	Operator	demo
Sample Name	isoleucine oil	Instrument	amazon SL
Comment	MeOH		

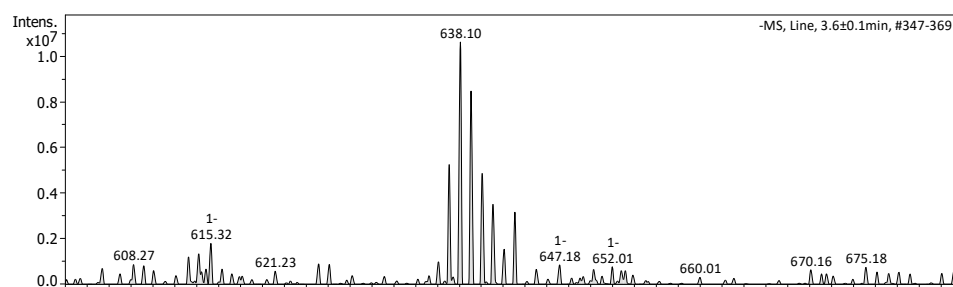
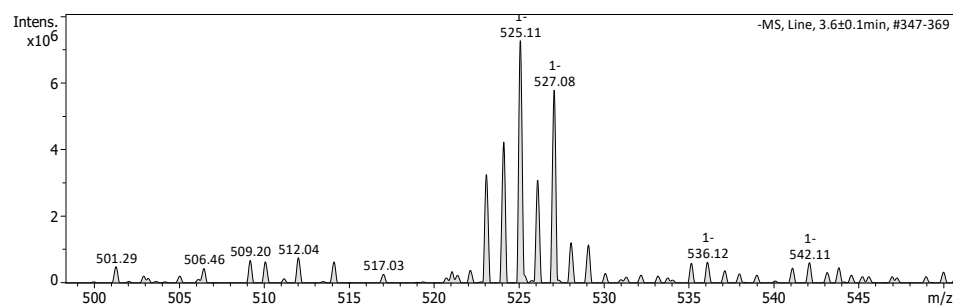
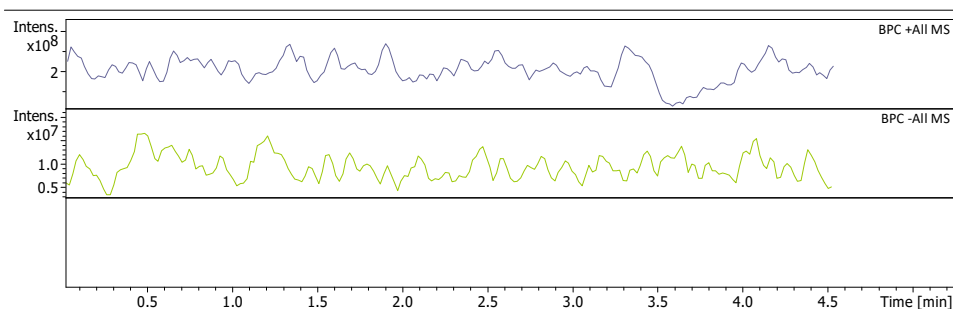


## Appendix 7: Mass spectrometry ESI (-) analysis of solid.

### (2.4.3 Synthesis of *cis*-[Pt(L-isoleucine)<sub>2</sub>])

#### Generic Display Report

<b>Analysis Info</b>		Acquisition Date	12-Apr-23 10:58:57 AM
Analysis Name	D:\Data\OneDrive - The University of Sydney (Staff)\Instrument_Data\BrukerAmazonSL\Data\Hambley\Vinitha\20230412_IsoPrecipitate.d	Operator	demo
Method	DEF_MS-NP.M	Instrument	amaZon SL
Sample Name	20230412_Iso Precipitate		
Comment	MeOH		

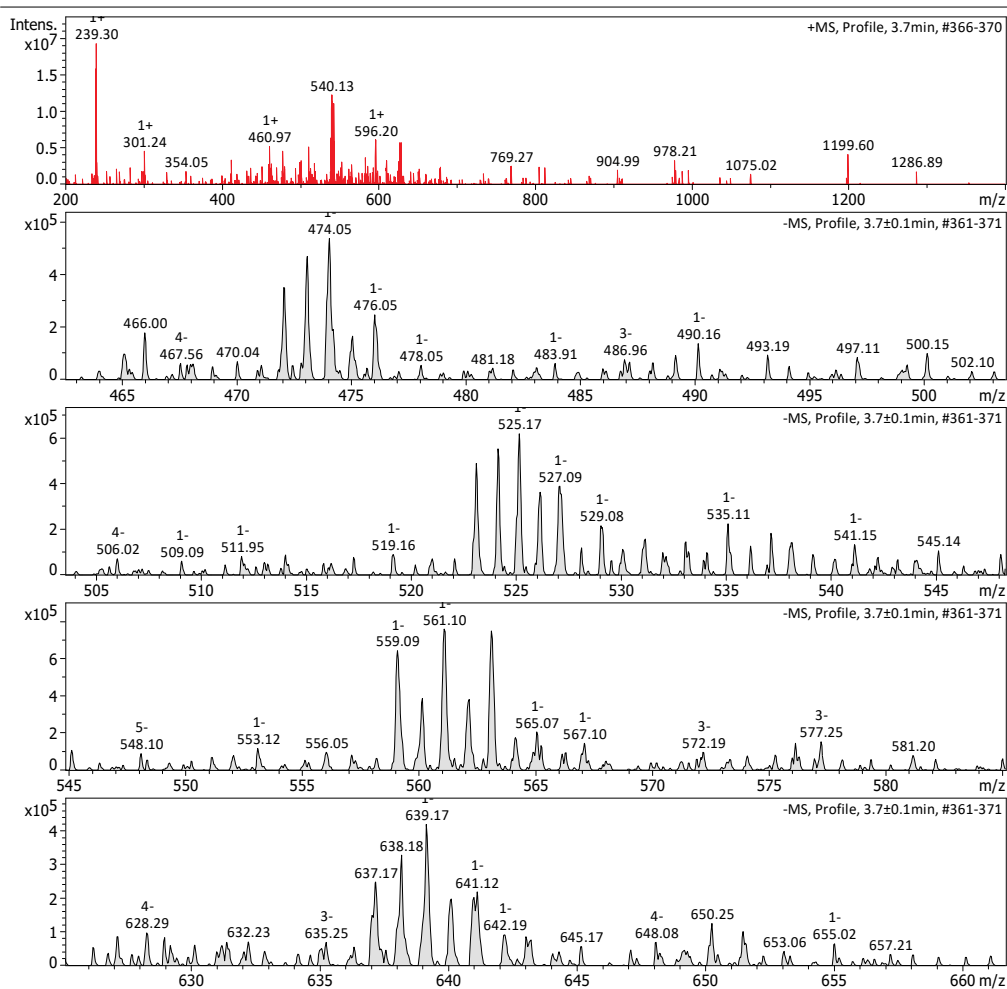


# Appendix 8: Mass spectrometry ESI (-) analysis of solution fraction.

## (2.4.3 Synthesis of *cis*-[Pt(L-isoleucine)<sub>2</sub>])


### Generic Display Report

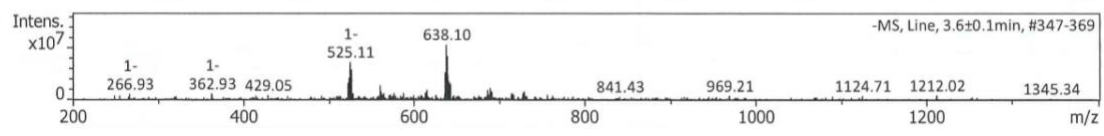
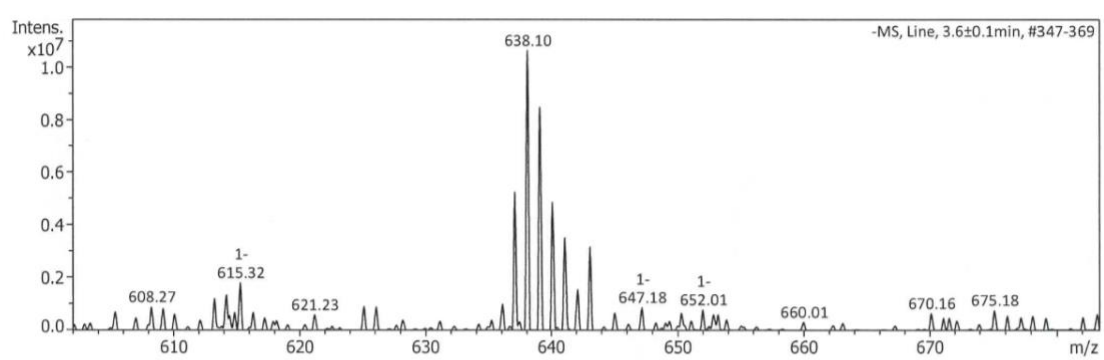
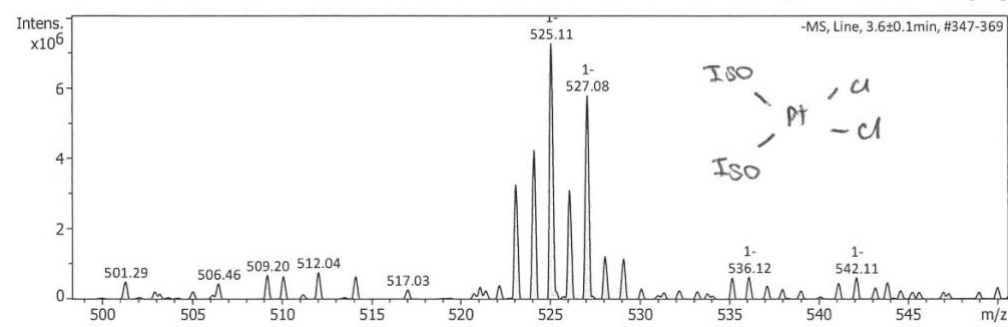
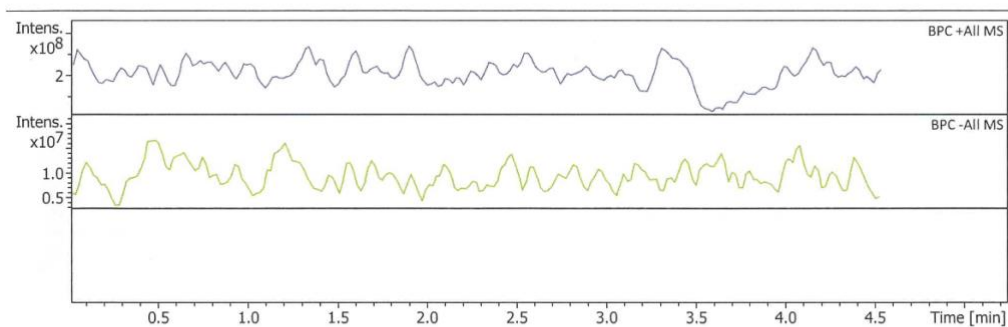
<b>Analysis Info</b>		Acquisition Date	13-Apr-23 10:52:02 AM
Analysis Name	D:\Data\OneDrive - The University of Sydney (Staff)\Instrument_Data\BrukerAmazonSL\Data\Hambley\Vinitha\220413_Isoleucine water soluble.d	Operator	demo
Method	DEF_MS-NP.M	Instrument	amaZon SL
Sample Name	220413_Isoleucine water soluble		
Comment	MeOH		



Appendix 9: Mass spectrometry ESI (-) analysis of precipitate.

(2.4.3 Synthesis of *cis*-[Pt(L-isoleucine)<sub>2</sub>])

Generic Display Report		<i>Precipitate collected when drying off MeOH</i>	
<b>Analysis Info</b>		Acquisition Date	12-Apr-23 10:58:57 AM
Analysis Name	D:\Data\OneDrive - The University of Sydney (Staff)\Instrument_Data\BrukerAmaZonSL\Data\Hambley\Vinitha\20230412_IsoPrecipitate.d	Operator	demo
Method	DEF_MS-NP.M	Instrument	amaZon SL
Sample Name	20230412_Iso Precipiate 		
Comment	MeOH		

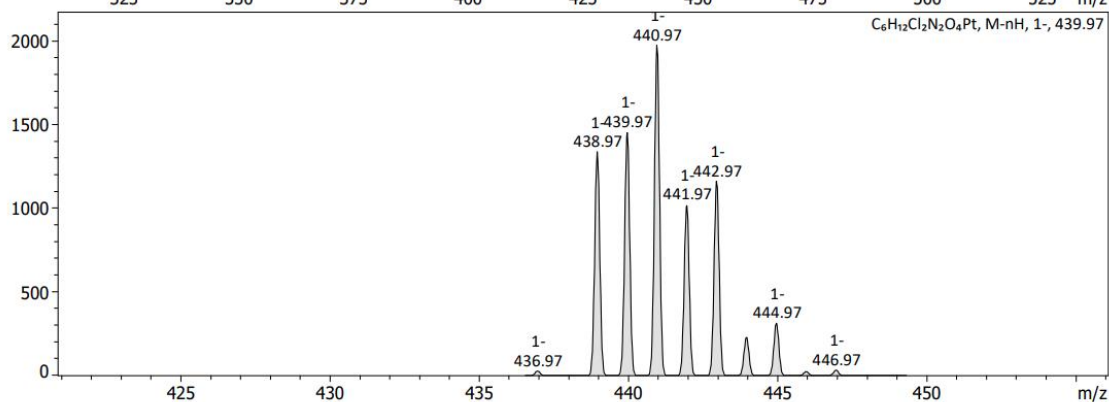
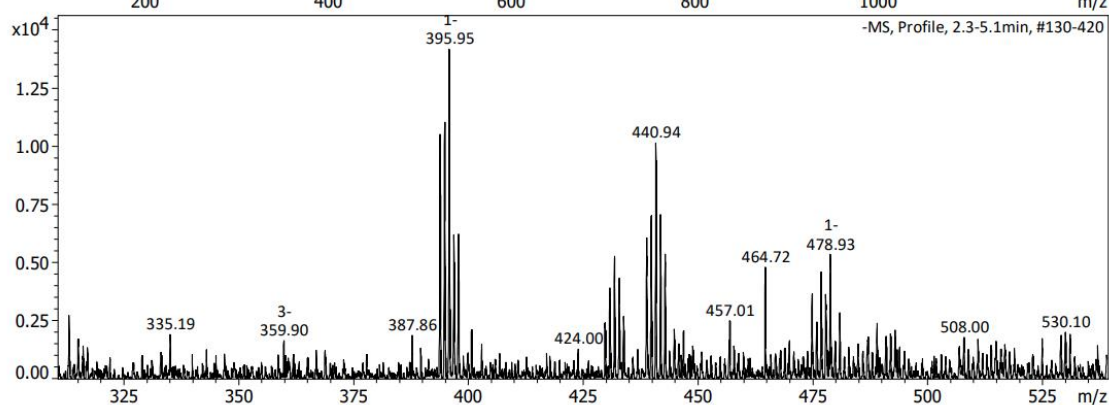
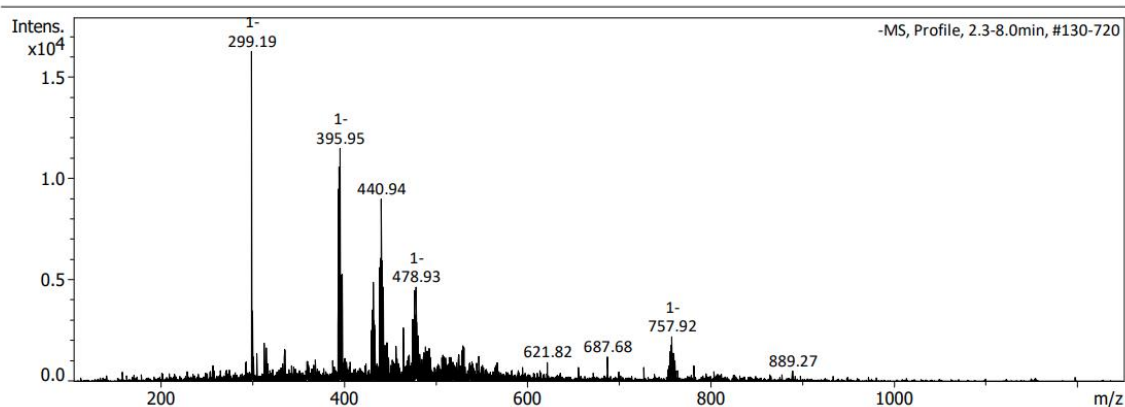


# Appendix 10: Mass spectrometry ESI (-) analysis of oil.

## (2.4.4 Synthesis of *cis*-[Pt(L-alanine)<sub>2</sub>] in 1-butanol)

### Generic Display Report

<b>Analysis Info</b>	Acquisition Date	10-Feb-23 10:14:13 AM
Analysis Name	D:\Data\OneDrive - The University of Sydney (Staff)\Instrument_Data\BrukerAmazSL\Data\MS Facility\Billy\2023-02-10\20230210_Service_ESI_00013.d	
Method	DEF_MS-NP.M	Operator demo
Sample Name	alanine oil	Instrument amaZon SL
Comment	MeOH	

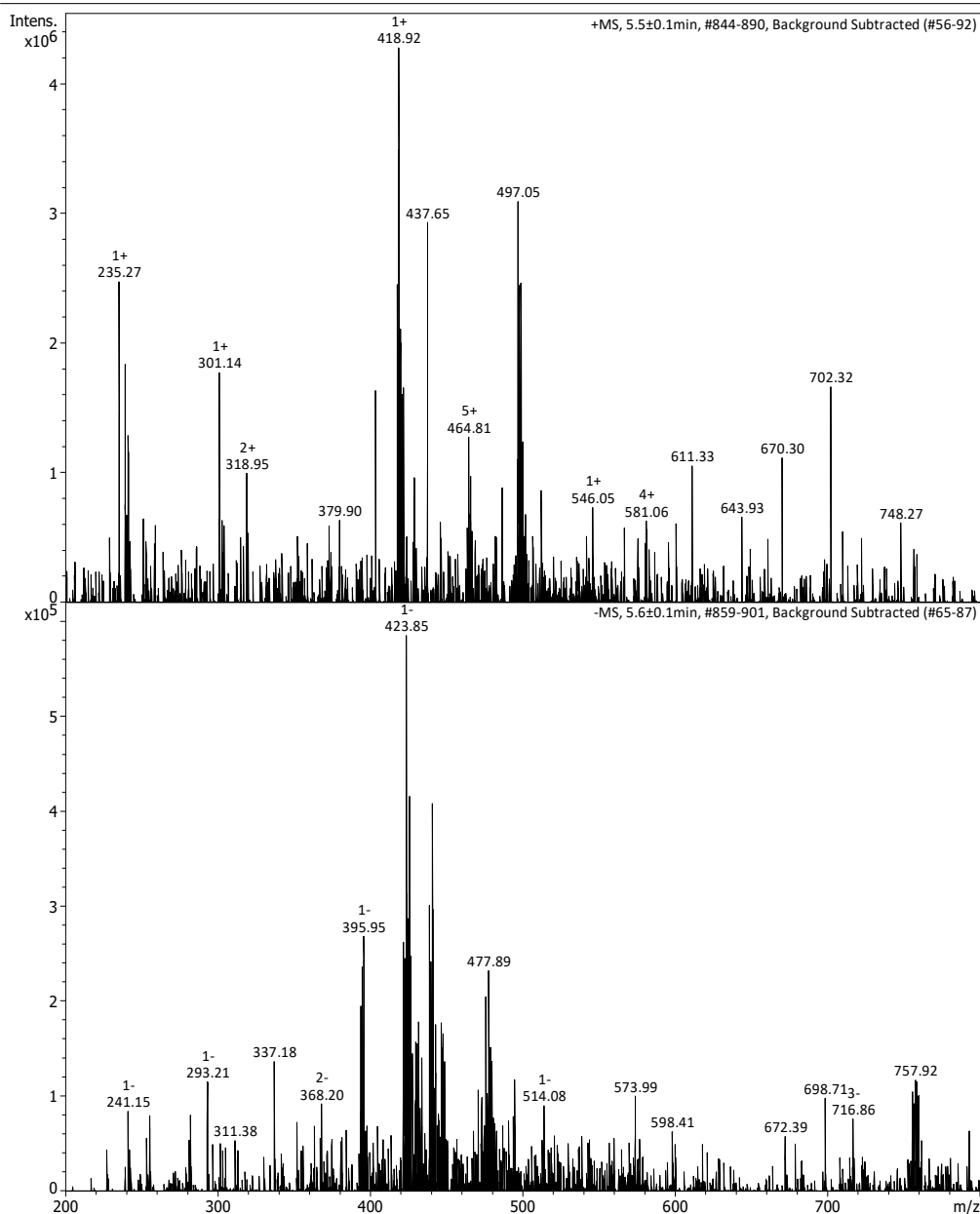


# Appendix 11: Mass spectrometry ESI (+) and (-) analysis of precipitate.

## (2.4.4 Synthesis of *cis*-[Pt(L-alanine)<sub>2</sub>] in 1-butanol)

### Generic Display Report

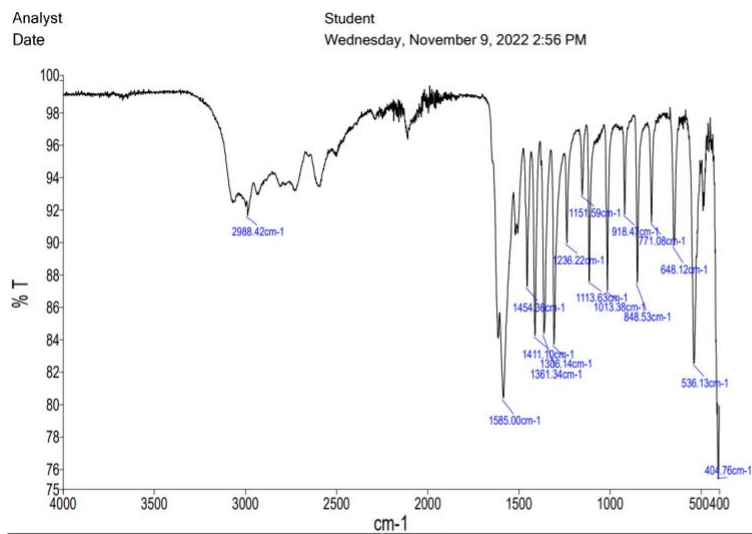
<b>Analysis Info</b>	Acquisition Date 28/03/2023 2:47:18 PM
Analysis Name E:\Data\AmaZon Data\MS Facility\Sarah\20230328\20230328_serviceESI00001.d	Operator demo
Method DEF_MS-NP.M	Instrument amaZon SL
Sample Name R13 Alanine Water fraction Structure	
Comment MeOH	





## Appendix 12: IR spectrum of L-alanine.

PerkinElmer Spectrum Version 10.5.0  
 Wednesday, November 9, 2022 2:56 PM



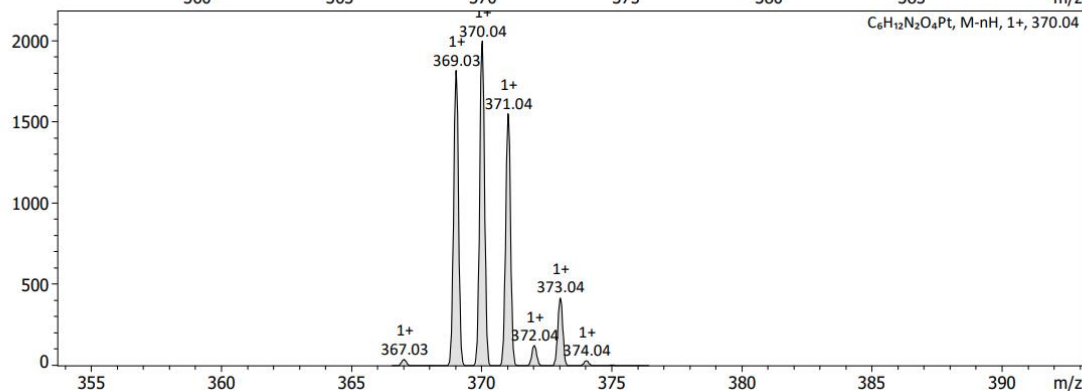
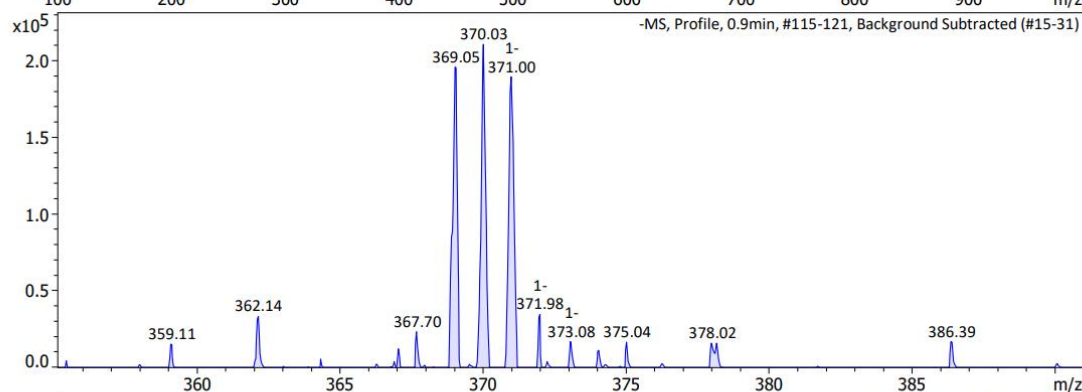
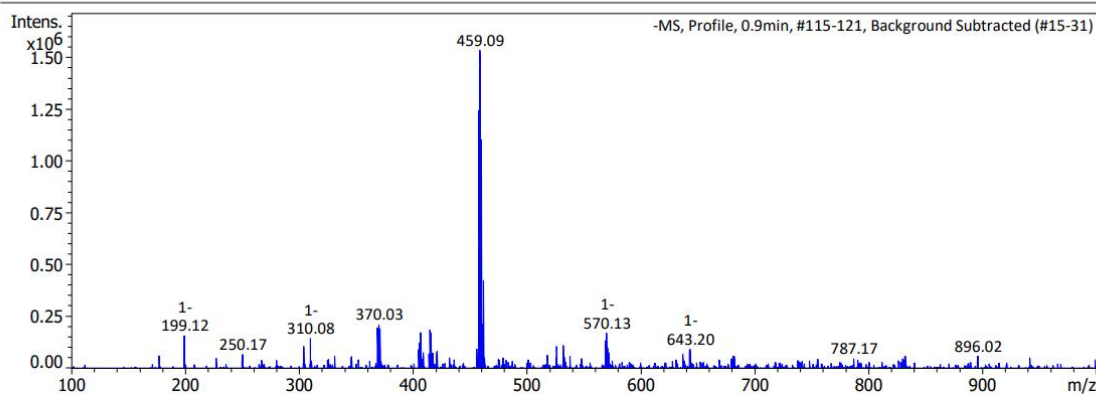
Sample Name	Description	Quality Checks
L-alanine	Sample 414 By Student Date Wednesday, November 09 2022	The Quality Checks give rise to multiple warnings for the sample.

## Appendix 13: Mass spectrometry ESI (-) analysis of crystals.

### (2.4.4 Synthesis of *cis*-[Pt(L-alanine)<sub>2</sub>] in 1-butanol)

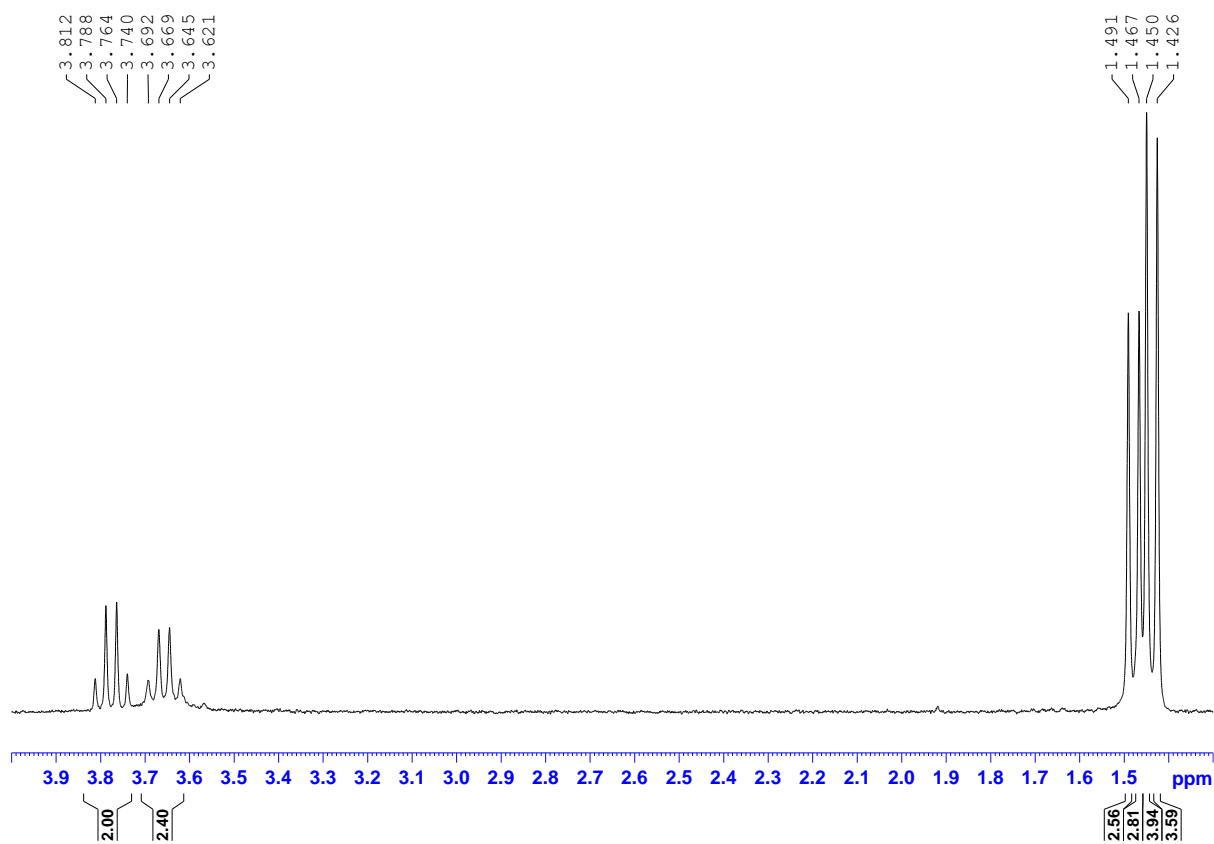
#### Generic Display Report

<b>Analysis Info</b>		Acquisition Date	11-Jan-23 7:35:38 AM
Analysis Name	D:\Data\OneDrive - The University of Sydney (Staff)\Instrument_Data\BrukerAmazonSL\Data\MS Facility\Chianna\2023-01-11\20230111_Service_ESI_00001.d		
Method	DEF_MS-NP.M	Operator	demo
Sample Name	3 Alanine crystals	Instrument	amaZon SL
Comment	H <sub>2</sub> O, diluted in MeOH		

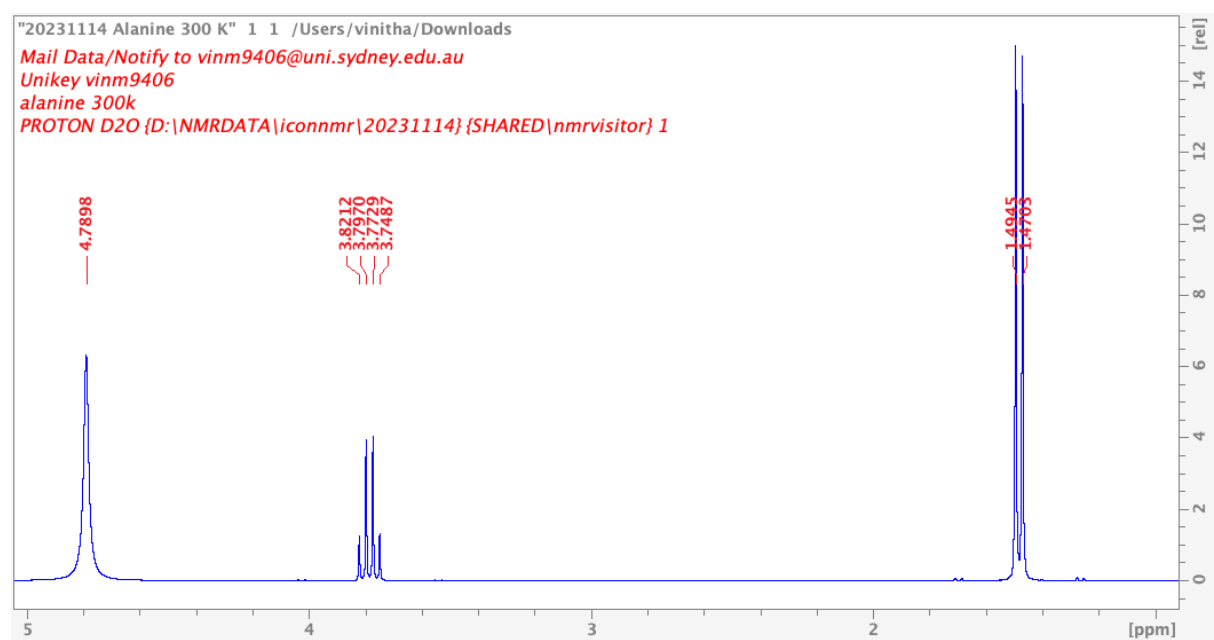


## Appendix 14: $^1\text{H}$ NMR spectrum of crystals.

### (2.4.4 Synthesis of *cis*-[Pt(L-alanine) $_2$ ] in 1-butanol)



## Appendix 15: $^1\text{H}$ NMR spectrum of L-alanine

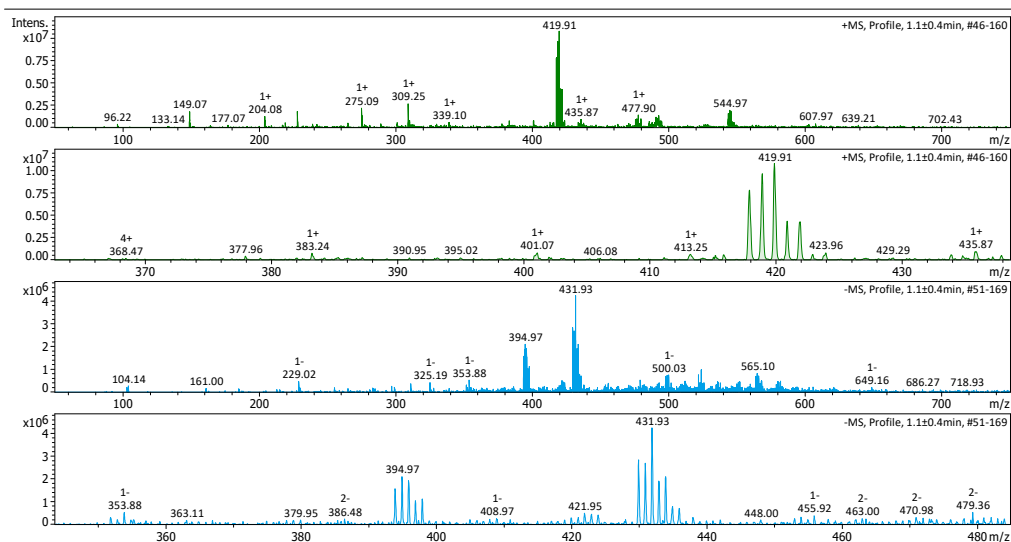


## Appendix 16: Mass spectrometry ESI (+) and (-) analysis of solid.

### (2.4.4 Synthesis of *cis*-[Pt(L-alanine)<sub>2</sub>] in 1-butanol)

#### Generic Display Report

<b>Analysis Info</b>		Acquisition Date	10-Mar-23 10:08:03 AM
Analysis Name	D:\Data\OneDrive - The University of Sydney (Staff)\Instrument_Data\BrukerAmazonSL\Data\MS Facility\Billy\2023-03-10\20230310_Service_ESI_00004.d		
Method	DEF_MS-NP.M	Operator	demo
Sample Name	R19 Alanine	Instrument	amaZon SL
Comment	MeOH Direct injection		



# Appendix 17: Mass spectrometry ESI (-) analysis of solid.

## (2.4.5 Synthesis of *cis*-[Pt(L-alanine)<sub>2</sub> in methanol)

### Generic Display Report

#### Analysis Info

Analysis Name D:\Data\OneDrive - The University of Sydney

Acquisition Date 20-Apr-23 1:41:23 PM

(Staff)\Instrument\_Data\BrukerAmaZonSL\Data\Hambley\Vinitha\230420 Li Ala solid (2).d

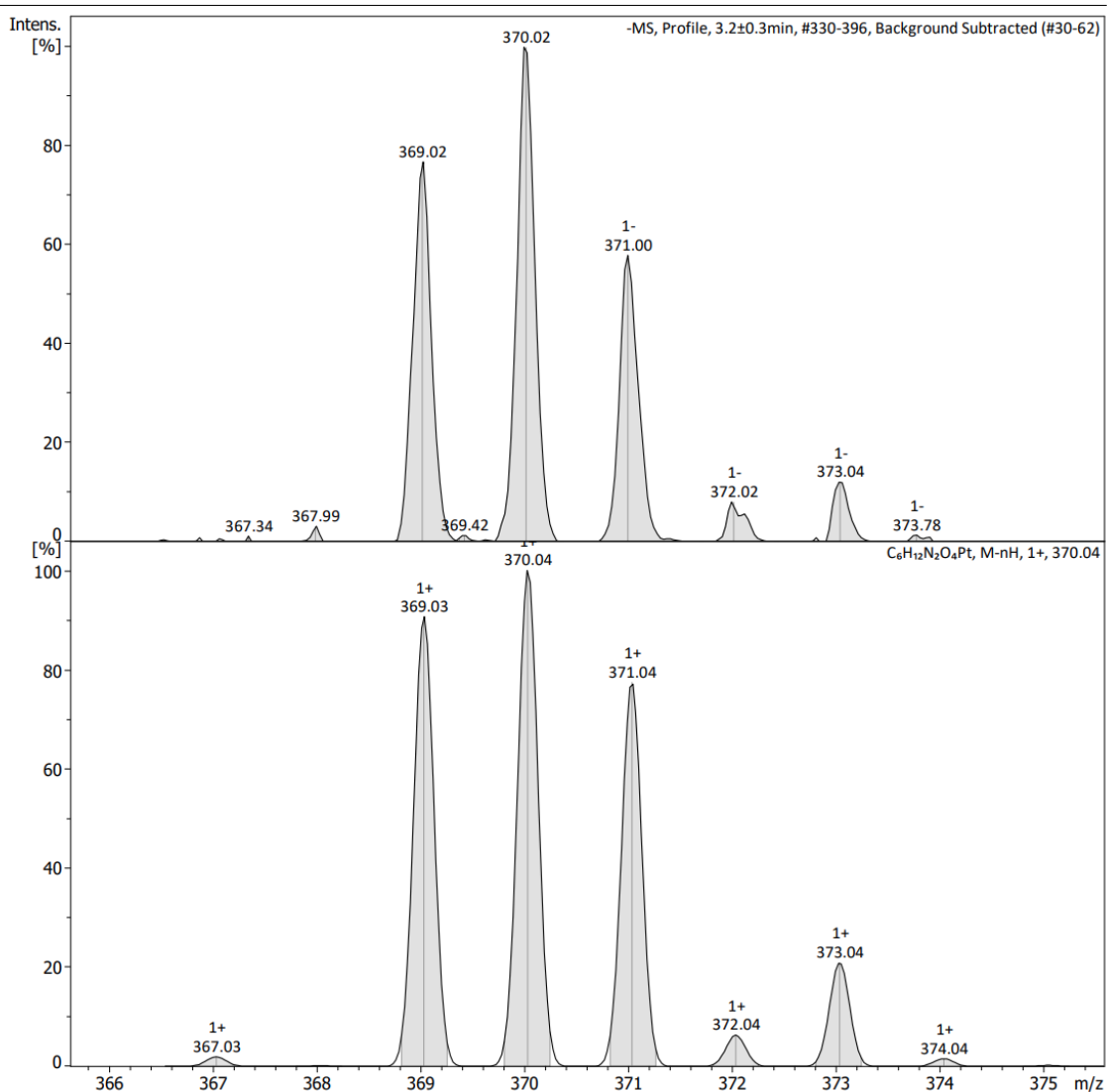
Method DEF\_MS-NP.M

Operator demo

Sample Name 230420 Li Ala solid (2)

Instrument amaZon SL

Comment MeOH



# Appendix 18: Mass spectrometry ESI (+) and (-) analysis of crystals.

## (2.4.5 Synthesis of *cis*-[Pt(L-alanine)<sub>2</sub>] in methanol)

### Generic Display Report

#### Analysis Info

Analysis Name D:\Data\OneDrive - The University of Sydney

Acquisition Date 17-May-23 1:04:12 PM

(Staff)\Instrument\_Data\BrukerAmaZonSL\Data\Hambley\Vinitha\20230517-R24Solid.d

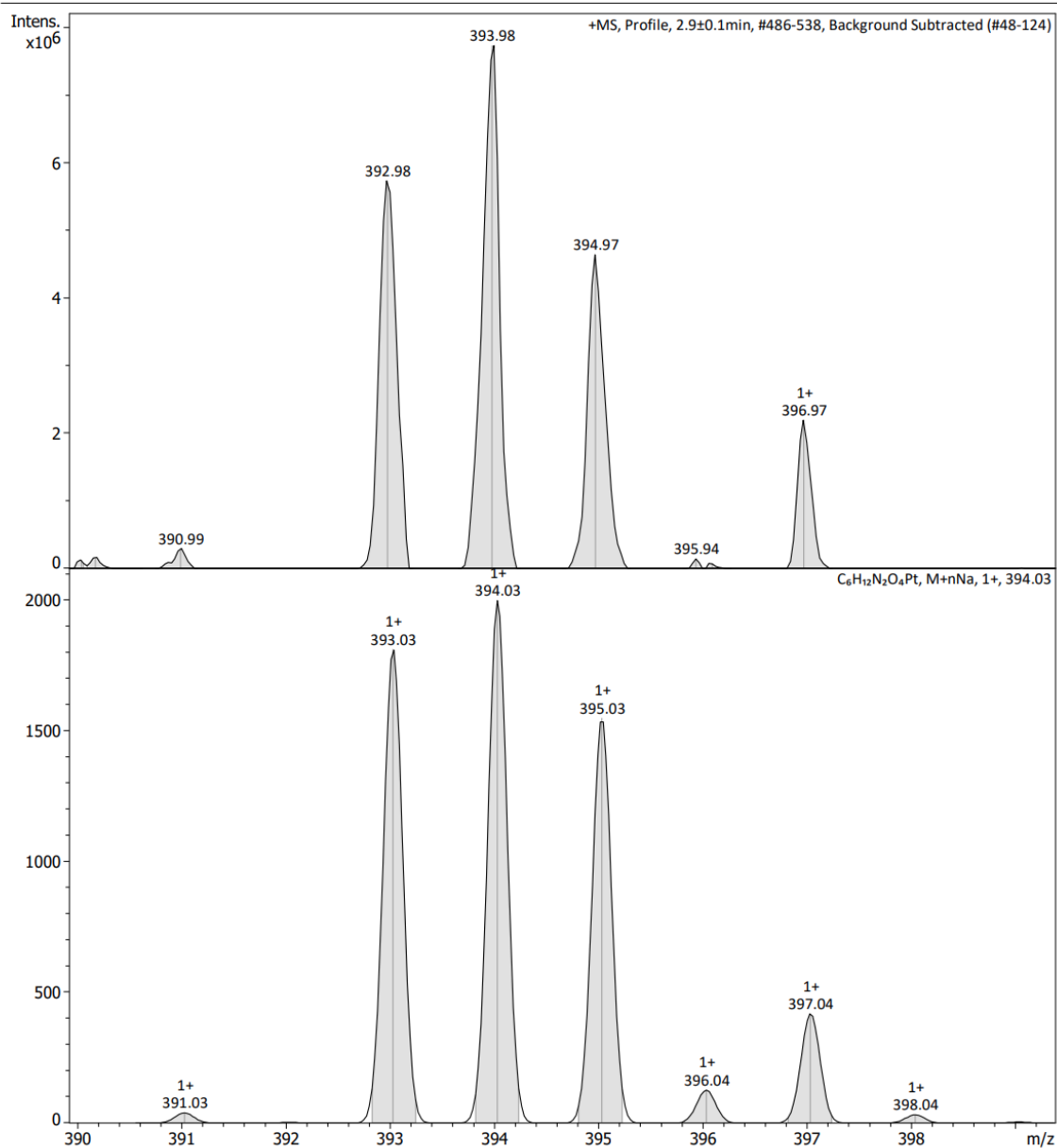
Method DEF\_MS-NP.M

Operator demo

Sample Name 20230517-R24 Solid

Instrument amaZon SL

Comment MeOH

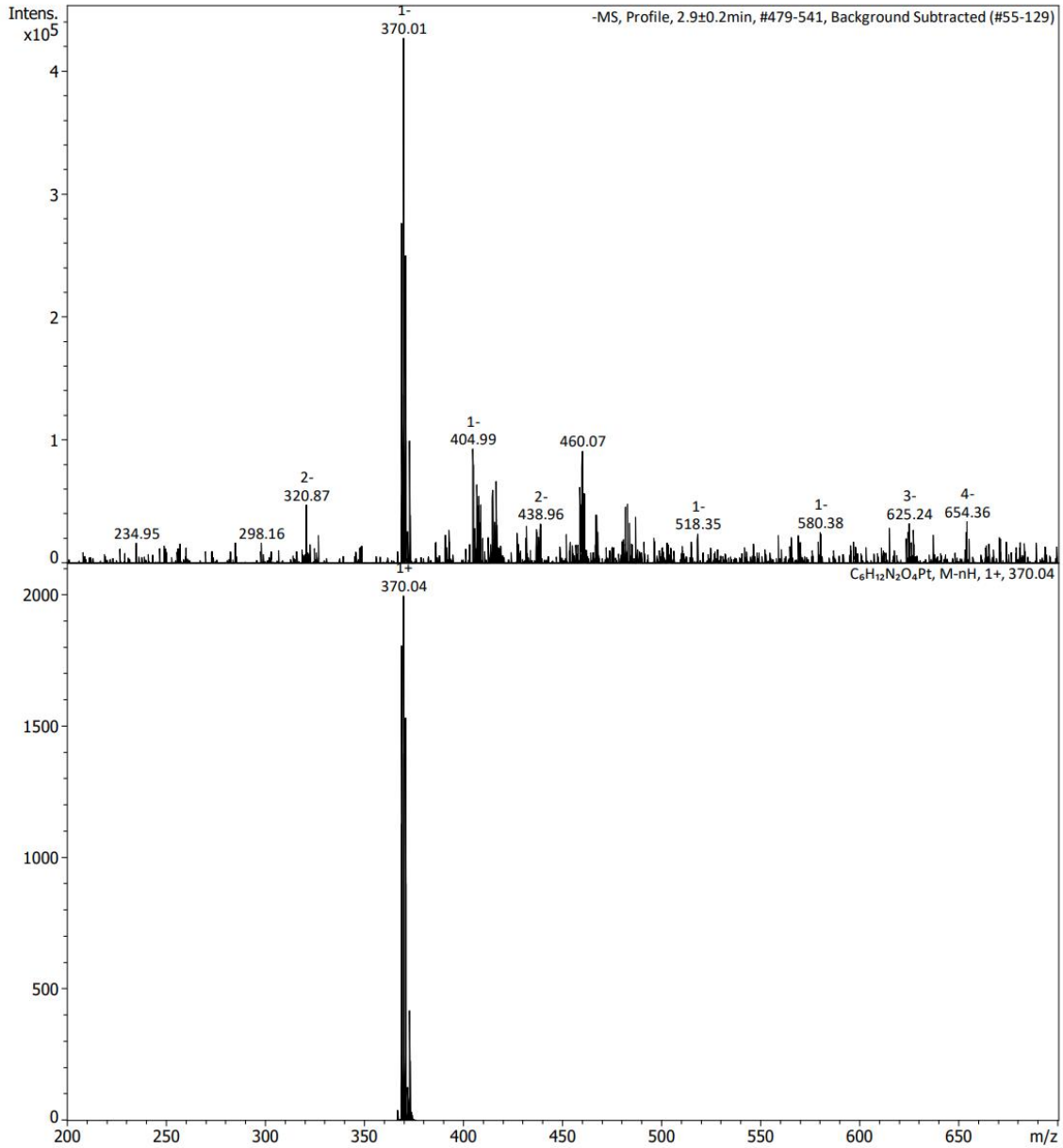


# Generic Display Report

## Analysis Info

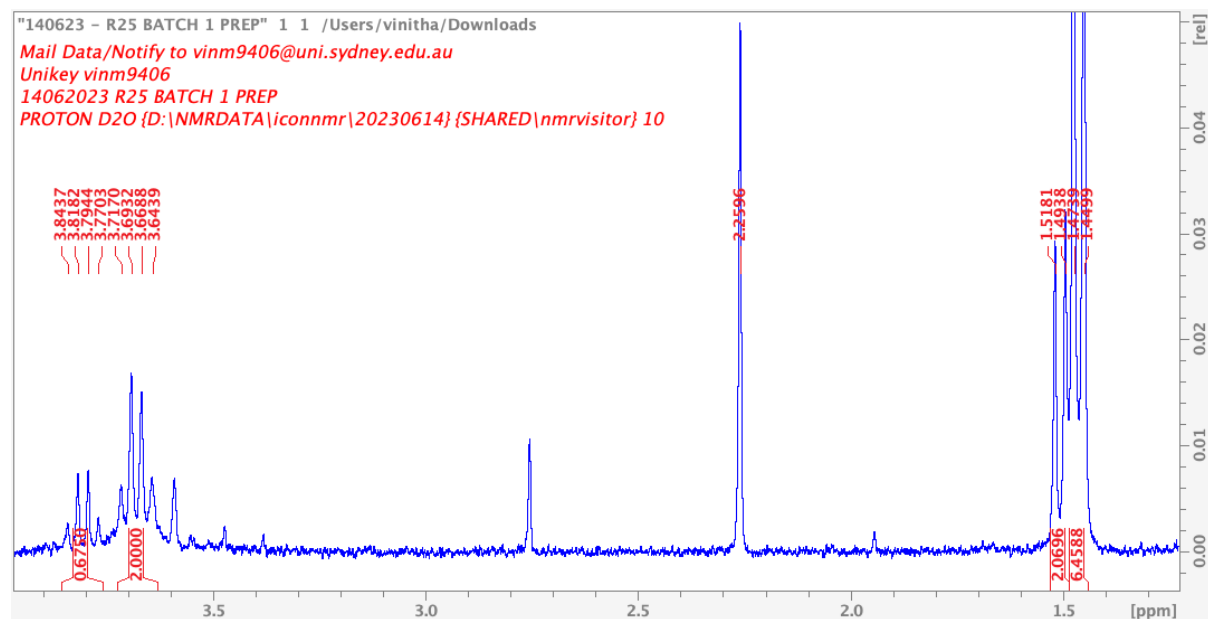
Analysis Name D:\Data\OneDrive - The University of Sydney  
(Staff)\Instrument\_Data\BrukerAmaZonSL\Data\Hambley\Vinitha\20230517-R24Solid.d  
Method DEF\_MS-NP.M Operator demo  
Sample Name 20230517-R24 Solid Instrument amaZon SL  
Comment MeOH

Acquisition Date 17-May-23 1:04:12 PM



Appendix 19: <sup>1</sup>H NMR spectrum of crystals.

(2.4.5 Synthesis of *cis*-[Pt(L-alanine)<sub>2</sub>] in methanol)





## Appendix 20: Mass spectrometry ESI (+) and (-) analysis of solid.

### (2.4.5 Synthesis of *cis*-[Pt(L-alanine)<sub>2</sub>] in methanol)

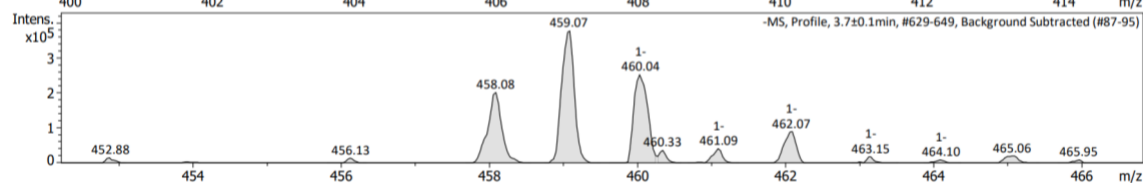
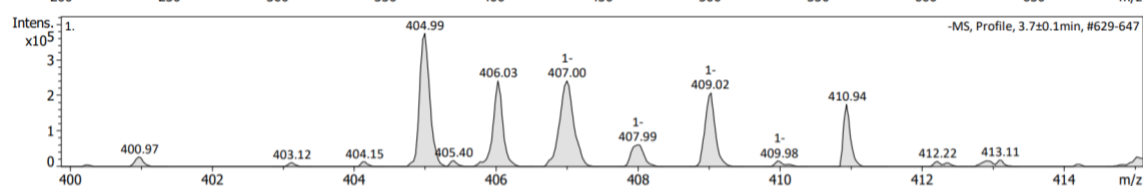
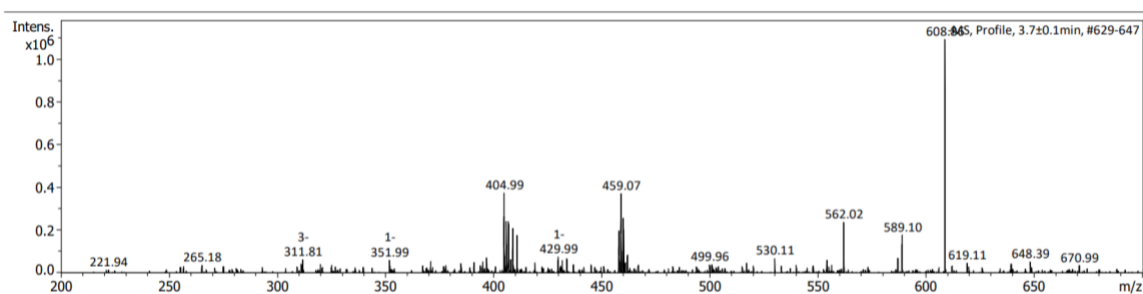
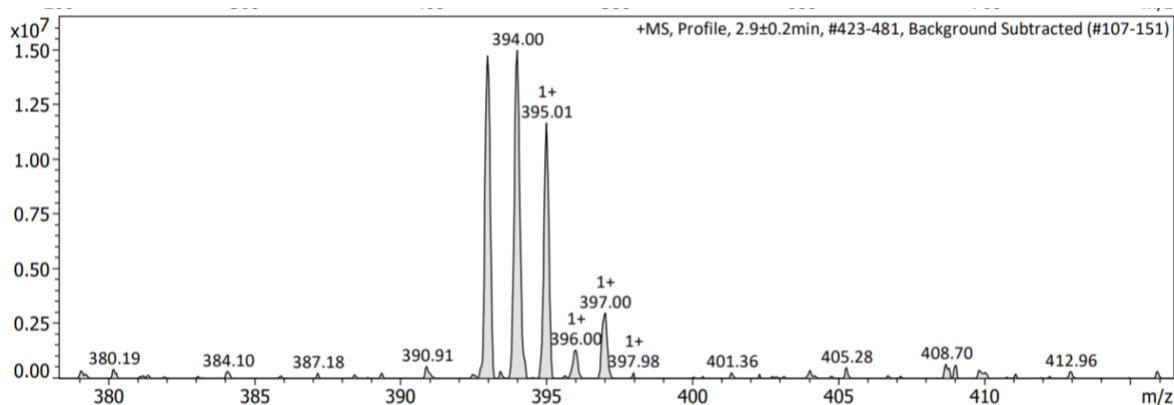
## Generic Display Report

### Analysis Info

Analysis Name D:\Data\OneDrive - The University of Sydney  
(Staff)\Instrument\_Data\BrukerAmazonSL\Data\Hambley\Vinitha\20230619\_R25 Batch 2 solid.d  
Method DEF\_MS-NP.M  
Sample Name 20230619\_R25 Batch 2 solid  
Comment MeOH

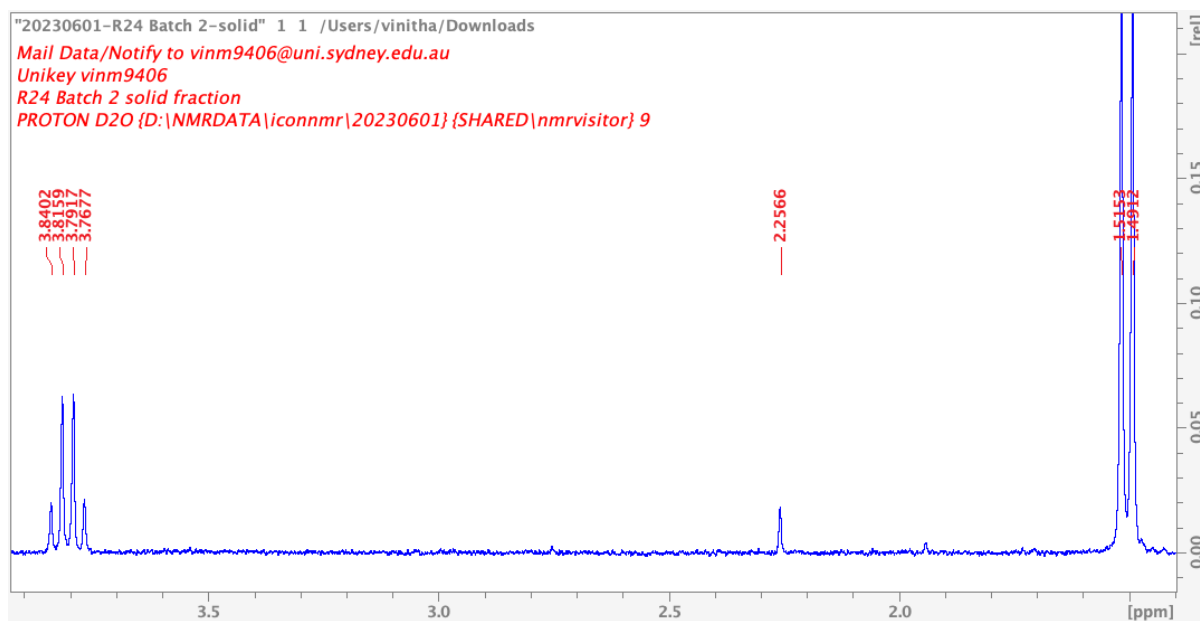
Acquisition Date 19-Jun-23 2:51:35 PM

Operator demo  
Instrument amaZon SL



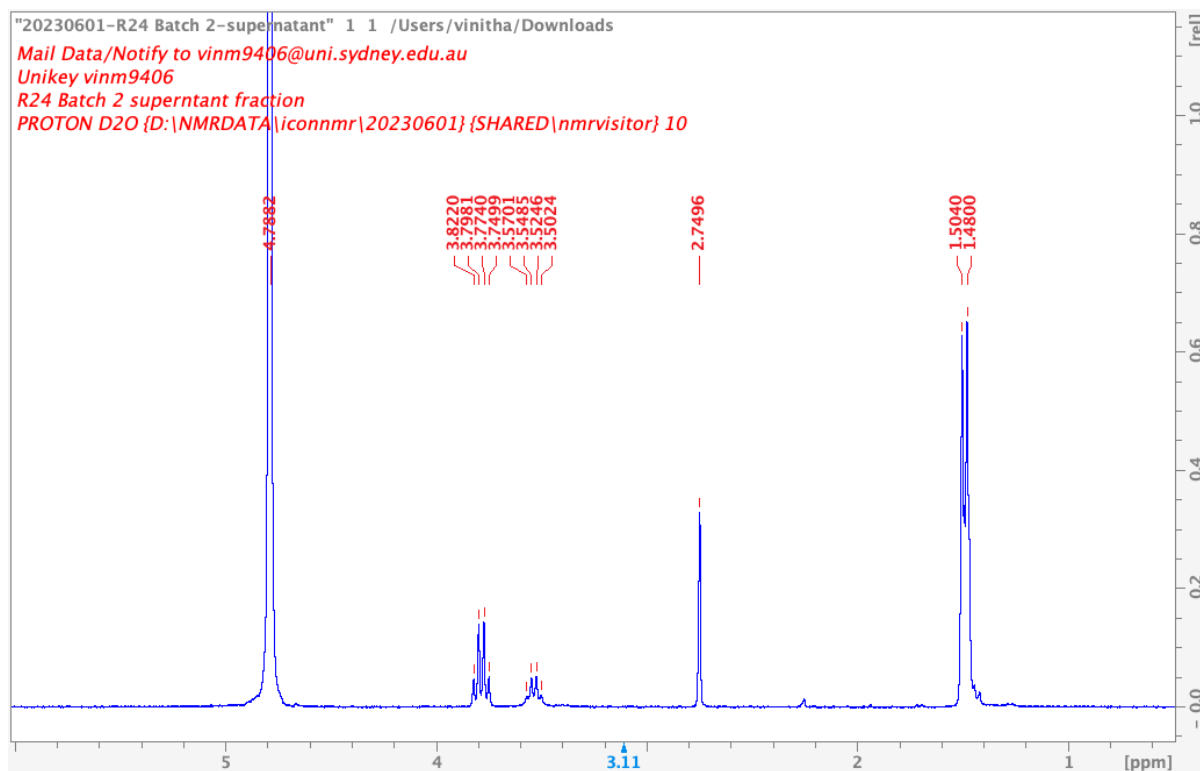
Appendix 21:  $^1\text{H}$  NMR spectrum of solid.

(2.4.5 Synthesis of *cis*-[Pt(L-alanine) $_2$ ] in methanol)



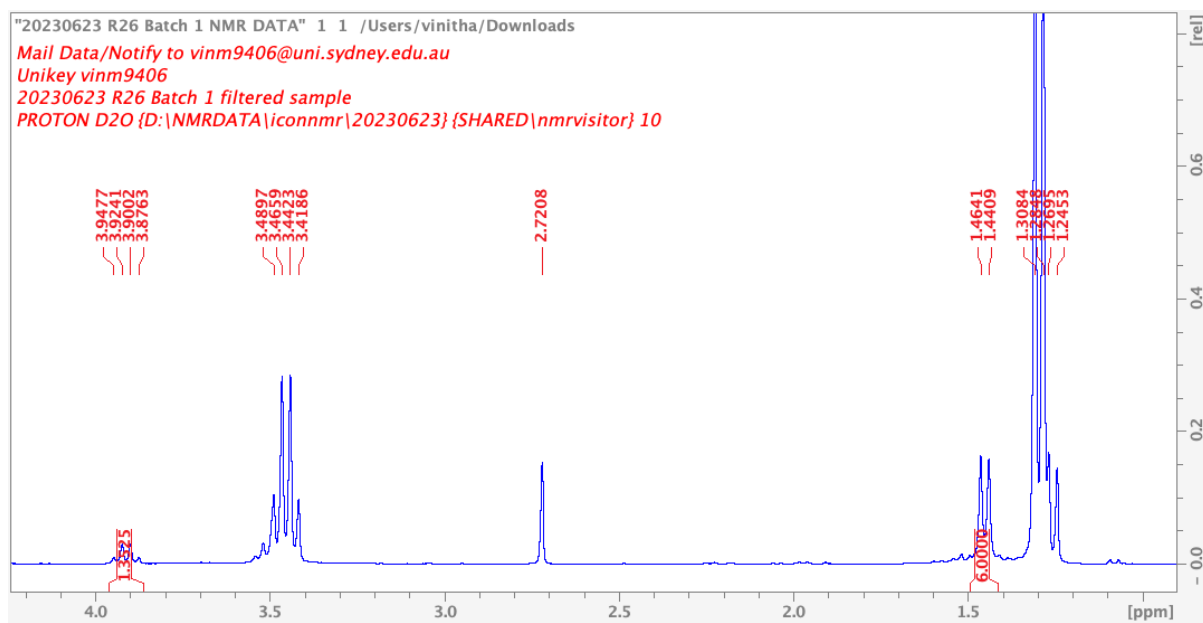
Appendix 22:  $^1\text{H}$  NMR spectrum of [Pt(L-alanine) $_3$ ] $^-$

(2.4.5 Synthesis of *cis*-[Pt(L-alanine) $_2$ ] in methanol)



Appendix 23:  $^1\text{H}$  NMR spectrum of solid.

(2.4.6 Synthesis of *cis*-[Pt(L-alanine) $_2$ ] in acetone)



## Appendix 24: Mass spectrometry ESI (+) and (-) analysis of solid.

### (2.4.6 Synthesis of *cis*-[Pt(L-alanine)<sub>2</sub>] in acetone)

#### Generic Display Report

Analysis Info		Acquisition Date 14-Jun-23 6:07:02 PM	
Analysis Name	D:\Data\OneDrive - The University of Sydney (Staff)\Instrument_Data\BrukerAmazonSL\Data\Hambley\Vinita\20230614 Batch 1 supernant.d	Operator	demo
Method	DEF_MS-NP.M	Instrument	amaZon SL
Sample Name	20230614 Batch 1 supernant		
Comment	MeOH		

